TURUN
YLIOPISTO
UNIVERSITY
OF TURKU

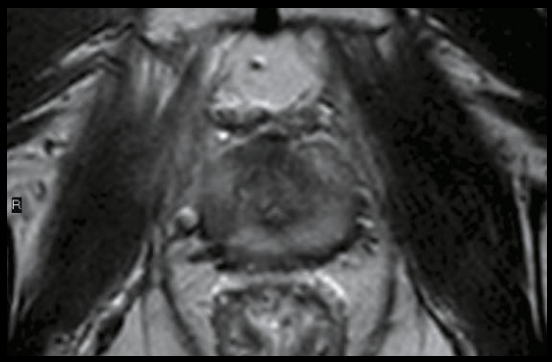
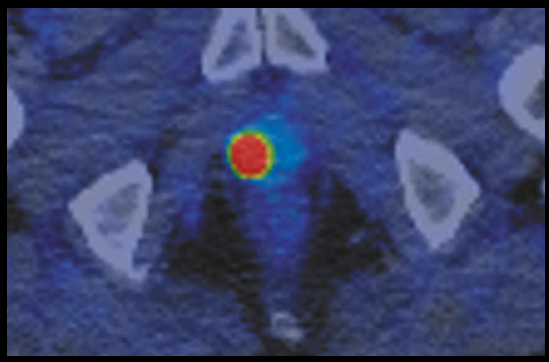
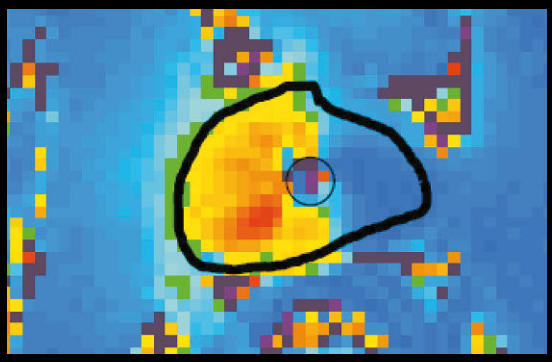
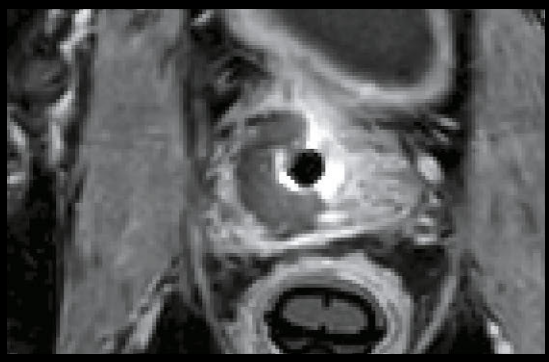

NOVEL IMAGING AND IMAGE-GUIDED THERAPY OF PROSTATE CANCER

Mikael H. J. Anttinen

TURUN YLIOPISTON JULKAISUJA – ANNALES UNIVERSITATIS TURKUENSIS
SARJA – SER. D OSA – TOM. 1555 | MEDICA – ODONTOLOGICA | TURKU 2021

TURUN
YLIOPISTO
UNIVERSITY
OF TURKU

NOVEL IMAGING AND IMAGE-GUIDED THERAPY OF PROSTATE CANCER

Mikael H. J. Anttinen

TURUN YLIOPISTON JULKAISUJA – ANNALES UNIVERSITATIS TURKUENSIS
SARJA – SER. D OSA – TOM. 1555 | MEDICA – ODONTOLOGICA | TURKU 2021

University of Turku

Faculty of Medicine
Surgery
Doctoral programme in Clinical Research
Department of Urology, Turku University Hospital

Supervised by

Adjunct Professor Peter J. Boström
Department of Urology
Turku University Hospital
Turku, Finland

Professor Roberto Blanco Sequeiros
Department of Diagnostic Radiology
Turku University Hospital
Turku, Finland

Associate Professor Pekka Taimen
Institute of Biomedicine
University of Turku and
Department of Pathology
Turku University Hospital
Turku, Finland

Reviewed by

Professor, Boris Hadaschik
Department of Urology
University of Duisburg-Essen and
University Hospital Essen
Essen, Germany

Adjunct Professor, Jukka Perälä
Department of Diagnostic Radiology
University of Oulu
Oulu, Finland

Opponent

Professor, Hashim U. Ahmed
Imperial Prostate
Division of Surgery
Department of Surgery and Cancer
Faculty of Medicine
Imperial College London
London, UK

The originality of this publication has been checked in accordance with the University of Turku quality assurance system using the Turnitin Originality Check service.

Cover picture: Mikael H. J. Anttinen

ISBN 978-951-29-8463-3 (PRINT)
ISBN 978-951-29-8464-0 (PDF)
ISSN 0355-9483 (Print)
ISSN 2343-3213 (Online)
Painosalama, Turku, Finland 2021

Suville, Leeville ja Matildalle

UNIVERSITY OF TURKU
Faculty of Medicine
Surgery
Department of Urology, Turku University Hospital
MIKAEL ANTTINEN: Novel imaging and image-guided therapy of prostate cancer
Doctoral Dissertation, 172 pp.
Doctoral Programme in Clinical Research
June 2021

ABSTRACT

Whole-gland prostate surgery and radiotherapy, the established approaches to localised prostate cancer (PCa), usually cause substantial adverse effects. Targeted image-guided cancer therapy has gained acceptance through improved PCa detection, localization and characterization by magnetic resonance imaging (MRI) and prostate-specific membrane antigen positron emission tomography-computed tomography (PSMA PET-CT). Focal therapy offers a potentially better trade-off between disease control and preservation of genitourinary and bowel function.

MRI-guided transurethral ultrasound ablation (TULSA), a recently introduced treatment modality, uses therapeutic ultrasound directed through the urethra to thermally ablate the prostate under real-time MRI control.

The applicability of TULSA to focal therapy of primary PCa, palliative therapy of symptomatic locally advanced PCa, and treatment of locally radiorecurrent PCa was investigated in a prospective setting. TULSA was shown to be a safe and effective method for local PCa control. Thermal injury was restricted to the planned treatment volume. This method enabled whole-gland ablation and focal ablation anywhere in the prostate. Furthermore, TULSA achieved local symptom relief in palliative care and encouraging preliminary oncological control in salvage care. These promising phase 1 study results enabled progression to phase 2 studies of patients with localised PCa and salvage of patients with radiorecurrent PCa.

The diagnostic accuracy of MRI and PSMA PET-CT was studied to determine the extent of primary PCa, to plan TULSA treatment and evaluate treatment response. PSMA PET-CT was found to be a more sensitive method for detecting metastatic disease and appeared to accurately reflect the extent of local disease before and after TULSA treatment. PSMA PET-CT appears to detect some false-positive bone lesions. The advantages of using MRI and PSMA PET-CT in treatment planning and monitoring treatment response are under further investigation.

These studies have shown ^{18}F-PSMA-1007 PET-CT to be effective in PCa diagnosis and TULSA to be effective in PCa therapy.

KEYWORDS: Prostate cancer, Focal therapy, MRI-guided transurethral ultrasound ablation (TULSA), Magnetic resonance imaging, Prostate-specific membrane antigen positron emission tomography-computed tomography

TURUN YLIOPISTO
Lääketieteellinen tiedekunta
Kirurgia
Urologia, Turun yliopistollinen keskussairaala
MIKAEL ANTTINEN: Modernit kuvantamismenetelmät ja kuvantamisohjatut hoidot eturauhassyövässä
Väitöskirja, 172 s.
Turun kliininen tohtoriohjelma
Kesäkuu 2021

TIIVISTELMÄ

Vakiintuneet paikallisen eturauhassyövän (PCa) hoitomenetelmät, leikkaus ja sädehoito, kohdistuvat koko rauhaseen ja aiheuttavat merkittäviä haittavaikutuksia. Magneettikuvantamisella (MRI) ja eturauhassyövän entsyymikuvantamisella (PSMA PET-TT) PCa:n havaitseminen, paikallistaminen ja karakterisointi ovat tarkentuneet. Kohdennetut kuvantamisohjatut syöpähoidot ovat siksi saaneet hyväksynnän ja tarjoavat mahdollisesti optimaalisemman vaihtoehdon hoidon hyödyn ja sen virtsa- ja sukupuolielimiin kohdistuvien haittojen suhdetta ajatellen.

MRI-ohjattu eturauhasen kuumennushoito (TULSA) on uusi menetelmä, jossa virtsaputken kautta kudosta tuhoavaa ultraääntä ohjataan eturauhaseen reaaliaikaisessa MRI-ohjauksessa ja -valvonnassa.

TULSA:n käyttökelpoisuutta primaarin PCa:n kohdennetussa hoidossa, paikallisesti edenneen PCa:n palliatiivisessa hoidossa ja sädehoidon jälkeen paikallisesti uusiutuneen PCa:n hoidossa tutkittiin prospektiivisessa tutkimusasetelmassa. TULSA-menetelmän todettiin tuhoavan turvallisesti ja tehokkaasti eturauhaskudosta. Lämpövaurio rajautui suunnitellulle hoitoalueelle. Menetelmä mahdollisti kuumennushoidon käytön kaikkialla eturauhasessa, koko rauhasessa tai paikallisemmin. Lisäksi TULSA-hoito lievensi paikallisoireita palliatiivisilla potilailla ja oli tehokas sädehoidon jälkeen paikallisesti uusiutuneessa PCa:ssä. Lupaavien ensimmäisen vaiheen tutkimustulosten takia olemme siirtyneet toisen vaiheen tutkimuksiin näillä uusilla indikaatioilla.

MRI:n ja PSMA PET-TT:n diagnostista tarkuutta tutkittiin primaarin PCa:n levinneisyyden selvittelyssä ja TULSA-hoidon suunnittelussa sekä hoitovasteen arvioinnissa. PSMA PET-TT:n havaittiin olevan herkempi menetelmä etäpesäkkeiden tunnistamisessa ja se näytti tarkasti taudin laajuuden ennen ja jälkeen TULSA-hoidon. PSMA PET-TT tunnistaa myös vääriä positiivisia luustomuutoksia. MRI:n ja PSMA PET-TT:n kliinistä hyötyä TULSA-hoidon suunnittelussa ja hoitovasteen seurannassa tutkitaan edelleen.

Tutkimuksemme ovat osoittaneet PSMA PET-TT:n hyödyllisyyden PCa:n diagnostiikassa ja TULSA:n turvallisuuden ja tehon PCa:n hoidossa.

AVAINSANAT: Eturauhassyöpä, Fokaaliterapia, MRI-ohjattu eturauhasen kuumennushoito, Magneettikuvantaminen, Eturauhassyövän entsyymikuvantaminen

Table of Contents

Abbreviations

ADT	androgen deprivation therapy
AUC	area under the receiver-operating characteristic curve
BCR	biochemical recurrence
BS	bone scintigraphy
CE	contrast-enhanced
CEM	cumulative equivalent minutes at 43°C
csPCa	clinically significant prostate cancer
CI	confidence interval
CT	computed tomography
DWI	diffusion-weighted imaging
EAU	European Association of Urology
GG	grade group
H&E	hematoxylin-eosin
HIFU	high-intensity focused ultrasound
IIEF	International Index of Erectile Function
IPSS	International Prostate Symptom Score
ISUP	International Society of Urological Pathology
LN	lymph node
mpMRI	multiparametric magnetic resonance imaging
MRI	magnetic resonance imaging
MRI-TBx	MRI-targeted biopsy
PCa	prostate cancer
PET	positron emission tomography
PI-RADS	Prostate Imaging Reporting and Data System
PSA	prostate-specific antigen
PSMA	prostate-specific membrane antigen
pTULSA	palliative TULSA
QoL	quality of life
RALP	robot-assisted laparoscopic prostatectomy
RCT	randomized controlled trial
RP	radical prostatectomy

RT	radiation therapy
SPECT	single-photon emission tomography
sTULSA	salvage TULSA
SUV	standardized uptake value
TRUS	transrectal ultrasound
TRUS-Bx	transrectal ultrasound guided prostate biopsies
TULSA	MRI-guided transurethral ultrasound ablation
TURP	transurethral resection of prostate
TYKS	Turku University Hospital
wb	whole-body

List of Original Publications

This dissertation is based on the following five original publications, which are referred to in the text by their Roman numerals:

I Mikael Anttinen, Pietari Mäkelä, Visa Suomi, Aida Kiviniemi, Jani Saunavaara, Teija Sainio, Antero Horte, Lauri Eklund, Pekka Taimen, Roberto Blanco Sequeiros and Peter J. Boström. Feasibility of MRI-guided transurethral ultrasound for lesion-targeted ablation of prostate cancer. *Scandinavian Journal of Urology*, 2019; 5: 295-302.

II Mikael Anttinen, Eemil Yli-Pietilä, Visa Suomi, Pietari Mäkelä, Teija Sainio, Jani Saunavaara, Lauri Eklund, Roberto Blanco Sequeiros, Pekka Taimen and Peter J. Boström. Histopathological evaluation of prostate specimens after thermal ablation may be confounded by the presence of thermally-fixed cells. *International Journal of Hyperthermia*, 2019; 1: 914-924.

III Mikael Anttinen, Pietari Mäkelä, Pertti Nurminen, Eemil Yli-Pietilä, Visa Suomi, Teija Sainio, Jani Saunavaara, Pekka Taimen, Roberto Blanco Sequeiros, Peter J. Boström. Palliative MRI-guided transurethral ultrasound ablation for symptomatic locally advanced prostate cancer. *Scandinavian Journal of Urology*, 2020; 8: 1-6.

IV Mikael Anttinen, Pietari Mäkelä, Antti Viitala, Eemil Yli-Pietilä, Visa Suomi, Teija Sainio, Jani Saunavaara, Roberto Blanco Sequeiros, Pekka Taimen, Peter J. Boström. Early experience of MRI-guided transurethral ultrasound ablation for radiorecurrent prostate cancer. *European Urology Open Science*, 2020

V Mikael Anttinen, Otto Ettala, Simona Malaspina, Ivan Jambor, Minna Sandell, Sami Kajander, Irina Rinta-Kiikka, Jukka Schildt, Ekaterina Saukko, Pentti Rautio, Kirsi L. Timonen, Tuomas Matikainen, Tommi Noponen, Jani Saunavaara, Eliisa Löyttyniemi, Pekka Taimen, Jukka Kemppainen, Peter B. Dean, Roberto Blanco Sequeiros, Hannu J. Aronen, Marko Seppänen, Peter J

Boström. A Prospective Comparison of 18F-prostate-specific Membrane Antigen-1007 Positron Emission Tomography Computed Tomography, Whole-body 1.5 T Magnetic Resonance Imaging with Diffusion-weighted Imaging, and Single-photon Emission Computed Tomography/Computed Tomography with Traditional Imaging in Primary Distant Metastasis Staging of Prostate Cancer (PROSTAGE). *European Urology Oncology*, 2020.

1 Introduction

Prostate cancer (PCa) is the most prevalent non-cutaneous cancer affecting men in developed countries and is considered one of the principal medical problems facing the male population. Fortunately, many men diagnosed with PCa will not suffer from any clinically significant consequences of this disease during their lifetime.

The overall extent of PCa is one of the main factors influencing prognosis and treatment choices. The spread of the disease to soft tissues and bone is traditionally assessed by computed tomography (CT) and bone scintigraphy (BS). However, these imaging methods are not sufficiently sensitive in detecting metastatic disease, which may explain why many men still suffer from metastases following locally radical PCa treatment.

The past decade has seen the rapid development of PCa imaging, particularly multiparametric magnetic resonance imaging (mpMRI) and prostate-specific membrane antigen (PSMA) positron emission tomography-computed tomography (PET-CT), which allow for earlier detection and better localization of PCa and more reliable exclusion of metastases. The diagnosis of PCa has been advanced to earlier stages of the disease, creating an opportunity to treat PCa locally.

Although PCa is often a multifocal disease, several studies have suggested that the prognosis is mainly determined by the largest and histopathologically most aggressive cancer focus, referred to as the index lesion, which can be identified and visualized by mpMRI and/or PSMA PET-CT with a high accuracy, becoming the target for image-guided cancer therapy.

While traditional radical therapy for localized PCa, including radical prostatectomy (RP) and conventional whole-gland radiation therapy (RT), provide effective local cancer control, they treat the entire gland irrespective of the underlying pathology, leaving many men with substantial long-term complications affecting urinary, bowel and sexual function, often significantly affecting the patient's quality of life (QoL). Given the relatively high overall cancer-specific survival in PCa, many men have to live much of their lives with these functional impairments. As a result, there is an unmet need for PCa therapy that can achieve sufficient control of local disease, with reduced morbidity.

In recent decades, minimally invasive ablative treatment methods have been introduced to PCa management, in which ablative energy is directed to the prostate directly through the perineum, transrectally or transurethrally. Most of these techniques exploit thermal energy, typically heating, to ablate prostate tissue. The newer technonology incorporates real-time imaging guidance, allowing targeted therapy to a specific area in the prostate, known as focal therapy (FT). Some devices use real-time tissue temperature monitoring connected to active dynamic feedback control, enabling spatially accurate conformal ablation, the prerequisite for successful FT. This approach has already become competitive with whole-gland therapy in selected PCa patients, with the goal of eradicating the cancer focus and sparing the surrounding healthy tissues, thus offering a potentially better compromise between disease control and morbidity. One of the challenges has been the ability of imaging methods to distinguish cancer from healthy tissues with sufficient accuracy. Another challenge has been to produce a more accurate energy delivery system. These two requirements are necessary for precise treatment margins to optimize the oncological and functional outcomes.

While ablative therapy is being increasingly utilized in PCa management, it remains experimental until further evidence can confirm a longer-term oncological efficacy. Thus, the patient selection criteria remain to be established. Furthermore, FT continues to face challenges in monitoring the treatment efficacy and oncological outcome. It is evident that novel imaging methods will play a key role in patient selection for FT and treatment response assessment.

2 Review of the Literature

2.1 Characteristics of prostate cancer

PCa includes a wide range of neoplasms with different malignant potential. Conventional acinar adenocarcinoma, characterized by a transformed glandular epithelial cell population, is the most common malignant neoplasm of the prostate gland and comprises more than 95% of prostate malignancies. Other histopathological PCa types include neuroendocrine PCa, as well as rare transitional and squamous cell carcinomas, sarcomas and lymphomas. The current thesis focuses only on patients with histopathologically verified conventional acinar adenocarcinoma of the prostate.

The prostate gland is anatomically divided into four histologically discrete zones (**Figure 1**) including the central zone, peripheral zone, transition zone and fibromuscular zone (McNeal 1981). The peripheral zone comprises the largest area of the glandular prostate and due to the posterior location is the only zone of the prostate, which can be reached by digital rectal examination (McNeal 1981). Two thirds of prostate adenocarcinomas originate from the peripheral zone, while the remaining originate mainly from the transitional zone (McNeal et al. 1988, Epstein et al. 1994). It has been reported that approximately 20% of patients with localized PCa have unilateral disease (Mouraviev et al. 2007, Nevoux et al. 2012). Up to 85% of primary prostate adenocarcinomas are multifocal with individual tumour foci harbouring different genetic alterations and aggressiveness (Byar et al. 1972, Nevoux et al. 2012, Wei et al. 2017, Løvf et al. 2019). The accumulating evidence indicates that the clinical outcome is determined predominantly by the index lesion that is characterized by the largest diameter, highest stage and highest grade (McNeal 1992, Mouraviev et al. 2011, Choi et al, 2019).

PCa can spread directly to the surrounding organs or through lymphovascular routes to other parts of the body. Local spread includes direct invasion of the tumour in the adjacent organs and lymphatic spread typically into the pelvic regional lymph nodes (LN). The most common distant metastatic sites are bone (84%) and non-regional LNs (11%), followed by extranodal soft tissues, typically liver (10%) and lung (9%) (Gandaglia et al. 2014).

PCa can be considered as a continuum of tumours with aggressiveness ranging from indolent tumours with no effect on the life expectancy to highly aggressive tumours that lead to death. Fortunately, the natural course of PCa is generally slow and has a good prognosis. Many men diagnosed with PCa will not suffer from the clinically significant consequences of the disease during their lifetime and the onset of the disease is relatively late in life, with most patients being over 70 years of age at diagnosis (Mottet et al. 2020).

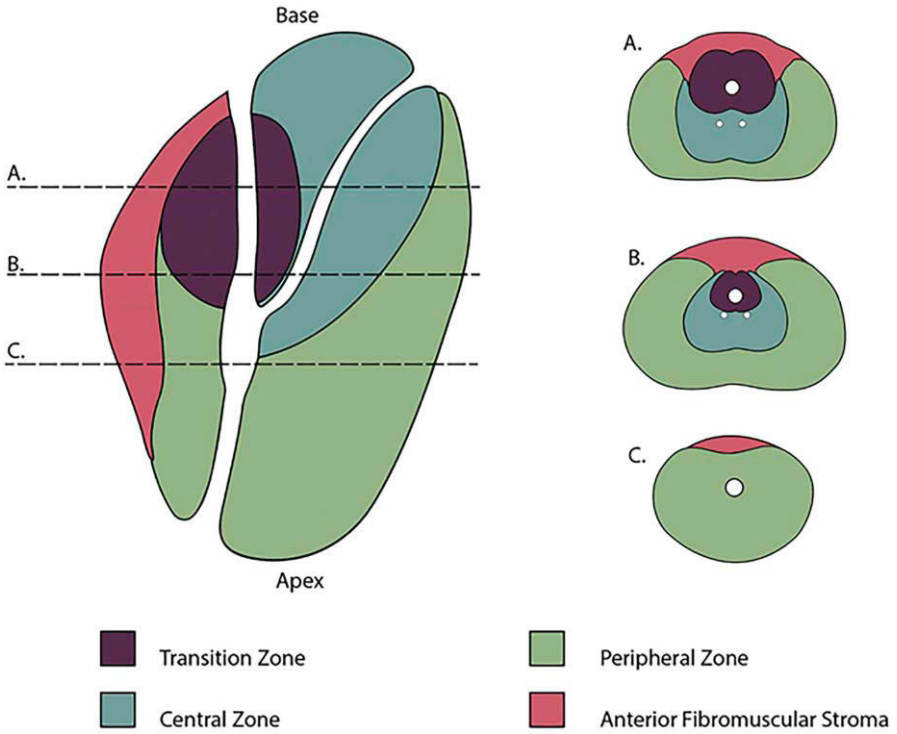

Figure 1. Schematic of the zonal anatomy of the prostate (Reproduced with permission from Yacoub, Oto. Radiol Clin 2018)

2.1.1 Incidence, aetiology and risk factors

Globally PCa is recognized as one of the most important health concerns affecting the male population, especially due to aging population in the developed countries. Based on the autopsy studies the frequency of autopsy-detected PCa is approximately the same worldwide (Haas et al., 2008) and up to 50% of men older than 50 years of age harbour latent PCa (Hølund et al. 1980, Zlotta et al. 2013). In the United States, it is estimated that a man has a 17% lifetime risk of developing PCa and a 2.6% risk of dying from it (American Cancer Society 2008). Further, 35%

of Swedish and 16% of US men diagnosed with PCa will die from it (Epstein et al. 2012). In Finland, 92% of men are alive 5 years after being diagnosed with PCa (Finnish Cancer Registry 2019).

Determining the worldwide incidence and mortality of PCa is problematic due to the significant proportion of latent cancers diagnosed through prostate-specific antigen (PSA)-based screening and surgery for benign prostatic obstruction. Significant geographical variations in PCa rates and trends is mainly explained by differences in access to medical care, detection rates, availability of treatment, environmental factors and underlying genetic susceptibility.

PCa is the most frequently diagnosed cancer among men worldwide by total incidence and the eight most common in total cancer mortality (Fitzmaurice et al. 2015) with an estimated 1 276 000 new cases and 359 000 deaths in 2018 (Bray et al. 2018). Comparing age standardized incidence rates, PCa is the second most commonly diagnosed cancer among men worldwide after lung cancer with the highest rates observed in the highest resourced areas of the world. Using the age standardized mortality rates, PCa is in the 6th place in cancer-related deaths in developed countries, and the second most common in non-developed countries (Bray et a. 2018). According to Finnish Cancer Registry, 5446 prostate cancers were diagnosed in Finland and 912 men died of prostate cancer in 2017, making it the most commonly diagnosed cancer and the second most common cause of cancer deaths (Finnish Cancer Registry, 2019). In Finland (and worldwide), the main reasons for the increase in PCa incidence in recent decades are screening and improved diagnostics, especially the introduction of PSA, and aan aging population.

The aetiology of PCa remain largely unknown although various exogenous and environmental factors may influence PCa incidence and the risk of progression. Therefore, no specific preventive or dietary measures are recommended to reduce the risk of developing PCa. The only well-established risk factors for PCa include advanced age, black race, and a family history of the disease (Mottet et al. 2020).

2.1.2 Grading

Grading of prostate acinar adenocarcinomas is based on the Gleason grading system, which is named after its inventor Donald Gleason, a pathologist at the Minneapolis Veterans Affairs Hospital (Gleason, 1966). The original Gleason grading system has since being significantly modified after three major consensus meetings conducted by the International Society of Urologic Pathology (ISUP) in 2005, 2014 and 2019 (Epstein et al. 2005, Epstein et al. 2016, van Leenders et al. 2020).

The Gleason grading system, which is used for the grading of both prostate biopsy and prostatectomy specimens, is based on the different patterns of prostate gland formation ranging from organized and uniform glands to disordered and

infiltrative as shown in **Figure 2**. The different patterns are graded to 1-5, of which the grade 5 represents the most aggressive type. The Gleason Score is obtained by using the sum of the most common (primary) pattern and, if present, the second most common (secondary) pattern detected in the prostate specimen. If only one pattern is present, the Gleason score is obtained by doubling the single score. For three grades in the prostate biopsy specimen, Gleason score comprises the most common grade plus the highest grade, irrespective of its extent. When an adenocarcinoma is mainly grade 4 or 5, small volume (< 5%) of lower grade carcinoma is no longer incorporated in the Gleason score. In addition to reporting Gleason score for each biopsy specimen/site, an overall (global) Gleason score is also recommended for systematic biopsies, which consider the extent of each grade from all biopsies. For MRI-targeted biopsies, a global Gleason score for each MRI lesion should be assigned (van Leenders et al. 2020). However, there is no consensus how to report global Gleason score in the case of both systematic and targeted biopsies on patient level. ISUP grading of prostatectomy specimens largely corresponds to grading of prostate biopsy specimens, except that for a third higher Gleason pattern of less than 5%, a separate tertiary Gleason grade 4 or 5, is also reported (**Figure 2**).

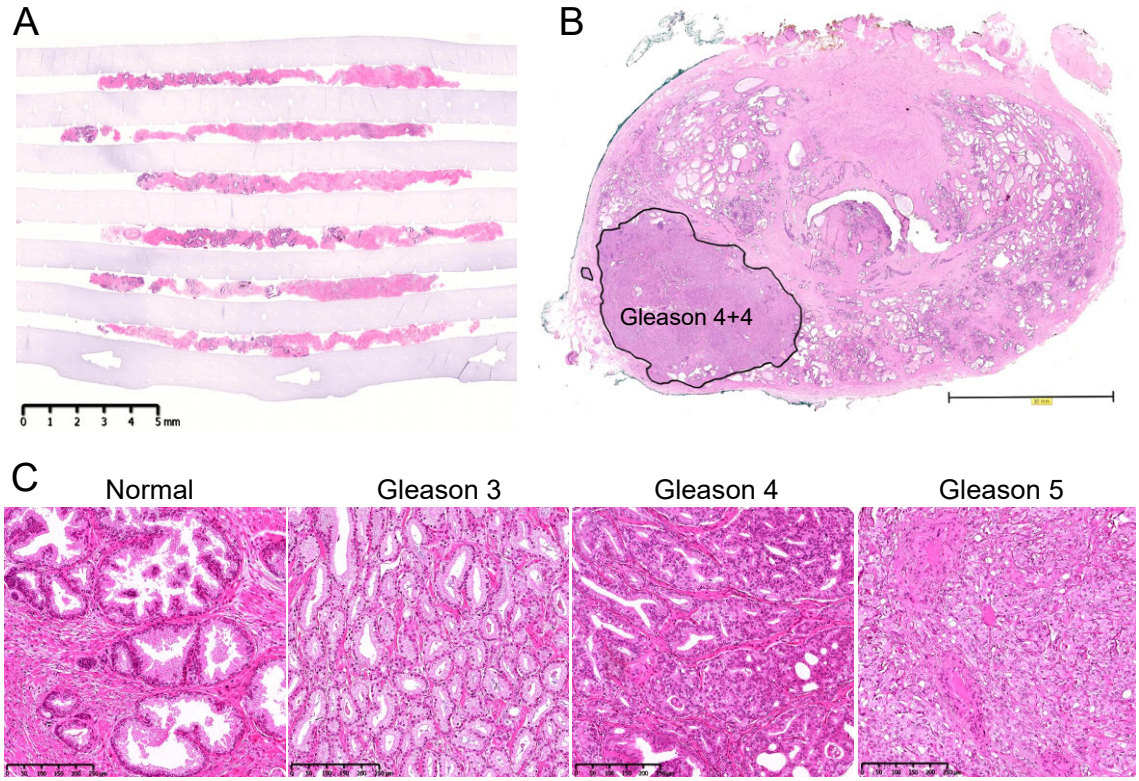

Figure 2. Six prostate biopsy cores on the orientation plate (Themis Biopsy Chip [BxChip™], CellPath Ltd, Newtown, United Kingdom) (A) and cross-section of radical prostatectomy specimen (B) with Gleason 4+4 tumour in the posterolateral corner. Different patterns of prostate gland formation (C).

The 2014 ISUP consensus conference established the concept of the ISUP grade groups (ISUP GG) of PCa, graded also from 1-5 (**Table 1**, ISUP GG), to eliminate the anomaly that the most highly differentiated PCa have a Gleason score 6 and to reflect more accurately the prognosis of disease especially in the case of Gleason score 7 (Epstein et al. 2016, Mottet et al. 2020). The ISUP GG are independently linked to biochemical recurrence (BCR) rate in men treated with RP or RT (Epstein, Zelefsky, et al. 2016) and to cancer-specific mortality (Erickson et al. 2018). Recent publications suggest superiority of the global biopsy ISUP GG in predicting prostatectomy ISUP GG (Sauter et al. 2016) and BCR (Cole et al. 2016). The ISUP GG system is also used in this thesis.

Table 1. ISUP Gleason grade group system (Modified from Epstein et al. Am J Surg Pathol 2016)

Gleason score	ISUP grade group	10-year biochemical recurrence free survival after radical prostatectomy
3+3	1	95%
3+4	2	80%
4+3	3	50%
4+4, 3+5, 5+3	4	38%
4+5, 5+4, 5+5	5	17%

Intraductal carcinoma of the prostate, characterized by carcinoma colonizing normal ducts and/or acini, is a histopathological subtype of adenocarcinomas that is associated with an adverse prognosis and clinical outcome (Tsuzuki et al. 2015). The 2014 ISUP consensus conference concluded that an intraductal carcinoma of the prostate without invasive carcinoma should not be assigned a Gleason grade.

Cribriform PCa is a morphological subtype of adenocarcinoma associated with poor prognosis. The 2014 ISUP consensus conference concluded that cribriform glands should be assigned a Gleason pattern 4 (Epstein et al. 2016). Both intraductal carcinoma of the prostate and cribriform pattern of PCa in prostate biopsies are independently associated with metastatic disease (Kweldam et al. 2016) and cancer-specific survival (Sæter et al. 2016). Therefore, their presence or absence should be systematically reported by pathologists.

2.1.3 TNM-staging classification

The World Health Organization (WHO) Tumour, Node, Metastasis (TNM) classification is used for staging of PCa with the objective of combining patients with a similar clinical outcome. It consists of three components: T = the extent of the primary tumour, N = the absence or presence of the regional LN metastasis, and M

= the absence or presence of distant metastasis (**Table 2**. TNM Classification) (Brierley, et al. 2017). The TNM classification is divided into two categories: clinical TNM (cTNM) and pathological TNM (pTNM). The clinical T stage is traditionally based only on digital rectal examination. The clinical N and M stages are based on imaging, the need for which depends on the risk stratification by the European Association of Urology (EAU) guidelines, as described in **Table 3** (Mottet et al. 2020). The pathological T stage is based on histopathological evaluation of the removed prostate and seminal vesicles in RP. The RP specimen is further studied to determine histopathological type, grade, the amount and extent of cancer and surgical margins, all of which have prognostic value, for example, for BCR (Mottet et al. 2020). For T stage, pathological staging is equivalent to clinical staging except for clinical stage T1c and the T2 substages. All histopathologically verified organ-confined PCa are pathological stage T2. Similarly, the pathological N stage is based on pelvic LN dissection during RP in certain men at increased risk for LN metastases, which is determined preoperatively by using validated nomograms such as Briganti nomogram (Gandaglia et al. 2017). With the increasing use of MRI in the diagnosis, local staging and treatment planning of PCa, radiological T stage (rT) has been introduced in clinical practice corresponding to cT stage. However, it should be noted that rT stage has not been incorporated in the EAU risk group classification, and therefore should not replace digital rectal examination. Prostate mpMRI have been included in some risk nomograms, for example, the rT stage and MRI-targeted biopsies (MRI-TBx) in addition to systematic biopsies has been combined to estimate the probability of LN invasion in the 2018 Briganti nomogram (Gandaglia et al. 2019).

Table 2. TNM classification (Modified from Bierley et al. Union for International Cancer Control (UICC) International Union Against Cancer. 8th edition 2017),

Clinical TNM classification		Pathological TNM classification	
TX	Primary tumour cannot be assessed	pTX	–
T0	No evidence of primary tumour	pT0	–
T1	Clinically inapparent tumour neither palpable nor visible by imaging	pT1	There is no pathological T1 classification
T1a	Tumour incidental histological finding in ≤5% of tissue resected	pT1a	–
T1b	Tumour incidental histological finding in >5% of tissue resected	pT1b	–
T1c	Tumour identified by needle biopsy (e.g. because of elevated PSA)	pT1c	–
T2	Tumour confined within prostate	pT2	Organ confined
T2a	Tumour involves ≤50% of one lobe		
T2b	Tumour involves >50% of one lobe but not both lobes		
T2c	Tumour involves both lobes		
T3	Tumour extends through the prostate capsule	pT3	Extraprostatic extension
T3a	Extraprostatic extension (unilateral or bilateral)	pT3a	Extraprostatic extension or microscopic invasion of bladder neck
T3b	Tumour invades seminal vesicle(s)	pT3b	Seminal vesicle invasion
T4	Tumour is fixed or invades adjacent structures other than seminal vesicles such as external sphincter, rectum, bladder, levator muscles, and/or pelvic wall	pT4	Invasion of rectum, levator muscle, and/or pelvic wall
NX	Regional lymph nodes were not assessed	pNX	Regional nodes not sampled
N0	No regional lymph node metastasis	pN0	No positive regional nodes
N1	Metastases in regional lymph node(s)	pN1	Metastases in regional node(s)
M0	No distant metastasis	pM0	No distant metastasis
M1	Distant metastasis	pM1	Distant metastasis
M1a	Non-regional lymph node(s)	pM1a	Non-regional lymph node(s)
M1b	Bone(s)	pM1b	Bone(s)
M1c	Other site(s) with or without bone disease	pM1c	Other site(s) with or without bone disease. When more than one site of metastasis is present, the most advanced category is used. pM1c is most advanced

Table 3. EAU risk groups for biochemical recurrence of localized and locally advanced PCa (Modified from Mottet et al. 2020), which is based on D´Amico risk stratification for PCa (D`Amico et al. 1998).

Low risk	Intermediate risk	High risk	
PSA < 10 ng/ml, Gleason score < 7 (ISUP grade group 1) and cT1-cT2a	PSA 10-20 ng/ml or Gleason score = 7 (ISUP grade group 2–3) or cT2b	PSA > 20 ng/ml or Gleason score > 7 (ISUP grade group 4–5) or cT2c	any PSA any Gleason score (any ISUP grade) cT3–4 or cN+
Localized			Locally advanced

2.2 Diagnosis and Imaging

Suspicion of PCa typically arises from elevated PSA or abnormal digital rectal examination of the prostate such as a hard mass or nodule, induration or asymmetry. The definitive diagnosis is made by confirming PCa by histopathological examination of prostate biopsy specimens. Sometimes the diagnosis is made incidentally due to prostate surgery, such as simple prostatectomy or transurethral resection of prostate (TURP), typically in the treatment of benign prostatic obstruction.

2.2.1 Prostate-specific antigen (PSA) and screening of men using PSA

PSA, also known as human kallikrein peptidase 3, is an androgen-regulated serine protease exclusively produced by prostate luminal epithelial cells, although small quantities of ectopic expression have been reported mainly in other malignancies, such as breast, colon, ovarian, liver, adrenal, kidney and parotid tumours (Levesque et al. 1995). It is in high concentrations secreted via prostatic ducts to the semen, where its function is to liquify the seminal coagulum to allow the release of spermatozoa.

PSA is normally present in small quantities in the serum of men without prostate pathology. Elevated serum PSA levels are suspected to be due to disruption of both the basement membrane and normal cellular architecture within the prostate gland, particularly in adenocarcinomas lacking basal cells, leading to more PSA leaked into the bloodstream (Wein et al. 2016). PSA is a continuous parameter with higher PSA levels indicating greater likelihood of PCa, and predictive of more advanced PCa (Thompson et al. 2004). Importantly, PSA is organ but not cancer-specific biomarker meaning it may be elevated in other prostate diseases including benign prostatic hyperplasia, prostatitis and other non-malignant conditions (Wein et al. 2016). Thus, limited PSA elevation alone in a single measurement should not prompt immediate

prostate biopsy, but should be based on a repeatedly elevated PSA level. A large proportion of men with organ-confined PCa present with low PSA values. Up to 6.7% of clinically significant PCa (csPCa) are diagnosed with a PSA value of 3-4, precluding an optimal PSA threshold for detecting csPCa (Thompson et al. 2004).

The use of the PSA as a serum biomarker has revolutionized the diagnosis of PCa by allowing earlier diagnosis. Serum PSA measurement was originally introduced in the 1980s to monitor treatment response after radically treated PCa patients (Kuriyama et al. 1981, Stamey et al. 1987). Shortly afterwards it was adopted in PCa screening, which still remains one of the most controversial topics in the medical literature. The most significant challenges in PSA screening include a high false positive rate of PCa suspicions and diagnosis of insignificant PCa, which led to increased patient anxiety, unnecessary biopsies and treatments, ultimately subjecting patients to the adverse effects associated with these procedures. The Cochrane systematic review from 2013, including results from up to five randomized controlled trials (RCT) randomizing more than 341.000 men with 7-20 years´ follow-up, concludes that there were no statistically significant differences in cancer-specific mortality or overall mortality observed between the screening and control groups (Ilic et al. 2013). However, the updated results from extended follow-up in the European Randomized Study for Prostate Cancer and Swedish Gothenburg Randomized Population-based Prostate Cancer Screening Trial indicated a decrease in PCa-specific mortality in screened men (Schröder et al. 2014, Carlsson et al. 2017). Based on these results, the European Association of Urology does not recommend population-based PCa screening but recommends an individualized risk-adapted strategy for early detection to men with a good performance status and a life-expectancy of at least ten to fifteen years.

To increase the specificity of total serum PSA in PCa diagnosis, various PSA derivatives and PSA kinetics have been introduced in clinical practice. PSA density is defined by total serum PSA divided by the prostate volume based on transrectal ultrasound measurement. The contributions of normal prostate epithelium, benign prostatic hyperplasia and PCa to serum total PSA levels have been estimated to be 0.1 ng/ml, 0.3 ng/ml, and 3.5 ng/ml, respectively (Stamey et al. 1987). The higher the PSA density, the greater likelihood is of csPCa. There are two methods of measuring PSA kinetics. PSA velocity is defined as absolute annual increase and PSA doubling time as an exponential increase in serum PSA over time. Compared to total serum PSA, the added value of these PSA kinetics is limited and therefore they are not recommended by contemporary EAU guidelines. Serum PSA predominantly occurs in a complex with proteases in the blood. Free form constitutes 5-40% of total PSA. A free to total PSA ratio is used to distinguish benign prostatic hyperplasia from PCa, when PSA level is between 4-10 ng/ml and digital rectal examination is negative. In a prospective multicentre study PCa was detected by

biopsy in 56% of men with free to total PSA <10%, but in only 8% with free to total PSA > 25% (Catalona et al. 1998). Due to novel serum biomarkers, the value of the free to total PSA ratio in clinical use is limited (Mottet et al. 2020).

2.2.2 Other kallikreins and biomarkers

In addition to PSA and its derivatives, many other prognostic biomarkers have been introduced for men with elevated PSA to refine the diagnosis and risk stratification of PCa. Commercially available tests include assays measuring a panel of kallikreins in serum (Prostate Health Index [PHI] and four kallikrein [4K] score test), serum- and urine-based tests (Prostate cancer antigen 3 score [Progensa], SelectMDX, MiProstate score, ExoDX), and tissue-based tests (ConfirmMDX, Oncotype Dx, Prolaris, Decipher, Decipher Portos, ProMark). Although these novel biomarkers may improve risk assessment in PCa diagnostics, their benefit is likely to be significantly affected by emerging imaging techniques, especially upfront mpMRI. Thus, the contemporary EAU guidelines have given a weak recommendation for the usage of these serum or urine-based tests in further risk assessment of asymptomatic men with a PSA level between 2-10 ng/ml prior to performing a prostate biopsy. Rather, in addition to risk-calculators, a strong recommendation has been given to perform mpMRI, which is also strongly recommended in re-biopsy setting for men with prior negative biopsy (Mottet et al. 2020).

2.2.3 Transrectal ultrasound and prostate biopsies

Transrectal ultrasound (TRUS) is traditionally used by urologists in outpatient clinics for the diagnosis of prostate diseases. TRUS provides insight into the prostate zonal anatomy, prostate size and periprostatic structures. Furthermore, TRUS provides a needle tract tool and guidance for prostate biopsies. Ultrasound guided biopsies are a cornerstone in PCa diagnosis. However, grey-scale TRUS is insufficient to reliably detect or stage PCa, and should be used solely to locate prostate tissue, and to assist in directing biopsy needle to the prostate (Mottet et al. 2020). Despite application of new sonographic modalities to improve PCa detection and staging, such as sonoelastography, contrast-enhanced (CE) ultrasound and high-resolution micro-ultrasound, there is no sufficient evidence to support their routine use (Mottet et al. 2020).

If PCa is suspected, and the patient is considered to benefit from a PCa diagnosis, ultrasound guided prostate biopsies are performed by either the transrectal or transperineal route using an 18-gauge needle gun. The TRUS-guided biopsy (TRUS-Bx) procedure is performed under a local infiltration anaesthesia to the periprostatic regions, while the transperineal procedure requires at minimum additional

anaesthesia to perineal skin and subcutis. An antibiotic prophylaxis should be given prior to the prostate biopsies. An antibiotic regimen of fluoroquinolone is still recommended in the TRUS-Bx, although emerging antibiotic resistance of Escherichia Coli have been reported. A single dose of intravenous cephazolin is recommended in the transperineal biopsies (Mottet et al. 2020).

Two thirds of PCa originate from the peripheral zone (McNeal et al. 1988, Epstein et al. 1994). Therefore, at the baseline biopsy (depending on the prostate size) 8-12 biopsy cores are taken systematically from the template distributed regions covering the peripheral zones (**Figure 3**), with more than 12 cores not being significantly more conclusive (Eicher et al. 2006, Ukimura et al. 2013, Mottet et al. 2020). In case of prevailing suspicion of PCa after first-line biopsies, repeated biopsies are indicated in certain cases, which are well described in the EAU guidelines (Mottet et al. 2020).

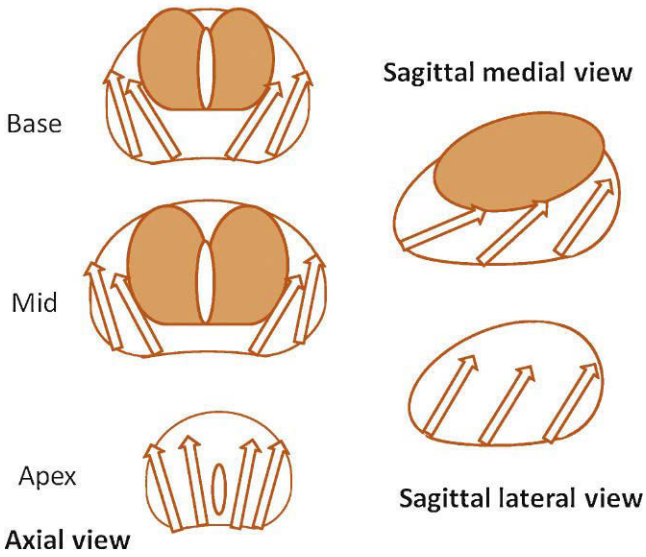

Figure 3. Recommended scheme for initial prostate biopsy covering the peripheral zone (Reproduced with permission from Ukimura et al. Eur Urol 2013).

2.2.4 Prostate MRI

The conventional diagnostic pathway in men with a suspicion of PCa has relied on systematic TRUS-Bx that focus on the posterolateral areas of the prostate where most of the PCa develop. However, 20-30% of csPCa, mostly in apical and anterior regions, are missed using this method (Mottet et al. 2020).

During the last decade, MRI has been adopted as an integral part of PCa diagnostics and is currently used primarily for the identification of csPCa, but also

for risk stratification, tumour staging, and treatment planning. Prostate MRI has evolved during the last decade. The multiparametricity of MRI consists of several different sequences used to search for signs of prostate pathology including anatomical (T1 and T2 weighted [T2w] imaging) and so-called functional (diffusion-weighted imaging [DWI] including apparent diffusion coefficient maps and dynamic contrast enhanced MRI, proton magnetic resonance spectroscopy) sequences. Prostate MRI is most commonly performed using T2w, DWI and dynamic contrast enhanced MRI sequences, although promising results have been achieved with biparametric MRI, including T2w and DWI only without the use of intravenous contrast agent, in prospective single- and multicentre studies (Jambor et al. 2019, Knaapila et al. 2020) in treatment naive men with a clinical suspicion of PCa. In a two-centre study conducted in 2011-2013 Jambor and coworkers demonstrated limited added values of dynamic contrast enhanced MRI and MRI-TBx in men with clinical suspicion of PCa before their first biopsy (Jambor et al. 2015). Moreover, recent meta-analysis shows that biparametric MRI offers comparable diagnostic accuracies to mpMRI in detecting PCa in treatment naive men with a clinical suspicion of PCa (Bass et al. 2020) (**Figure 4**).

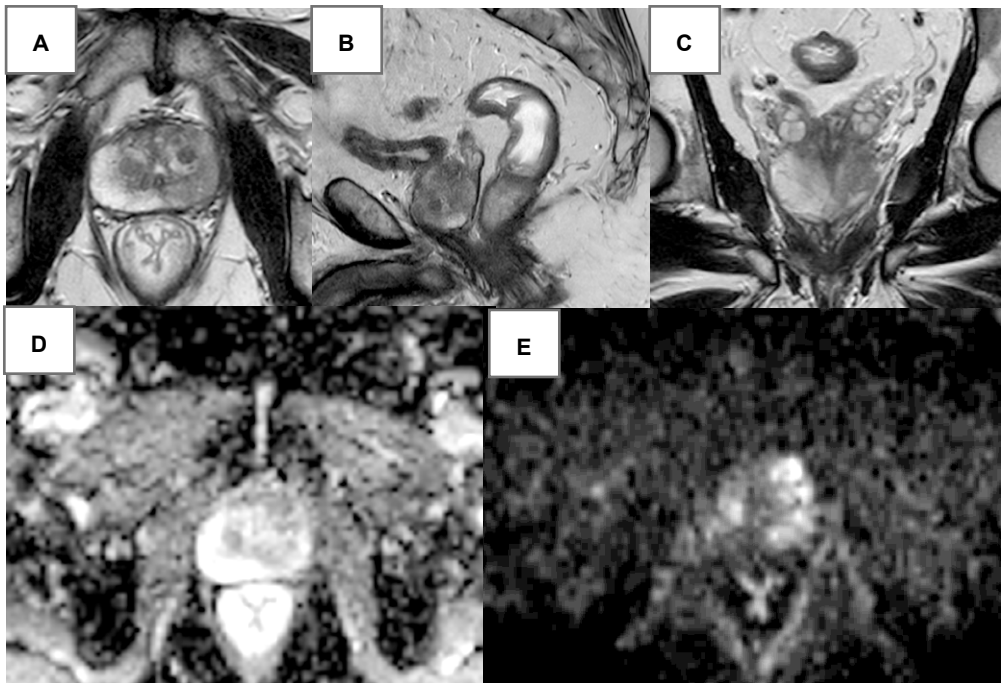

Figure 4. Case example of a prostate biparametric MRI. Axial (A), sagittal (B) and coronal (C) T2-weighted images, and apparent diffusion coefficient map (b-value 0, 2000 s/mm^2) (D) and diffusion-weighted image (b-value 2000 s/mm^2) (E) of the left lobe situated PI-RADS 5 lesion from a study patient.

Large inter-centre variations in the performance of prostate MRI exist, likely driven by differences in prostate MRI acquisition protocol, reporting and application of prostate MRI, and reference standard for performance measures of prostate MRI. In order to address inter-centre variations, the European Society of Urogenital Radiology in collaboration with American College of Radiology developed consensus-based guidelines for prostate mpMRI called Prostate Imaging–Reporting and Data System (PI-RADS). PI-RADS is a structured reporting scheme for mpMRI in treatment naive men with suspected or diagnosed PCa (Purysko et al. 2020).

In several studies using a prostatectomy specimen or prostate template biopsies as reference, both mpMRI and biparametric MRI has been shown to be highly sensitive to the detection and localization of csPCa with increasing detectability according to tumour size and grade, and is less sensitive to the detection of insignificant PCa (Bratan et al. 2013, Drost et al. 2019, Merisaari et al. 2019). Furthermore, several prospective clinical studies have reported on superior detection rates of csPCa and reduced detection rates of insignificant PCa by using MRI-targeted biopsies (MRI-TBx) compared to systematic biopsies in biopsy naive men (Siddiqui et al. 2015, Ahmed et al. 2017, Kasivisvanathan et al. 2018, Van der Leest et al. 2019, Rouvière et al. 2019), although contrary to these results, the superiority of MRI-TBx over TRUS-TBx could not be demonstrated by a RCT conducted in Finland (Tonttila et al. 2016). Nevertheless, recent systematic review and meta-analysis of RCT addressing this topic concluded that MRI-TBx improves detection of csPCa compared to TRUS-TBx (Woo et al. 2019). This improvement is even more evident in the repeat-biopsy setting, with marginal added value for systematic biopsies, whereas in biopsy naive patients, systematic biopsies remain a higher added value for the detection of csPCa and therefore commonly combined with MRI-TBx in case of positive mpMRI (PI-RADS ≥3) (Mottet et al. 2020). Thus, if mpMRI is available, it is strongly recommended by the EAU guidelines in both biopsy-naive patients and in patients with prior negative biopsy.

Three techniques are currently available for MRI-TBx, none of which has yet proven to be superior to the others: cognitive registration under TRUS guidance, MRI/TRUS fusion-guided biopsy using software-assisted fusion registration and in-bore biopsy (Wegelin et al. 2017). Currently, it is generally recommended to take 2-5 biopsies per lesion depending on the size of the lesion. In our centre, cognitive registration is used for MRI-TBx and approximately 2-4 biopsies are taken per lesion.

The most widely used reporting system for mpMRI of treatment-naive prostate remains PI-RADS systems, which uses explicit criteria on a zonal mpMRI to rate the suspicion of PCa on a 5-point scale, where a score of 1 represents very low risk for csPCa while a score of 5 represents very high risk for csPCa. PI-RADS was designed to promote standardization and diminish variation in the acquisition, interpretation, and reporting of prostate mpMRI, and the current version used is 2.1 (Padhani et al. 2019). Multiple

additional reporting systems, such as IMPROD biparametric MRI Likert score (Jambor et al. 2017), have been proposed by different centres which present the likelihood of csPCa on a Likert scale as 5-point rating system adapted to the radiologist's experience for overall impression. **Table 4** shows the proportion of csPCa and insignificant PCa at a lesion level in MRI-TBx in different MRI suspicion scores using data from the Met Prostate MRI Meer Mans (4M), MRI-FIRST and Improved Prostate Cancer Diagnosis (IMPROD) and Multi-IMPROD studies (Van der Leest et al. 2019, Rouvière et al. 2019, Knaapila, Jambor & Perez, et al. 2020). **Table 5** presents the prevalence of PCa at the patient level according to the highest biparametric MRI Likert score.

Table 4. Prevalence of clinically significant PCa (csPCa) (ISUP GG ≥2) and insignificant PCa (insPCa) (4M/IMPROD/Multi-IMPROD ISUP GG 1; MRI-FIRST ISUP 1 with maximum cancer core length <6mm) in MRI-TBx in relation to mpMRI score in the prospective MRI-FIRST and 4M studies (Rouvière et al. 2019, Van der Leest et al. 2019). For comparison, the results of a biparametric IMPROD/Multi-IMPROD MRI studies conducted at our centre (Modified from Knaapila´s thesis entitled "Challenges in diagnostics of prostate cancer" 2020). The PI-RADS score was used in the 4M study, while the MRI-FIRST used Likert score and IMPROD/Multi-IMPROD studies used biparametric MRI Likert score to assess MRI-visible lesions.

MRI score (PI-RADS/ Likert/biparametric MRI Likert)	mpMRI-targeted biopsies				biparametric MRI-targeted biopsies	
	4M (n=626)		MRI-FIRST (n=251)		IMPROD and Multi-IMPROD (n=499)	
	csPCa %	insPCa %	csPCa %	insPCa %	csPCa %	insPCa %
3	18	18	12	5	8	12
4	40	32	31	15	35	20
5	70	26	77	0	72	15

Table 5. Prevalence of PCa, clinically significant PCa (csPCa) and insignificant PCa (insPCa) according to the highest Likert score at the patient level from the pooled data of the prospective studies including IMPROD, IMPROD 2.0, Multi-IMPROD and PROMANEG, where patients underwent MRI-TBx (Likert score ≥3) in addition to systematic biopsy (Data from Knaapila et al. 2020).

Pooled data from IMPROD, Multi-IMPROD, IMPROD 2.0 and PROMANEG (n=639)									
MRI score (biparametric MRI Likert)		Benign n=239		PCa n=410		csPCa (ISUP GG ≥2) n=307		insPCa (ISUP GG=1) n=103	
Score	n	n	~%	n	~%	n	~%	n	~%
1	74	64	87	10	14	4	5	6	5
2	59	47	80	12	20	5	8	7	12
3	110	71	65	39	35	13	12	26	24
4	112	32	27	80	71	49	44	31	63
5	284	15	5	269	95	236	83	33	12

mpMRI has shown its superiority in the detection of index lesion, but in the detection of non-index/secondary lesion, even in high-grade lesions, it is limited based on correlation studies with whole-mount histopathology (Le et al. 2015). In a retrospective analysis by Johnson et al. whole-mount pathology of RP specimens from 588 operated men was correlated with their 3T mpMRI prior to RP to determine per-lesion detection rate for PCa foci by mpMRI. A total of 1213 histopathologically-confirmed PCa foci were included in the final analysis, of which mpMRI detected 45%, including 65% of csPCa, and 80% of high-grade tumours. 73% and 31% of missed csPCa were solitary and multifocal tumours, respectively. Furthermore, mpMRI missed at least one csPCa focus in 34% of patients overall, and in 45% of men with multifocal lesions (Johnson et al. 2019). In whole-gland treatments, knowledge of the presence of csPCa is often sufficient at the patient level, but in FT, accurate information at the lesion level is required to ensure the eradication of all csPCa foci. Another challenge for FT is the tendency of MRI to underestimate the size and extent of prostate tumours, and the degree of underestimation seems to be increased with smaller radiological tumour size and lower PI-RADS scores (Pooli et al. 2021). Priester et al. evaluated the accuracy of MRI in determining the size and shape of localized PCa in 114 men who underwent MRI before RP (Priester et al. 2017). The patient specific moulds were used to correlate images with whole-mount pathology. The study found that PCa foci had an average diameter of 11 mm longer and a volume 3 times greater than T2w MRI segmentations. A similar conclusion was reached by Merisaari and coworkers in a similar type of study, suggesting that 10-12 mm margin in all direction was required to cover the whole tumour (Merisaari et al. 2019).

2.2.5 Traditional imaging modalities

Accurate staging is paramount in PCa, since stage is an important prognostic factor which also drives treatment decisions (Daneshmand et al. 2004). The most important anatomic locations for PCa metastasis imaging are the LNs, bones and extranodal soft tissues. Tumour spread to soft tissues, especially LN, is traditionally assessed with a thorax, abdomen, pelvis CT, or abdominopelvic MRI, which have limited sensitivity of less than 40% (Hövels et al. 2008). Both CT and T1-T2-weighted MRI indirectly assess nodal invasion by using LN diameter and morphology. The sensitivity and specificity of these methods depend directly on the threshold of LN diameter used for suspicious LN. Traditionally, LN with a short axis of more than 8 mm in the pelvis, and more than 10 mm outside the pelvis are considered suspicious for malignancy. Increasing this threshold will improve specificity but at the expense of sensitivity (Mottet et al. 2020). Detection of PCa bone metastases commonly uses methodology with also limited accuracy, such as bone scintigraphy (BS) and CT

(Suh et al. 2018, Jambor et al. 2018) (**Figure 5**). The results of several studies have questioned whether BS is effective for confirming or excluding metastatic bone disease (Even-Sapir et al. 2005). The sensitivity for BS in detection of PCa bone metastasis is only about 50-70% (Venkitaraman et al. 2009, Lecouvet et al. 2007).

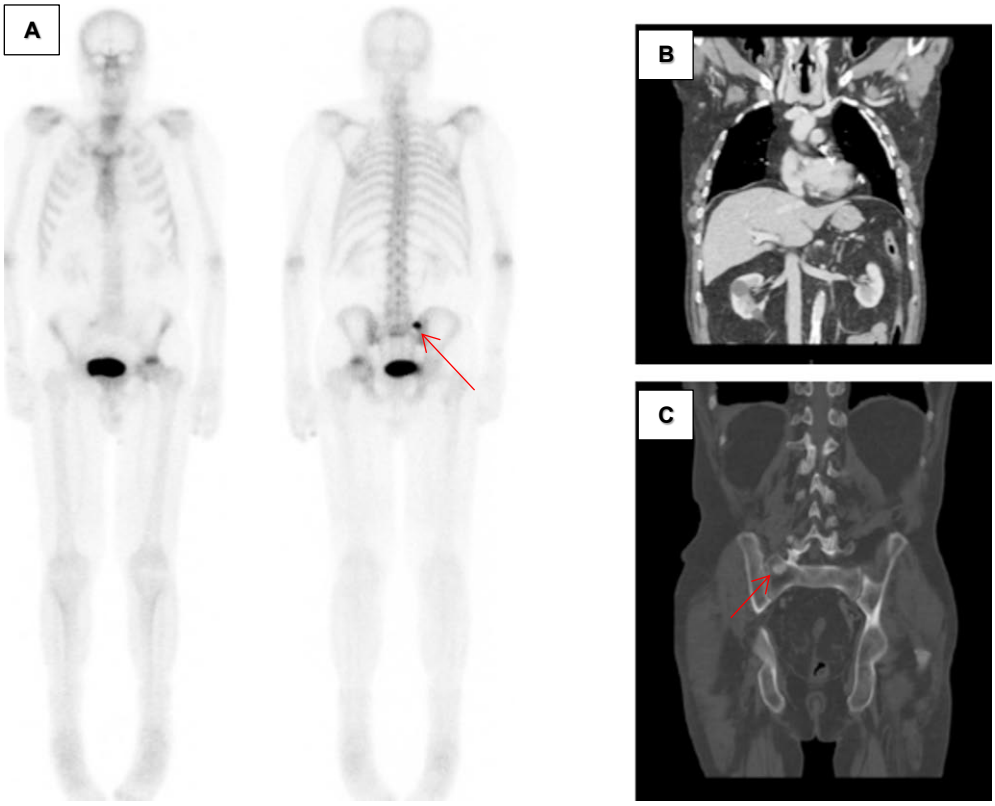

Figure 5. A case example of standard imaging modalities in primary metastasis staging of PCa. Images of the planar bone scintigraphy (BS) (A) and thorax and abdominopelvic coronal CT with (B) and without contrast (C) from a study patient. Note the red arrows pointing to the lesion suspicious for PCa bone metastasis in the sacrum with radiotracer uptake on BS (A) and sclerosis on CT (C).

2.2.6 Advanced imaging modalities

After radical treatment of PCa, many men are diagnosed with metastatic recurrence. This raises the question of whether metastatic spread was already present at the time of initial diagnosis but was not detected by traditional imaging. BS and CT are still used for the detection of distant metastases in primary staging (Mottet et al. 2020). However, these methods are not sensitive or accurate in detecting distant metastases from PCa (Hövels et al. 2008, Suh et al. 2018, Jambor et al. 2016).

The detection of bone metastases in patients with high-risk PCa is significantly improved by single-photon emission computed tomography (SPECT) (Even-Sapir et al. 2004, Jambor et al. 2016) compared with BS (**Figure 6**). The diagnostic accuracy for the interpretation of equivocal bone lesions is also significantly improved by SPECT-CT compared with BS (Helyar et al. 2010). The other imaging modalities with potentially improved accuracy to detect bone metastases include whole-body MRI (wbMRI) and positron emission tomography (PET).

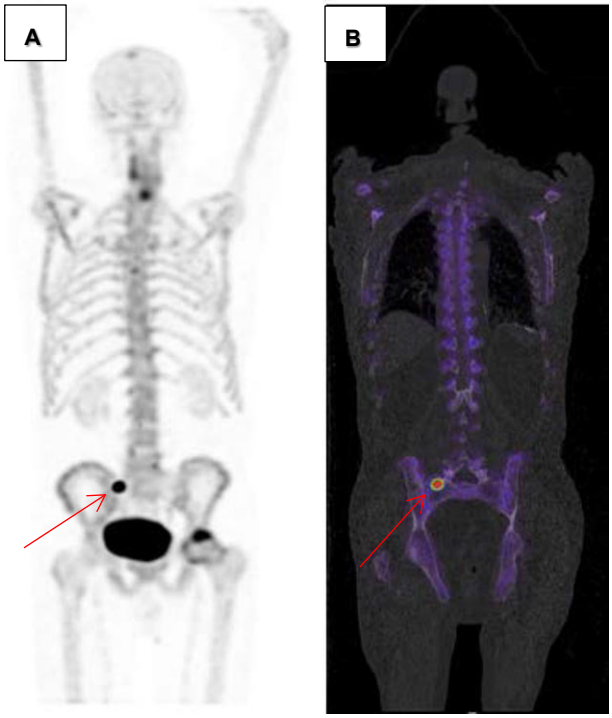

Figure 6. A case example of single-photon emission computed tomography-CT (SPECT-CT) in primary metastasis staging of PCa. Images of the maximum intensity projection **(A)** and SPECT integrated with CT **(B)** from a study patient with high-risk PCa. Note the red arrows pointing to the lesion suspicious for PCa bone metastasis in the sacrum.

wbMRI is an effective tool for overall staging in PCa allowing bone and soft tissue evaluation in a single imaging session (Pasoglou et el. 2014) and has been shown to outperform traditional imaging (combination of BS and CT) in primary staging of high-risk PCa (Lecouvet et al. 2017) (**Figure 7**). wbMRI with and without DWI has shown to significantly improve detection of bone metastases compared to BS (Lecouvet et al. 2007, Jambor et al. 2016). DWI can detect metastases in normal-sized LNs and early intramedullary bone metastases before the appearance of cortical destruction or reactive processes (Thoeny et al. 2014, Komori et al. 2007, Luboldt et al. 2008).

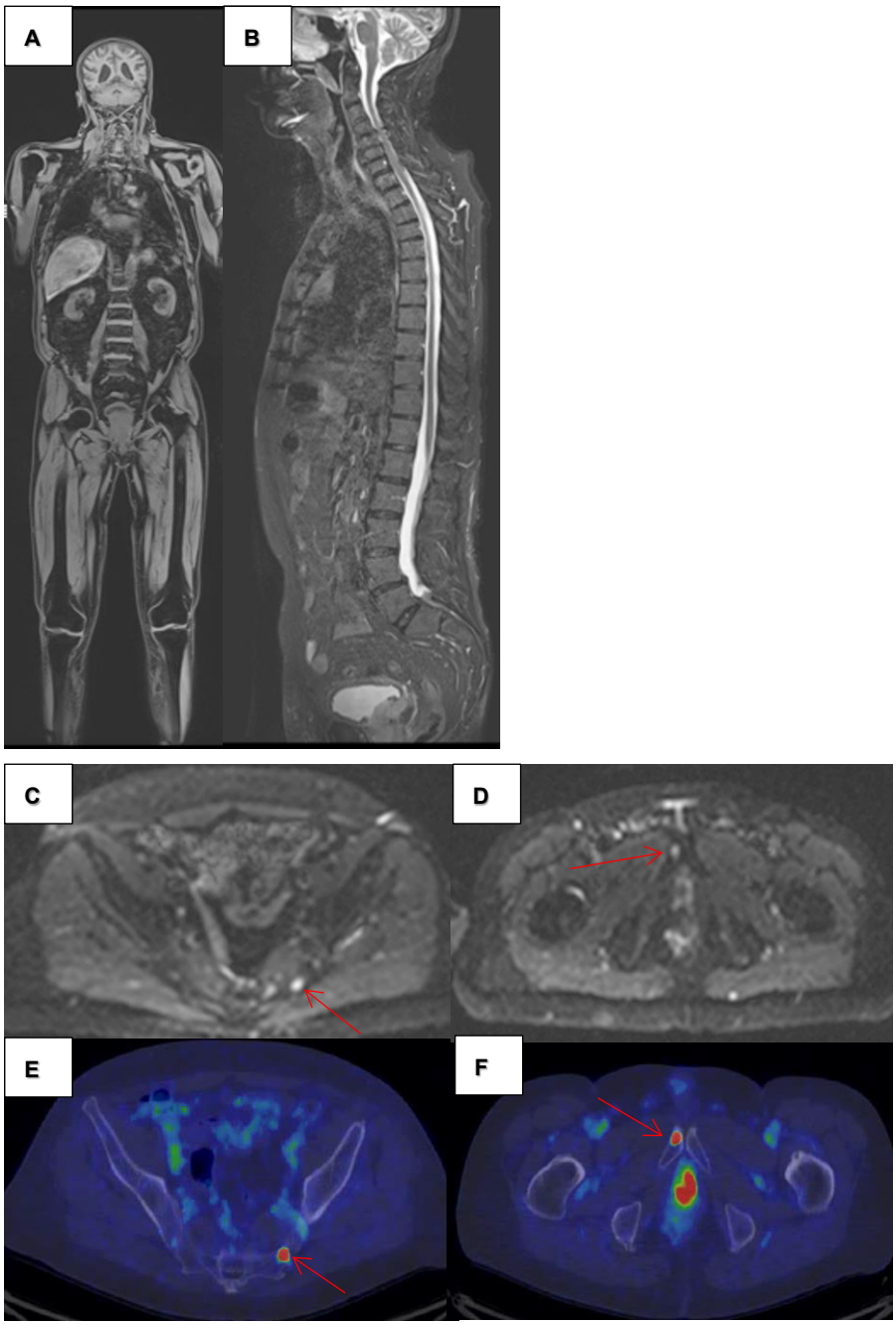

Figure 7. A case example of 1.5T whole-body MRI in primary metastasis staging of PCa. A coronal T1-weighted **(A)** and sagittal T2-weighted **(B)** image from a study patient with high-risk PCa. Diffusion-weighted images show two lesions with diffusion restriction in the left sacral ala **(C)** and right pubic bone **(D)**, both concordant with ^{18}F-PSMA-1007 PET-CT **(E** and **F)**. Note the red arrows pointing to the lesions suspicious for PCa bone metastasis.

PET imaging with various markers based on the demonstration of increased amino acid or lipid metabolism in PCa has increased over the last decades (Wallitt et al. 2017). The value of PET imaging depends on the sensitivity and specificity of used isotope tracer to identify lesions accurately of the imaged tumour type. When bone is imaged with PET, ^{18}F-sodium fluoride has been shown to be a sensitive tracer for the detection of PCa bone metastasis (Even-Sapir et al. 2006, Tateishi et al. 2010). The sensitivity and accuracy of this bone-seeking ligand was shown to the same range that of wbMRI with DWI (Jambor et al. 2016). ^{18}F-sodium fluoride is not capable of detecting soft tissue metastasis and therefore ^{11}C /^{18}F-choline has commonly been combined with ^{18}F-sodium fluoride to include also soft tissues for metastasis staging, although the pooled sensitivity of choline PET-CT for detection of pelvic LN metastasis is modest, only 62% (von Eyben et al. 2014). Both ^{18}F-sodium fluoride and ^{18}F/^{11}C-choline tracers have been lately replaced by tracers targeting prostate-specific membrane antigen (PSMA) (Maurer et al. 2016).

PSMA is an enzymatic trans-membrane protein located on the cell membrane. Approximately 98% of primary tumours and metastases in PCa express this enzyme, the amount of which increases as the degree of differentiation of the disease decreases (Silver et al. 1997, Sweat et al. 1998, Mease et al. 2013, Su et al. 1995, Uprimny et al. 2017). However, despite its name, PSMA is not purely prostate-specific, but is also found in the ganglia (Rischpler et al. 2018), salivary glands, liver, spleen, small intestine, and kidney. Many other benign and malignant tumours may also express PSMA (Sheikhbahaei et al. 2019). Minor PSMA-uptakes are also observed in infections and inflammatory changes. In addition, depending on the PSMA ligand, and the isotope with which it is labelled, due to different secretory pathways, tracer accumulations are seen either in the urinary tract (^{68}Ga-PSMA-11, ^{18}F-DCFPyl) or in the liver and bile ducts (^{18}F-PSMA-1007) (Kesch et al. 2017).

Currently, the most widely used PSMA-tracer ^{68}Gallium-PSMA-11 (^{68}Ga-PSMA-11) has high specificity for PSMA-positive tumour cell allowing evaluation of soft and bony tissue metastases (Eder et al. 2012). ^{68}Ga-PSMA-11 PET-CT can detect different types of bone metastases in PCa patients including osteolytic, osteoblastic and bone marrow metastases (Janssen et al. 2017). ^{68}Ga-PSMA-11 PET-CT has been used primarily in the restaging of patients with BCR (Perera et al. 2020), and this tracer was recently shown to outperform ^{18}F-fluciclovin tracer in restaging of men experiencing BCR after RP (Calais et al. 2019). Several prospective studies have demonstrated improved diagnostic accuracy with ^{68}Ga-PSMA regarding intraprostatic tumour detection (Bahler et al. 2019, Rhee et al. 2016, Kalapara et al. 2020 [retrospective study]), T- and N-staging (Herlemann et al. 2016, van Leeuwen et al. 2017, Yilmaz et al. 2019 [retrospective study], van Kalmthout et al. 2020) also in the primary staging. Recently, a multicentre RCT reported superiority of ^{68}Ga-

PSMA-11 PET-CT over conventional imaging in primary staging of high-risk PCa (Hofman et al. 2020).

Lately, the novel ^{18}F-labeled PET tracers, DCFPyl and PSMA-1007, have been developed as a promising PSMA targeting ligands for PCa imaging (Kesch, Vinsensia et al. 2017, Giesel et al. 2018, Cardinale et al. 2017) (**Figure 8**). The half-life of ^{18}F-PSMA-1007 is longer than that of ^{68}Ga-PSMA (Kesch et al. 2017) and it offers superior energy characteristics with smaller average positron range and higher image resolution. ^{18}F-PSMA-1007 is primarily eliminated via the hepatobiliary excretion route leading to less urinary tract activity which may improve local and pelvic nodal staging compared to ^{68}Ga-PSMA (Kesch et al. 2017, Privé et al. 2020). ^{18}F-PSMA is also cyclotron produced, allowing centralized production in larger quantities and long-distance transport, which could provide a more practical option for PCa imaging (Kesch et al. 2017).

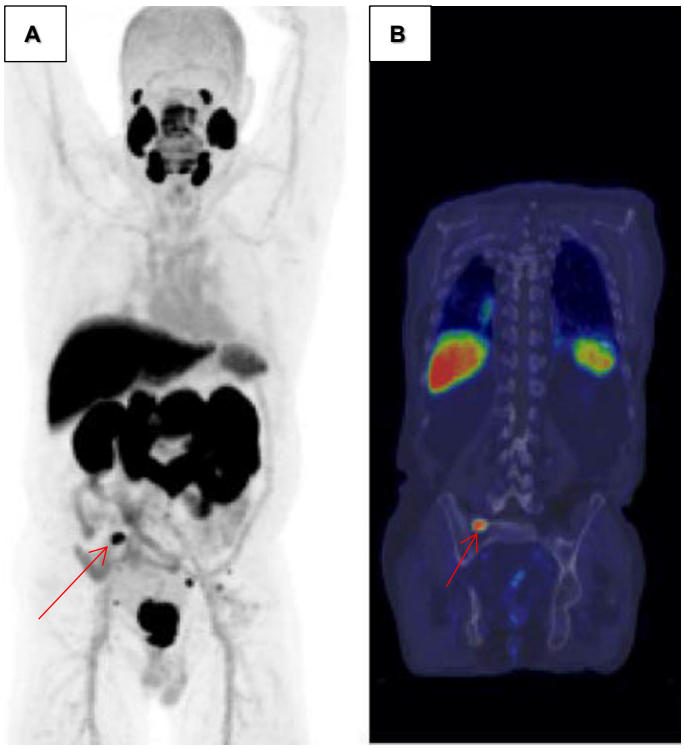

Figure 8. Maximum intensity projection **(A)** and fused image of ^{18}F-PSMA-1007 PET-CT **(B)** in a study patient. Note the red arrows pointing to the lesion suspicious for PCa bone metastasis in the sacrum. Normal physiological uptake areas are shown in the image A including lacrimal and salivary glands, liver, spleen, bowel, kidneys, bladder and sympathetic ganglion.

2.2.7 Current practise in initial staging

The field of metastasis staging of PCa with novel and more sensitive imaging methods is evolving rapidly enabling earlier detection of metastatic disease. The ultimate benefit of earlier metastasis detection upon prognosis, patient management, and survival has yet to be established. For these reasons CT and BS are still the methods of choice for metastasis staging in men with newly diagnosed unfavourable intermediate and high risk PCa (Mottet et al. 2020).

2.3 Treatment of localized PCa

2.3.1 Standard radical treatment methods

Increased public and professional awareness of PCa, improving diagnostic methods and screening of men with PSA are all attributable to earlier detection of PCa with more favourable disease characteristics (Albertsen et al. 2005, Cooperberg et al. 2005, Fenton et al. 2018). Because many diagnosed PCa are indolent and the risk of progression is low, and to reduce overtreatment and possible subsequent genitourinary morbidity, low risk cases are increasingly treated with active surveillance (AS). The idea of AS is the concept of deferred treatment strategy, where a patient with reasonably good life expectancy (> 10 years) is followed up regularly and definitive curative intent treatment is given in the case of disease progression. AS should be distinguished from passive surveillance, in other words watchful waiting, which refers to conservative management for a patient deemed unsuitable for curative treatment. Typically, it is offered for men with comorbidities, life expectancy < 10 years, and in more advanced disease stages. These patients are monitored for the development of local or systemic progression with disease-related morbidity at which stage they are then treated palliatively according to their symptoms.

There are some variation and heterogeneity related to AS protocols in terms of patient selection and eligibility, follow-up policies, reclassification criteria and outcome measures triggering active treatment (Godtman et al. 2012, Klotz et al. 2015, Tosoian et al. 2015). PRIAS (Prostate cancer Research International: Active Surveillance) protocol is the most used AS program in Finland with the following inclusion criteria: men fit for curative treatment, PSA at diagnosis < 10 ng/ml, PSA density < 0.2, ≤ 2 biopsy cores involving PCa, ISUP GG 1 and digital rectal examination T1c ≤T2. These inclusion criteria for AS are also currently generally accepted, although good results have also been achieved with ISUP GG 2 PCa in men over 70 years of age (Klotz et al. 2015). Follow-up protocol in PRIAS is intensive including regular PSA testing, digital rectal examination and repeated

prostate biopsies. Nowadays prostate MRI is recommended for men undergoing AS (Mottet et al. 2020). Results from PRIAS study demonstrated that after 10 years of follow-up, 27% of patients continued in AS, while the others discontinued due to the following reasons: reclassification (41%), anxiety/patient request (5%), switch to passive surveillance or death from another cause without reclassification (15%) and discontinuation for other reasons without reclassification (12%) (Bokhorst et al. 2016). Although no formal RCT is available comparing AS to standard treatment in men with screening-detected low-risk PCa, the results from prospective and retrospective cohorts including over 4500 patients have shown excellent 10-year overall survival and cancer-specific survival of 93% and 100%, respectively (Mottet et al. 2020).

The traditional radical treatments for localized PCa include RP and RT. RP is the only treatment modality that has been shown to reduce metastatic progression and to improve survival in the RCT setting (Bill-Axelson et al. 2018). Scandinavian Prostate Cancer Group study number 4 (SPCG-4) randomized 695 patients with localized PCa to undergo watchful waiting (WW) or RP. During 29 years of follow-up, 292/348 men in the WW group and 261/347 men in the RP group had died. Significantly lower mortality was observed in the RP group, both overall mortality (relative risk [RR] 0.74, 95% CI 0.62-0.87) and cancer-specific mortality (RR 0.55, 95% CI 0.41-0.74). At 23 years, a mean of 2.9 extra years of life were gained with RP. In another RCT, the Prostate Cancer Intervention versus Observation Trial (PIVOT), RP and WW were also compared in localized PCa (Wilt et al. 2017). However, during almost 20 years of follow-up (median 12.7 years) no overall survival or cancer-specific survival benefit for RP was shown. The difference in the results of these two RCT studies may be explained by the fact that there were more low-risk and comorbid patients in the PIVOT study than in the SPCG study. In addition, PIVOT recruited patients in the PSA testing era (1994-2002), while SPCG-4 included patients before the PSA testing era. To date only one RCT has compared RP to RT and non-formal AS, including repeated PSA testing, in the treatment of localized PCa. Prostate cancer Testing for Cancer and Treatment (ProtecT) trial randomized 1643 men to undergo AS (545 men), RT (545) and RP (553) (Hamdy et al. 2016, Neal et al. 2020). At a median of 10 years follow-up, there were no statistically significant differences in cancer-specific survival or overall survival among the treatment modalities. However, RP and RT were associated with lower rate of disease progression and metastases than AS.

RT is a well-established primary treatment for localized PCa (Neal et al. 2020, Bolla et al. 2010). Recent technological advances have improved the safety and efficacy of RT, allowing an increase in radiation dose to the tumour while sparing critical surrounding structures (Mottet et al. 2020). External beam RT with intensity-modulated RT (IMRT), with or without image-guided RT (IGRT), is the gold

standard of RT for PCa. Dose escalation to 74-80 grays (Gy) has been shown to improve 5-year BCR free survival by several RCT (Mottet et al. 2020), and also overall survival in men with intermediate- or high-risk PCa by a non-randomized propensity-matched retrospective analysis including a total of 42.481 patients (Kalbasi et al. 2015). The combination of RT with ADT has proven its superiority over RT alone followed by deferred ADT on relapse. The role of ADT depends on the risk stratification of the disease. 2- to 3-year ADT is recommended in high-risk disease (Bolla et al. 2010), while 4-6 months is considered sufficient in intermediate-risk disease (Jones et al. 2011).

Low-dose-rate brachytherapy, in which radioactive seeds are permanently implanted into the prostate, has been used to treat PCa with or without external beam RT. However, high-dose-rate brachytherapy (HDR-BT), in which radioactive source is temporarily introduced into the prostate to deliver radiation, provides a more promising treatment option for external beam RT of PCa. It can be delivered in a single or multiple fraction and is often combined with external beam RT to achieve dose escalation for the prostate and to avoid radiation injury of surrounding tissues (Mottet et al. 2020). RT is also used as a part of multimodality treatment approach in locally advanced PCa, but also as an adjuvant or salvage treatment with or without ADT following RP for patients with high-risk features and/or BCR.

Diagnosis of PCa and passive nature of AS can both lead to psychological burden affecting to treatment decisions and pushing men with low-risk disease to pursuing radical therapy (Reeve et al. 2012, Taylor et al. 2018). Standard therapy for localized PCa including RP and RT provide proven cancer control and improved survival, but at the expense of treatment related adverse effects to genitourinary and bowel function (Sanda et al. 2008, Resnick et al. 2013, Donovan et al. 2016, Matta et al. 2019). Data from a population-based cohort study (Prostate Cancer Outcome Study) on men diagnosed with localized PCa in the mid-1990s and followed prospectively for 15 years was used to compare functional outcomes after RP and RT. Depending on the timepoints of 15-years of follow-up, severe urinary incontinence, characterized by no control or frequent urinary leakage, varied between about 10-18% in men receiving RP and 3-9% in men receiving RT. The corresponding percentages for severe erectile dysfunction, characterized by erections insufficient for intercourse, were about 75-87% in RP group and 61-94% in RT group. In addition, up to 36% of RT-treated men experienced bowel urgency and up to 16% of bowel frequency/pain/urgency (Resnick et al 2013). It should be noted that in addition to treatment modality and the technique used, the risk of functional impairment is also affected by age, baseline health status, sexual and urinary function before treatment, and nerve-sparing among other factors. In the systematic review De Carlo et al. compared surgical, functional and oncological outcomes of open RP, laparoscopic RP and robot-assisted laparoscopic prostatectomy (RALP) (De Carlo

et al. 2014). The study reported that 17-29% of men had some level of urinary incontinence, while 19-56% of men had erectile dysfunction at 12 months after RP. The study confirmed the well-known perioperative advantages of laparoscopic RP and RALP, but the data was insufficient to prove the superiority of any surgical approach regarding functional and oncological outcomes. These results were also supported by the recent Cochrane review (Ilic et al. 2017). Intra- and peri-operative complications of open RP, laparoscopic RP and RALP are well reported by Ramsay et al. in their systematic review (Ramsay et al. 2012, Mottet et al. 2020). Depending on the surgical technique, the perioperative complications included bladder neck contracture (1-9%), anastomotic leak (1-4.4%), infection (0.8-4.8%), organ injury (0.4-2.9%), ileus (0.3%-2.4%) and deep venous thrombosis (0.2-1.4%) (**Table 6**). Late complications related to RT include gross haematuria (10-14%), rectal bleeding (19-28%), and urinary obstruction (6-9%) (Matta et al. 2019).

Table 6. Intra- and peri-operative complications of retropubic radical prostatectomy (RRP), lapascopic radical prostatectomy (LRP) and robot-assisted laparoscopic prostatectomy (RALP) (Modifed from Mottet et al. 2020 [adapted from Ramsay et al. Health Technol Assess 2012]).

Predicted probability of event	**RALP (%)**	**Laparoscopic RP (%)**	**RRP (%)**
Bladder neck contracture	1.0	2.1	4.9
Anastomotic leak	1.0	4.4	3.3
Infection	0.8	1.1	4.8
Organ injury	0.4	2.9	0.8
Ileus	1.1	2.4	0.3
Deep-vein thrombosis	0.6	0.2	1.4
Predicted rates of event	**RALP (%)**	**Laparoscopic RP (%)**	**RRP (%)**
Clavien I	2.1	4.1	4.2
Clavien II	3.9	7.2	17.5
Clavien IIIa	0.5	2.3	1.8
Clavien IIIb	0.9	3.6	2.5
Clavien IVa	0.6	0.8	2.1
Clavien V	< 0.1	0.2	0.2

2.3.2 Ablative therapy

In addition to conventional therapy including RP, external beam RT and brachytherapy, other treatment modalities have emerged as potential therapeutic options for patients diagnosed with localized PCa. Minimally invasive ablative therapy may offer an effective and safer alternative for selected patients with PCa (**Figure 9**).

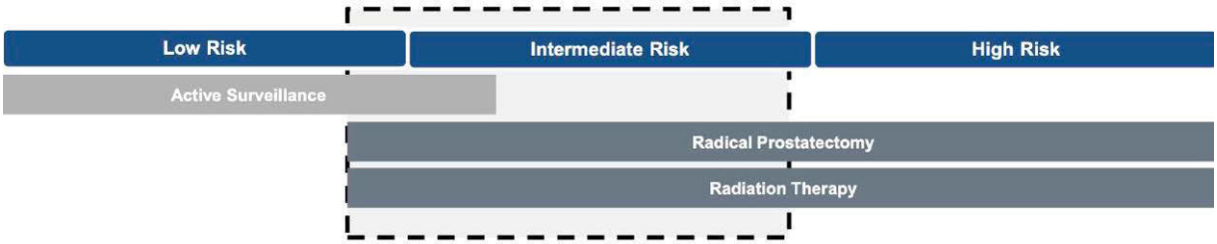

Figure 9. The dotted box illustrates "the sweet spot" for ablative therapy (Courtesy of Profound Medical Inc)

This is typically achieved by directing tissue-destroying energy to the prostate without incision through natural body channels (rectum and urethra) or perineum. Most ablative methods use thermal energy to ablate prostate tissue, typically heating prostate tissue with radiofrequency, laser or high-intensity focused ultrasound (HIFU) energy (Chu et al. 2014, Valerio et al. 2018). Some modern heat-based treatment systems exploit real-time MRI for guiding therapy into targeted regions (Woodrum et al. 2018). While ablative therapy is increasingly utilized in PCa management, they are still considered experimental due to insufficient evidence confirming their longer-term oncological efficacy (Van der Poel et al. 2018).

HIFU

Since 1990, transrectal HIFU has been investigated for the whole-gland (Crouzet et al. 2014) and focal treatment of primary (Rischmann et al. 2017, Stabile et al. 2019) and radiorecurrent PCa (Reddy et al. 2020). Some preliminary experience has also been obtained for salvage HIFU in the treatment of local recurrence after RP (Asimakopoulos et al. 2012). HIFU exploits thermal energy for tissue ablation. By rapidly raising temperature over 60°C using focused high-intensity ultrasound beam, the target tissue undergoes coagulation necrosis primarily due to hyperthermia and acoustic cavitation (Van Leenders et al. 2000, Biermann et al. 2010). In contrast to older generation devices that used ultrasound to guide and monitor treatment, modern devices utilize in-bore MRI guidance or MRI-transrectal ultrasound fusion software (Napoli et al. 2013). Crouzet and colleagues published whole-gland HIFU results from a largest prospective cohort of 1002 patients with localized PCa in 2014 (Crouzet et al. 2014). 60% of patients received a single HIFU session, while 38% received two sessions and 2% three sessions. Eight-year BCR free survival rates were 76%, 63%, and 57% for low-, intermediate-, and high-risk patients, respectively. At 10 years, the cancer-specific survival and metastasis-free survival rates were 97% and 94%, respectively. The administration of ADT to downsize the prostate prior to HIFU is a potential bias in survival analysis. During the study

period, severe incontinence and bladder outlet obstruction decreased with improvement of the technology, from approximately 6% and 35% to 3% and 6%, respectively. Potency was preserved in approximately 53% of younger previously potent patients. The main adverse event associated with HIFU in the whole-gland treatment of primary localized PCa include acute urinary retention (10%), erectile dysfunction (23%), urethral stricture (8%), rectal pain or bleeding (11%), recto-urethral fistula (5%) and urinary incontinence (10%) (Ramsay et al 2015).

Cryotherapy

Cryotherapy also utilizes thermal energy, but in this case extreme cold temperatures, to ablate prostate tissue by a number of mechanisms such as osmotic injury, cytolysis, apoptosis and vascular damage. Freezing of the prostate is performed through 17-gauge cryoneedles positioned in the target through the perineum under TRUS guidance. A given distance between needles form a homogenous ice ball with no gaps in the middle. Traditionally, two freeze-thaw cycles are used resulting in an ablative temperature of -40°C in the midgland and at the neurovascular bundle. Placement of thermosensors at the level of the external sphincter and rectal wall and insertion of a urethral warmer ensure protection of these organs. Cryotherapy has been investigated for whole-gland (Oishi et al. 2019) and more recently for FT of primary (Shah et al. 2019) and radiorecurrent (Reddy et al 2020) PCa, and has been shown to be safe and to provide acceptable medium-term oncological outcomes. The main adverse effects related to this method in the whole-gland treatment of primary localized PCa include erectile dysfunction (18%), urinary incontinence (2-20%), urethral sloughing (0-38%), rectal pain and bleeding (3%) and recto-urethral fistula formation (0-6%) (Ramsay et al. 2015).

Photodynamic therapy

Photodynamic therapy is based on the activation of a vascular photosensitizer within the prostate, leading to the formation of superoxide and hydroxyl radicals causing vascular occlusion and subsequent coagulation necrosis of the targeted tissue. In this method laser activating fibres are positioned transperineally in the prostate, and the photosensitizer is administered intravenously. Photodynamic therapy has been evaluated in the treatment of localized PCa (Gill et al. 2018).

Other ablative methods

Other ablative treatment options, such as laser interstitial thermotherapy, irreversible electroporation and radiofrequency ablation, have also been utilized for the treatment

of localized PCa, but they are in the early phase of evaluation with limited amount of data available. Laser interstitial thermotherapy uses direct thermal energy, in which the laser fibres are positioned transperineally or transrectally in the prostate. Irreversible electroporation employs high voltage low energy electric current and radiofrequency ablation uses medium frequency alternating current to ablate targeted tissue. In all cases, this is accomplished by inserting needles through the perineum into the prostate under TRUS guidance (Valerio et al. 2017).

Ablative therapy as a salvage intervention

As previously described, ablative therapy has also been investigated in the salvage setting, most commonly in the treatment of local recurrence after primary RT. Despite improvements in RT techniques, up to half of all men undergoing RT will still experience BCR, which is estimated to remain localized in the majority of cases (Zumsteg et al. 2015). However, even if the recurrence remains local, 98% of patients will receive ADT, which is not curative and has harmful side effects (Tran et al. 2014). Salvage RP is known to offer proven oncological control, but is a technically demanding procedure offered at limited centres for carefully selected favourable-risk patients. It carries a high risk of complications and an increased likelihood of adverse functional outcome (Chade et al. 2012). Because of invasiveness of the salvage RP, many patients are ineligible due to comorbidities. As a result, studies of various alternative ablative techniques in the treatment of locally radiorecurrent disease have been conducted including HIFU (Crouzet et al. 2017), cryotherapy (Siddiqui et al. 2016), brachytherapy (Tisseverasinghe et al. 2018), along with preliminary results from focal reirradiation stereotactic body RT (Maenhout et al. 2017, Jereczek-Fossa et al. 2019) and focal irreversible electroporation (Scheltema et al. 2017), all of which carry their own deficiencies in terms of oncological control and/or toxicity (Peters et al. 2013). Ablative techniques with most experience, including HIFU, cryotherapy and brachytherapy have an estimated risk of BCR between 31% to 42% and are also associated with increased risks of complications and genitourinary and gastrointestinal toxicity (Ingrosso et al. 2020).

2.3.3 Focal therapy (FT)

Because of the significant risk of toxicity associated with whole-gland treatments and the earlier diagnosis of PCa leading to the identification of smaller tumours that cover only a small portion of the prostate with a greater propensity for unifocal and/or unilateral disease, the concept of FT has gained interest (Donaldson et al. 2015, Postema et al. 2016, Tay et al. 2017, Tay et al. 2019). New ablative

technologies such as cryotherapy, HIFU, photodynamic therapy, irreversible electroporation and focal RT with brachytherapy or CyberKnife ® Robotic Radiosurgery System technology (Accuray Inc., Sunnyvale, Ca, USA), have emerged in the past decades enabling focal treatment of PCa. The novel technology of MRI-guided transurethral ultrasound ablation (TULSA), the method under investigation in this thesis, is described more detailed in the next section. FT strives for a tissue preservation strategy to provide the best compromise between oncological control and morbidity. The main objective is to eliminate clinically significant tumour with a margin, when applicable, while preserving as much tissue as possible to lower the risk of complications and to maintain genitourinary function. The key structures for the protection of functionality include neurovascular bundles, external sphincter, bladder neck, urethra and rectum (**Figure 10**).

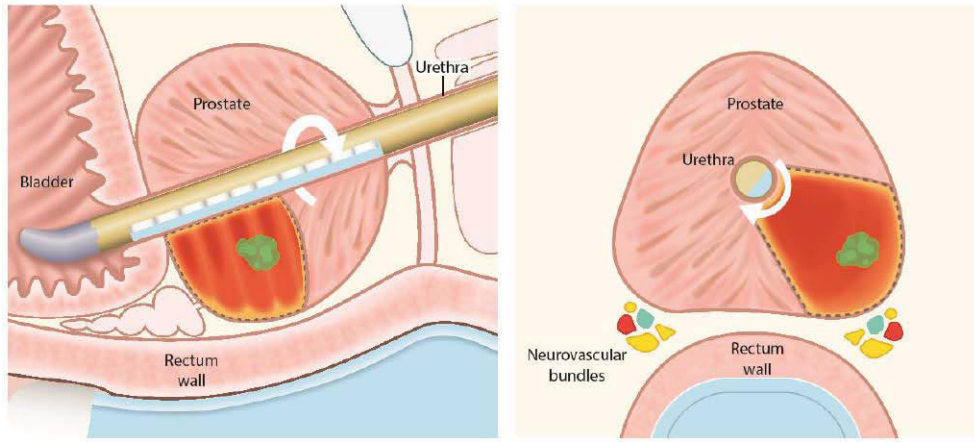

Figure 10. The concept of focal therapy is illustrated using MRI-guided transurethral ultrasound ablation (TULSA) as an example for targeted quadrant ablation of unifocal tumour (marked in green) with treatment margins. The goal is tissue-sparing eradication of the clinically significant tumour while preserving vital organs surrounding it. Fluid circuit in the transurethrally-inserted ultrasound applicator and endorectal cooling device protects these organs from thermal injury (Courtesy of Profound Medical Inc).

Even though PCa is often multifocal, evidence indicates that the clinical outcome of PCa is determined predominantly by the index lesion, and secondary low-grade lesions appear to have an indolent behaviour (Ahmed et al. 2012, Algaba et al. 2010, Arora et el. 2004, Karavitakis et al. 2011, Wise et al. 2002). Disease characterization and localization at a regional level have improved significantly due to the advent of mpMRI resulting in more accurate risk stratification. The accuracy of mpMRI with targeted prostate biopsy for the detection of the index lesion is over 90%, and for the exclusion of the clinically significant lesions also over 90% (Fütterer et al. 2015). With modern molecular imaging, in particular PSMA PET, exclusion of

extraprostatic disease is more reliable (Hofman et al. 2020), and promising results have also been obtained from intratumoral detection and local staging (Rhee et al. 2016).

Valerio et al. summarized the evidence regarding the effectiveness of FT in localized PCa (Valerio et al. 2017). In their systematic review including data from 3230 patients across 37 studies covering HIFU, cryotherapy, photodynamic therapy, laser interstitial thermotherapy, focal brachytherapy, irreversible electroporation and radiofrequency ablation, it was shown that FT has a favourable toxicity profile but its oncological effectiveness remains unproven due to lack of comparative studies against standard therapy. To date, there is only one RCT available for FT (Gill et al. 2018). Gill and co-workers compared FT using padeliporfin-based vascular-targeted photodynamic therapy to AS in men with low-risk PCa. At a median follow-up of 24 months, they reported superior progression free survival rate in the photodynamic therapy arm over AS arm (adjusted hazard ratio: 0.34, 95% CI 0.24-0.46) with fewer patients needing radical treatments in the photodynamic therapy arm (6% and 29%, $p<0.0001$). These benefits were maintained after four years according to updated results (Gill et al. 2018). The main limitations of the study included comparison to AS, which lacked any repeated biopsies or prostate MRI and active treatment of very low-risk patients. In addition, limitation included unusually high progression rate in AS arm (58% in two years) and more patients in the AS arm undergoing radical treatments without clinical indication.

With the onset of mpMRI and PSMA PET imaging, and their capability to isolate radiorecurrent disease, focal salvage therapy has also gained popularity (Duijzentkunst et al. 2016). Cryotherapy has been used primarily for recurrent anterior tumours because it offers less spatial control. In addition, the organ-protective warming tool may impair the effectiveness of treatment in apical and periurethral tumours (Van Son et al. 2018, Ganzer et al. 2018). HIFU meanwhile is used more often for posterior tumours, since it is delivered transrectally. However, anterior tumours may be challenging to treat with HIFU (Ingrosso et al. 2020).

2.3.4 MRI-guided transurethral ultrasound ablation (TULSA)

TULSA is a newer technology, which combines real-time MRI guidance, thermal ultrasound and closed-loop temperature feedback control to provide customizable incision-free prostate ablation (**Figure 11** and **Figure 12**). The entire procedure takes place in the MRI suite with the patient preferably under general anaesthesia, although spinal anaesthesia has also been used (Chopra et al. 2012).

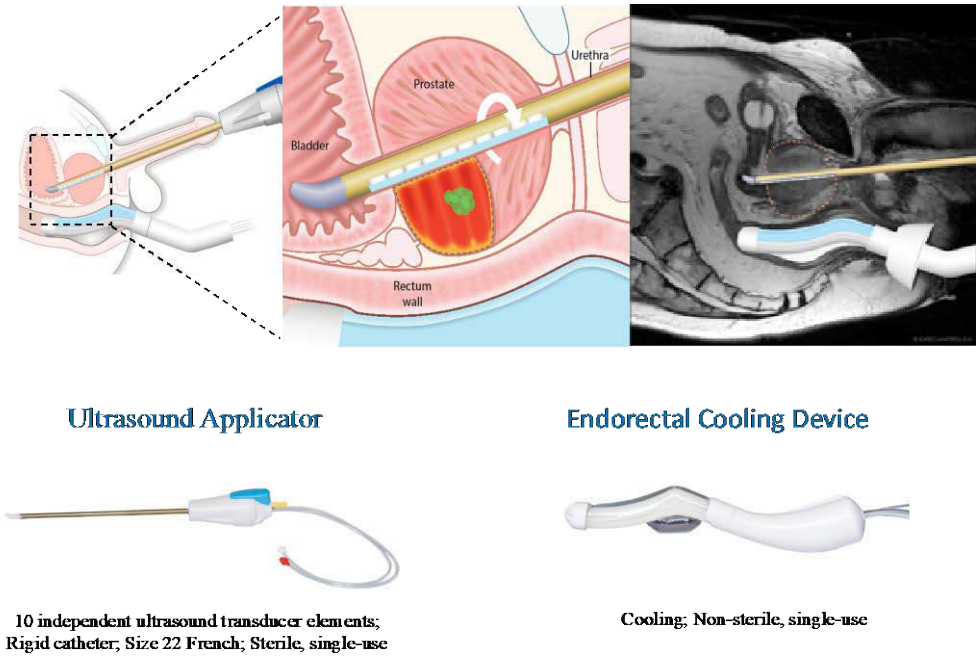

Figure 11. Instruments and operation of the TULSA device: the transurethrally inserted ultrasound applicator and endorectal cooling device in place. Inside-out ultrasound energy is delivered using an unfocused (directional) high-intensity ultrasound beam directed from the acoustic window of ultrasound applicator within prostatic urethra to the targeted prostatic tissue. Ablation volume is planned using MRI images acquired on treatment day and ablation progress is monitored in real-time using MRI-thermometry. Endorectal cooling device protects the rectal wall from thermal injuries (Courtesy of Profound Medical Inc).

TULSA utilizes transurethrally-delivered high intensity directional ultrasound to thermally ablate prostate tissue. By rapidly raising and maintaining elevated tissue temperatures above 55°C within the prescribed region, the target tissue is destroyed by undergoing acute coagulation necrosis (Boyes et al. 2007) (**Figure 12**). This is followed by delayed thermal injury, which depends mainly on cumulative thermal dose (Sapareto et al. 1984), which is measured and displayed in real-time from the MRI-thermometry acquired during treatment. Correlation between a thermal dose of 240 cumulative equivalent minutes at 43°C (CEM) with delayed migration of the outer limit of thermal injury up to 3mm beyond the region of acute coagulation necrosis within two days after ablation, has been shown in pre-clinical studies (Burtnyk et al. 2015, Siddiqui et al. 2010). The ablated volume is confirmed immediately post-treatment on CE-MRI as a non-perfused volume indicating complete cell death (Böni et al. 1997, Rouvière et al. 2001, Rosset et al. 2017). The acute non-perfused volume is surrounded by the rim of enhancement indicating the

outer limit of thermal injury, which represents an uncertain area where some tissue is irreversibly destroyed and some survives.

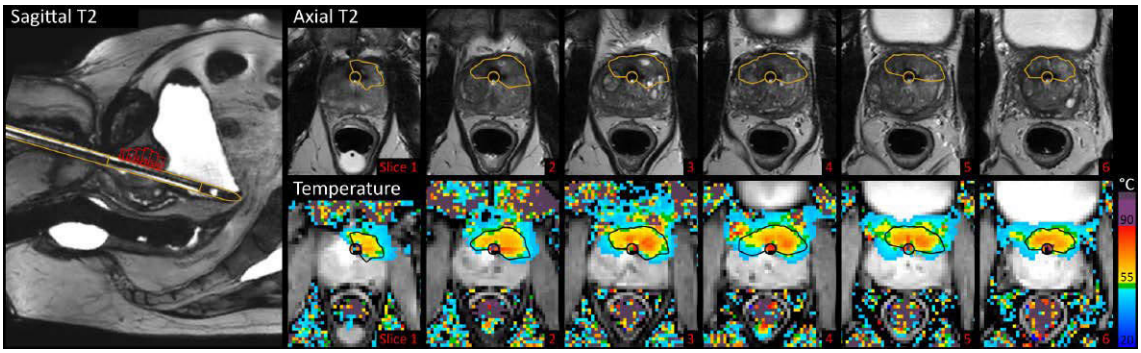

Figure 12. Treatment-day MRI-images of the TULSA-treated study patient. On the left, a sagittal MRI-image of the pelvic area with the instruments in place. In the top right row, the treatment area (yellow boundary) is contoured on T2-weighted axial images. Each axial image corresponds to one transducer element in the ultrasound applicator. Real-time magnetic resonance thermometry images are acquired from the area of each transducer element (red bars 1-6 in the sagittal image) to monitor changes in the temperature during treatment. The treatment delivery system utilizes this information by modifying the rotational speed, ultrasound frequency and energy, so that the tissue-destroying temperature is precisely limited to the pre-planned treatment area (from original publication I).

TULSA technology has been developed since the early 2000s through rigorous preclinical studies, which at first focused on *in vivo* evaluation of MRI-compatible robotics, transurethral directional ultrasound applicators, MRI-thermometry and the feedback control algorithm. Chopra and co-workers were one of the first to investigate various interstitial ultrasound applicators for MRI-guided thermal ablation. They developed one of the first MRI-compatible transurethral multi-element heating applicator incorporated to a temperature feedback control algorithm to enable conformal thermal ablation of prostate gland with high spatial and temporal accuracy of the heating pattern (Chopra el al. 2001, Chopra et al. 2003, Chopra et al. 2005, Tang et al. 2007, Chopra et al. 2008, Burtnyk et al. 2009, Burtnyk et al. 2010, Siddiqui et al. 2010). Preclinical canine studies with treat-and-immediate-resect (Boyes et al. 2007, Chopra et al. 2009, Siddiqui et al. 2010) and treat-and-delayed-resect settings (Burtnyk et al. 2015) have both shown the feasibility and safety of this technique to generate accurate thermal coagulation of prostate tissue with ablation margins of ± 3mm and ablation accuracy of ± 1.5 mm on histology with urethral protection and no unintended damage on periprostatic tissues on acute or 28 day time-points (Boyes et al 2007, Chopra et al 2009, Siddiqui et al. 2010, Burtnyk et al. 2015).

The first treat-and-immediate-resect study in humans was also performed by the Chopra research group (Chopra et al. 2012). In this proof of concept study, eight men with localized PCa who had been selected to undergo RP were included. Prior to surgery, the prostate was ablated with a single element using extremely conservative margin without a therapeutic intent with a prototype of the current TULSA system under spinal anaesthesia. The study showed that the method is safe and feasible for prostate ablation with spatial targeting accuracy of -1.0 mm ± 2.6. Histopathology was compared to MRI-thermometry acquired during treatment, indicating that 55°C at the boundary of the planned treatment region corresponded to the edge of acute coagulation necrosis.

In another treat-and-immediate-resect study using a similar prototype, Ramsay et al. investigated the applicability of the method in FT of PCa using histopathology as a comparison (Ramsay et el. 2017). The study included five men who had been diagnosed with MRI-visible organ-confined PCa and who were scheduled to undergo tumour-targeted ablation immediately prior to RP. Comparison of whole-mount histological sections parallel to the MRI treatment planes showed treatment accuracy of -0.4 ± 1.7 mm and spatial targeting accuracy of -1.5 ± 2.8. All targeted index tumours were inside the histological outer limit of thermal injury. This was also the first clinical study to demonstrate the capability of cytotoxic heat, and subsequent acute coagulation necrosis on histology, to reach the prostate capsule.

The first phase 1 clinical study investigating whole-gland ablation for therapeutic purposes in 30 men with mostly low-risk PCa, using the now CE-marked commercial TULSA system, was published by Chin et al. in 2016 (Chin et al. 2016). For safety reasons 3-mm margins sparing 10% of peripheral prostate tissue was mandatory. This pivotal study confirmed the safety and feasibility of the method in the treatment of localized PCa. The reported spatial ablation precision of ± 1.3 mm on MRI-thermometry was in line with the previous studies. A fairly favourable safety profile was demonstrated and TULSA-related Common Terminology Criteria for Adverse Events included haematuria (43% grade 1; 6.7% grade 2), urinary tract infections (33% grade 2), acute urinary retention (10 % grade 1; 17% grade 2) and epididymitis (3.3% grade 3). There were no rectal injuries observed. At the 12-month follow-up, the treatment was well tolerated with overall minor impact on sexual and urinary function with no bowel-related toxicity observed. The median reduction in PSA from baseline to nadir was 90%, which was consistent with the planned 90% ablation volume of the total prostate. As expected, due to conservative treatment margins, 9/29 of patients had csPCa and 16/29 of patients had any PCa on biopsies at one year of treatment.

Based on the meticulous quantitative analysis of the treatment day and 12-month MRI measurements from these 29 of 30 TULSA-treated patients, Bonekamp et al reported the median prostate volume reduction of 88% at 12 months, which was in

excellent agreement with the planned ablation volume and measured thermal ablation volume using 240 CEM thermal dose isocontour (Bonekamp et al. 2018). On the contrary, immediate post-treatment non-perfused volume predicted only 53% volume reduction, and underestimated acute thermal ablation volume (55°C isotherm) and delayed thermal ablation volume (240 CEM thermal dose isocontour) by 36% and 51%, respectively (Bonekamp et al. 2018).

3-year outcomes of this phase 1 study were recently reported by Nair et al. (Nair et al. 2020). No new severe adverse event occurred between 1 and 3 years. Functional ability was maintained at 3 years with leak-free, pad-free continence of 100% (22/22 patients) and erections sufficient for penetration (International Index of Erectile Function [IIEF] Q2 ≥2) of 50% (11/22 patients) at 3 years. Per-protocol systematic prostate biopsies were performed 1 and 3 years after TULSA treatment. A total of 10/29 patients had csPCa and 17/29 patients had any cancer on biopsies at 3 years, all but two of whom were diagnosed at one-year biopsies. However, 3/22 patients refused biopsy at 3 years. By 3 years, seven patients had received salvage therapy including six salvage RP without major complications. Nair et al. included four of these cases in their report on the feasibility and efficacy of salvage open RP for recurrent PCa following TULSA (Nair & Stern et al. 2020). No perioperative complications occurred and no major technical difficulties were encountered during the operations. Intraoperatively some fibrotic reaction of endopelvic and Denonvilliers fascia was observed. Whole-mount histopathology sections confirmed persistent PCa mainly in the untreated peripheral safety region with positive surgical margins in two patients who subsequently received salvage radiation and one of them in addition long-term ADT. All patients had reduced erectile function after surgery requiring medication, and one patient received an artificial urinary sphincter.

In addition to above studies, a retrospective subgroup analysis of this same phase 1 patient population was performed on nine patients with symptomatic concomitant benign prostatic obstruction in addition to local PCa (Elterman et al. 2020). At 12 months after TULSA International Prostate Symptom Score (IPSS) improved by 58% to 6.3 ± 5.0 (p=0.003), with at least a moderate (≥ 6 points) reduction in 8/9 patients. Also, IPSS QoL improved in 8/9 patients. In five patients who experienced more severe symptoms maximum flow rate increased from 11.6 ± 2.6 ml/s to 22.5 ± 14.2 ml/s at 12 months. These retrospective results suggest that TULSA could be used also to treat bladder outlet obstruction.

The 12-month results from the pivotal TULSA-PRO Ablation Clinical Trial (TACT) was recently published (Klotz et al. 2020). This prospective 13-centre phase 2 study enrolled 115 patients with low to intermediate risk PCa to undergo urethra and apical sphincter sparing whole-gland ablation with curative intent. 72 (63%) had ISUP GG 2 and 77 (67%) intermediate-risk disease according to EAU risk group classification. 55% of patients were discharged on the operation day and 45% were

admitted overnight. Median suprapubic catheter time was 17 (IQR 11-24) days. The rate and nature of attributable serious (Common Terminology Criteria for Adverse Events, Grade 3) adverse events were similar to the phase 1 study by Chin et al. and occurred in 9 (8%) patients including genitourinary infection (4%), urethral stricture (2%), urinary retention (1.7%), urethral calculus (1%) and urinoma (1%). Also, in this study, no rectal injuries were observed. The primary endpoint of PSA reduction ≥75% was met in 110/115 (96%) patients with median PSA reduction of 95% and nadir of 0.34 ng/ml (IQR 0.16-0.60). Of 111 men with 12-month biopsy data available, including a median of 10 biopsy cores (IQR 10-12) from the markedly reduced median prostate volume of 3 cc (IQR 1.7-4.7) with sampling density of 0.4 cc/core, 72 (65%) had no evidence of cancer and 16 (14%) had low-volume ISUP GG 1. Multivariate analysis revealed that among men with ISUP GG 2 disease before TULSA and without calcifications at screening, 51/60 (85%) were free of ISUP GG 2 disease. The other predictors of persistent ISUP GG 2 at 12 months involved undertreatment on MRI-thermometry and a PI-RADS ≥3 lesion at 12-month MRI ($p<0.05$). Furthermore, absence of PI-RADS ≥3 lesion on MRI at one-year had 92% negative predictive value for absence of GG2 disease on one-year biopsies. Based on patient reported functional and QoL questionnaires including Expanded Prostate Cancer Index Composite-50, IPSS and IIEF-15, TULSA had relatively low impact on functional abilities. There was no occurrence of severe erectile dysfunction, and 69/92 (75%) of previously potent patients maintained their erections sufficient for penetration at 12 months with the trend and recovery similar to that in the phase 1 study. Moreover, 96% of men returned to baseline urinary continence. Comparing the safety, functional and oncological outcomes of these landmark phase 1 and 2 TULSA studies, intensifying thermal ablation coverage from 90 to 98% of the prostate seems to improve substantially oncological outcome without affecting safety and functional outcomes (Klotz et al. 2020, Hatiboglu et al. 2020).

3 Aims of the study

Novel imaging methods are rapidly changing the management of PCa. MRI is increasingly used in PCa diagnosis, risk stratification and treatment planning. MRI enables reliable visualization of csPCa, providing a target for image-guided therapy. Extraprostatic disease can be ruled out more reliably with PSMA PET-CT imaging. Accumulating evidence supports the use of PSMA PET-CT for the restaging PCa after BCR. Recently, the effectiveness of PSMA PET-CT for primary staging has also been supported by a randomized controlled cross-over study (Corfield et al. 2018, Hofman et al. 2020).

Standard whole-gland therapy for localized PCa, RP and external beam RT, both offer proven cancer control but carry a high risk of functional impairment. Modern imaging methods have shifted PCa diagnosis from the glandular level to the subglandular level, enabling focal treatment of the malignancy while sparing the remainder of the prostate gland, thus providing better protection of the surrounding structures responsible for urogenital function. There is an unmet need for effective cancer therapy that has minimal impact on the QoL. TULSA is a minimally invasive technology that can ablate prostate tissue using real-time MRI guidance and monitoring. Previous TULSA studies have demonstrated safe and effective ablation of organ-confined PCa using conservative treatment margins. The specific aims of the current study were:

1. To assess the safety and feasibility of TULSA for the following indications:
    a. lesion-targeted ablation of MRI-visible and biopsy concordant PCa
    b. palliative ablation of symptomatic locally advanced PCa
    c. ablation of locally radiorecurrent PCa
2. To compare standard staging modalities (BS and CT) with newer and potentially more accurate imaging modalities (SPECT-CT, wbMRI and PSMA PET-CT) in primary metastasis staging of men with high-risk PCa.

4 Materials and Methods

4.1 Study population

The study population for the five substudies of this doctoral thesis stem from two prospective registered studies, HIFU-PRO and PROSTAGE, conducted at the Turku University Hospital (TYKS) between 2017-2020 (**Table 7**). The source population of both studies included all patients with a clinical suspicion of prostate pathology and/or clinical condition, as described in more detail in the next section, who lived in the TYKS catchment area and were eligible for inclusion in the studies according to specific inclusion and exclusion criteria. Study patients were identified and selected for both studies in the Department of Urology at TYKS. After patient referral to TYKS, a tentative eligibility for the studies was confirmed by the investigating urologist. If the patient met eligibility criteria, he was informed of the study verbally and given the appropriate consent documents approved by the Ethics Committee. If the patient agreed to participate in the study, a signed informed consent was obtained in the presence of designated personnel at the TYKS urological outpatient clinic or ward.

Table 7. Details of the two prospective studies used in this doctoral thesis

Study	Clinicaltrials.gov identifier	Purpose	n	Essential inclusion criteria	Essential exclusion criteria
HIFU-PRO	NCT03350529	treat-and-3-week-resect	6	men with newly-diagnosed MRI-visible biopsy-concordant localized csPCa scheduled for RALP procedure	metastatic disease, contraindications for MRI
		palliation	10	men in need of palliative surgical intervention due to local symptoms/ complications caused by locally advanced PCa	life-expectancy less than 3 months, contraindications for MRI
		salvage	10	men with biopsy-proven localized PCa recurrence after radiotherapy	evidence of extraprostatic disease on restaging including seminal vesicle invasion, contraindications for MRI
PROSTAGE	NCT03537391	primary staging	80	men with newly diagnosed biopsy-proven high-risk PCa according to the EAU risk group classification	any previous PCa imaging for metastasis staging, PCa treatment before enrolment, contraindications for MRI

4.2 Study design and eligibility

HIFU-PRO is a prospective registered (NCT03350529), non-randomized, investigator-initiated, single-centre phase 1 study. This open-label, four-parallel-arm study was geared to investigate safety and feasibility of TULSA method in the treatment of various prostate diseases including indications as follows:

1. lesion-targeted TULSA of MRI-visible biopsy-concordant csPCa before RALP procedure; treat-and-3-week-resect group
2. palliative TULSA (pTULSA) for men in need of palliative surgical intervention due to urinary retention and gross haematuria caused by locally advanced PCa; palliative group
3. salvage TULSA (sTULSA) for men with biopsy-proven localized PCa recurrence after RT; salvage group
4. TULSA for men with symptomatic benign prostatic obstruction in need of surgical intervention (these results are not included in the thesis)

Due to entirely new indications for TULSA, combined with a limited amount of early-stage data on TULSA in the treatment of localized PCa worldwide, plans were made to recruit 10 patients for each arm without a comparative arm. The eligibility criteria for the HIFU-PRO study are shown in **Table 8.**

Table 8. The inclusion and exclusion criteria in HIFU-PRO study

STUDY	Shared inclusion criteria	Specific inclusion criteria within each group			Shared exclusion criteria
		Treat-and-resect	Palliation	Salvage	
HIFU-PRO	Informed consent: The pts must sign the appropriate Ethics Committee approved informed consent documents in the presence of the designated staff Eligible for MRI Eligible for spinal or general anaesthesia (ASA 3 or less) Patency of the urethra and rectum for device instrumentation (confirmed if needed with pre-TULSA cystoscopy and with TRUS/digital rectal examination)	Pts with csPCa scheduled for RALP with normal standards of care were candidates if they met the following additional criteria: MRI-TBx from MRI-visible lesion(s) (PI-RADS ≥3) combined with systematic 10-12-core TRUS-Bx Histopathologically significant MRI-visible (PI-RADS ≥3) and biopsy-concordant PCa-lesion(s) Histopathologically significant PCa-lesion was defined from MRI-TBx as follows: ISUP GG ≥2 or ISUP GG 1 with cancer core length >6mm, and/or >50% in a core and/or >2 positive cores from the targeted lesion	Pts with symptomatic locally advanced and/or metastatic PCa in need of palliative surgical intervention due to local complications Life expectancy greater than 3 months	Pts with histopathologically verified radiorecurrent PCa without seminal vesicle or extraprostatic involvement	Prostate calcifications or cysts with a largest diameter >1cm in the anticipated line-of-sight of the treatment region Contraindications for MRI (e.g. cardiac pacemaker, intracranial clips, claustrophobia, etc.) Chronic inflammatory conditions affecting rectum (also includes rectal fistula and anal/rectal stenosis) Known allergy or contraindication to gastrointestinal anti-spasmodic drug or gadolinium Hip replacement surgery or other metal in the pelvic area Severe kidney failure (glomerular filtration rate <30ml/min/1.73m2) excluding usage of gadolinium unless clinically justifiable based on the clinical judgment of the responsible physician

PROSTAGE is also a prospective registered (NCT03537391), non-randomized, investigator-initiated, single-centre study. The purpose of this study was to compare the diagnostic accuracy of advanced imaging modalities with that of traditional ones in primary staging of men with high-risk PCa. The results of distant metastasis staging are included in the thesis. The T- and N-staging are being reported separately. The eligibility criteria of the PROSTAGE study are shown in **Table 9**.

Table 9. The eligibility criteria in the PROSTAGE study.

	Inclusion criteria	Exclusion criteria
PROSTAGE	Men with newly diagnosed histopathologically confirmed high-risk PCa were eligible if they met at least one of the following criteria: - ISUP GG ≥3 - PSA ≥20 ng/ml - clinical T-stage ≥3a Men aged at least 18 years Adequate physical status defined by treating physician as capability to undergo some form of active treatment for the PCa and the physical status allowing the patient to undergo all studied imaging modalities	Any previous PCa imaging for metastasis staging PCa treatment before enrolment, except administration of ADT at enrolment was permitted if necessary for symptomatic very high-risk patients Contraindications for MRI (e.g., pacemaker, intracranial clips, etc.) Claustrophobia

4.3 Study methods

4.3.1 HIFU-PRO-study

Detailed description of the TULSA intervention

Patient preparation before TULSA included fasting with no oral intake 8 hours prior to the operation. Bowel preparation with oral Bisacodyl was administered the day before, with Bisacodyl enema on the morning of the study intervention. Single–dose prophylaxis of levofloxacin 500 mg was administered intravenously. The entire procedure was conducted in the MRI suite, with the patient in supine position. General or spinal anaesthesia was administered according to manufacturer recommendations and normal clinical practice at TYKS. Device instrumentation occurred on the MR table in the magnet room. An endorectal cooling device was inserted into the rectum. After preloading the urethra with 2% lidocaine gel, a 16

French Foley catheter with perforated tip was inserted via urethra into the bladder, which was fully emptied, unless suprapubic catheter was inserted. If a suprapubic catheter was inserted, the bladder was first filled through a transurethrally-inserted catheter with sterile saline to at least 3 dl. The 14-16 French Foley catheter was then inserted into the bladder through the abdominal wall with two finger widths above the pubic joint in the midline using ultrasound guidance. The balloon was filled with sterile saline up to 10 ml. Catheter selection (suprapubic catheter or transurethral catheter) as well as duration of post-TULSA catheterization were influenced by many factors including the indication of treatment (primary treatment/salvage/palliation), the extent of treatment (whole-gland vs focal), logistical factors (long-distance patients), patient's urine flow prior to the procedure, the patient's desire and what type of catheter treatment was chosen. A maximum 0.96 mm nitinol guidewire was inserted through the transurethral catheter into the bladder, and the catheter was then removed, leaving the guidewire in place. Subsequently, the ultrasound applicator was inserted over the guidewire into the bladder and the guidewire was removed (**Figure 13**).

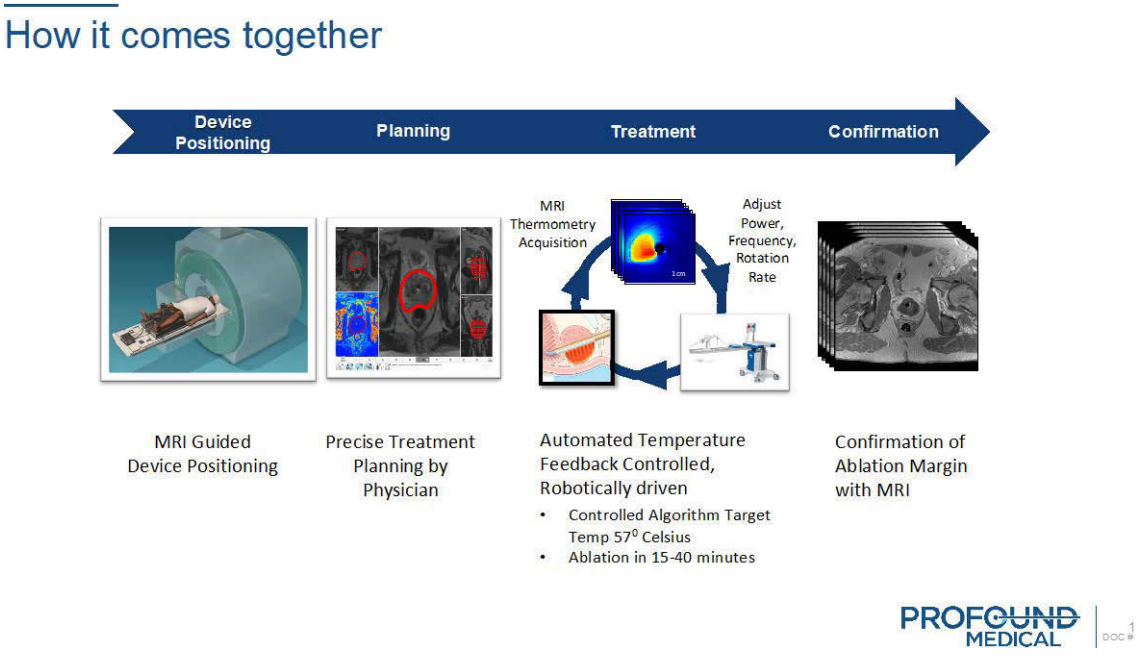

Figure 13. The workflow of TULSA (Courtesy of Profound Medical Inc).

The treatment planning workflow in the console room followed the steps as first described by Chin el al. (Chin et al. 2016). The planned treatment strategy depended on which of the study arms the patient belonged to:

1. In treat-and-resect cohort the treatment plan targeted ablation of all MRI-visible biopsy-concordant PCa lesions. The ablative effect was planned to cover the lesion(s) with a 5 mm overlap up to the prostate capsule when feasible, to account for MRI underestimation of tumour size. For this treat-and-resect-study where patients do not receive benefits from TULSA treatment, it was paramount to minimize the risk of any negative functional impact on genitourinary function related to the study intervention prior to nerve-sparing RALP. Therefore, in the vicinity of the neurovascular bundles, safety margins up to 3 mm were applied regardless of tumour extent, based on the concern that necrosis may migrate beyond the region of acute coagulation necrosis.
2. In palliation patients, the treatment approach was dependent on the individual disease characteristics. If visible, the ablation was targeted to the dominant tumour section compressing and/or invading the prostatic urethra, otherwise the objective was to debulk the prostate. As more experience was obtained, any tissue obstructing the bladder neck was also targeted, regardless of if a tumour was present.
3. In salvage patients the ablative effect was planned to cover all areas deemed suspicious by imaging (PSMA PET and/or MRI) and/or contained cancer in biopsies, and if applicable, with a 5 mm margin of the visible tumour up to the prostate capsule. Per patient, two sonication sweeps were performed.

TULSA treatment was delivered under real-time feedback control, with a clinical objective of reaching a temperature of 55ºC at the prostate boundary (**Figure 14**). Due to MRI-thermometry uncertainty where the edge of the prostate meets extraprostatic fat, the system achieves this goal by making real-time feedback control decisions using more reliable temperature measurements at a control boundary set 2 mm inside the drawn prostate boundary. Based on previous clinical studies (Ramsay et al. 2017), the controller objective is to reach 57ºC at the control boundary, which is expected to achieve a cytocidal thermal dose of 240 CEM at the prostate capsule (**Figure 14**). Post-treatment CE-MRI was acquired following weight-adjusted intravenous injection of standard institutional gadolinium-based contrast agent (0.1 mmol/kg) (**Figure 14**). Both dynamic and static CE sequences were obtained:

1. Dynamic images with high temporal resolution including 70 prostate scans within 4 min 55 s, the spatial resolution was 1,08 x 1,08 x 3,0 mm.

2. Static CE-images (3D T1-weighted fat-saturated images) with higher spatial resolution of 0,78 x 0,78 x 1 mm were acquired immediately after the dynamic scan. The sequences enabled both high temporal and spatial resolution, thus giving complementary information about perfusion in a detailed level.

After finishing therapy, if no suprapubic catheter had been inserted, a transurethral 16 French Foley catheter was inserted using sterile technique into the bladder and balloon was inflated with 10 ml sterile saline. The patients were transferred into the recovery room, where special attention was paid to free flow of urine through the catheter. Intravenous hydration was adjusted so that urine output was at least 2 ml/kg/h to prevent possible clotting. Patients were admitted overnight if deemed appropriate by the investigator.

Due to anticipated thermal injury derived oedema after TULSA, catheter removal trial was planned within 1-2 weeks of treatment. When removing the catheter, completeness of bladder emptying was confirmed with the post-void residual estimation. If the patient had a suprapubic catheter, the patient also completed a post-void residual diary for 3 days prior to catheter removal to ensure that the bladder is emptied reliably.

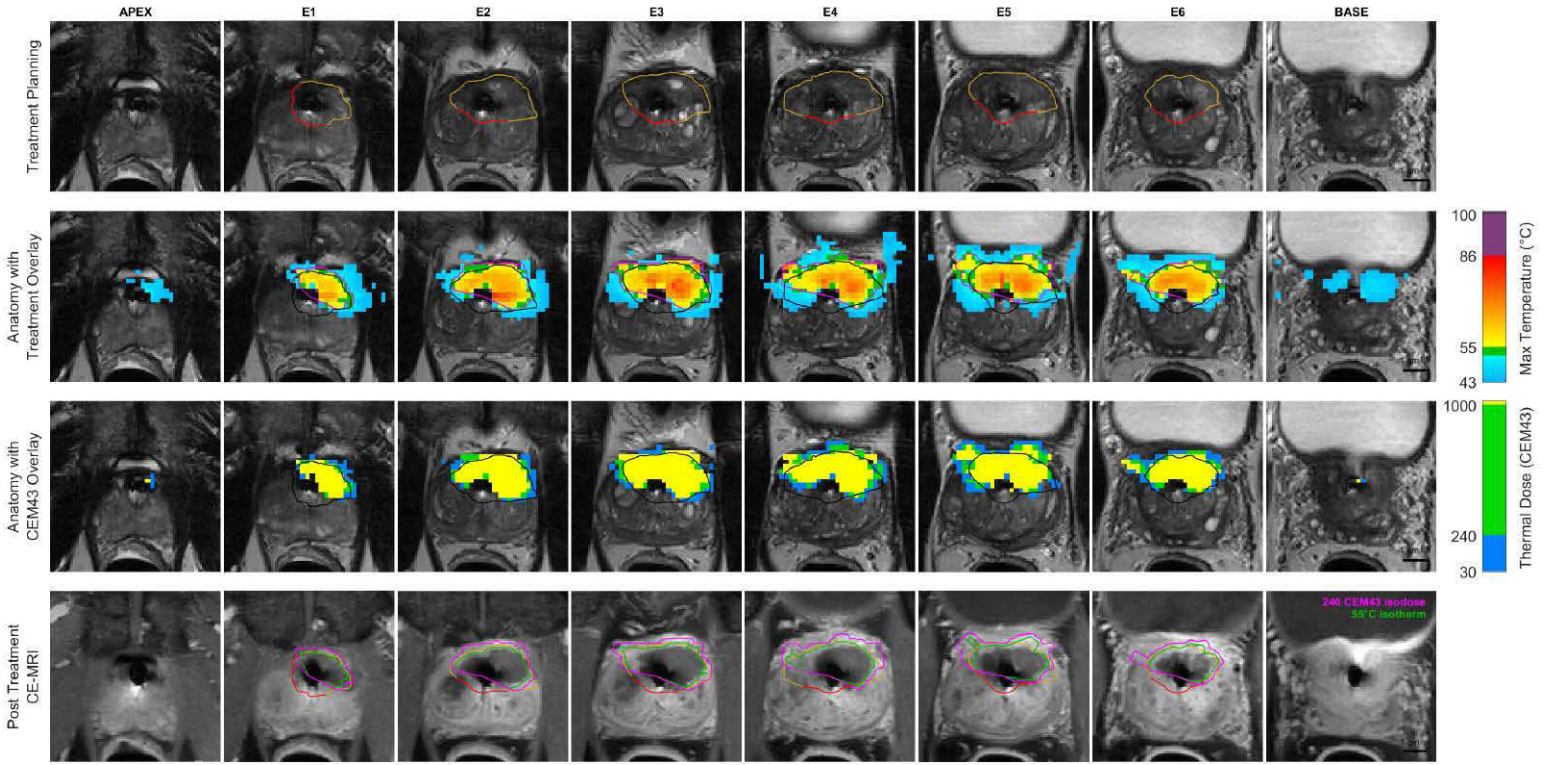

Figure 14. Intra-procedural MRI images of the study patient, with contoured target volume (top row), 55°C isotherm volume (cytocidal temperature, second row), thermal dose coverage (third row), and non-perfused-volume (fourth row) (from original publication I).

Follow-up procedures

In the HIFU-PRO study follow-up visits were scheduled at 0-3 weeks, depending on the study arm, and, 3, 6, 9, and 12 months (**Table 10**). A catheter removal trial was performed at the first follow-up visit. Adverse events were recorded at every follow-up visit using the Clavien-Dindo classification for surgical complications, as well as PSA, uroflowmetry (post-void residual, average flow rate, maximum flow rate, voided volume), and functional questionnaires (Expanded Prostate Cancer Index Composite-26, IPSS, IPSS quality -of -life, IIEF-5) and Visual analog scale for pain (**Table 10**). At 12 months, salvage patients underwent ^{18}F-PSMA-1007 PET-CT and pelvic 3-T mpMRI followed by an MRI-TBx using TRUS for cognitive registration. The biopsy protocol included two to four infield biopsies and additional biopsies from any other regions deemed suspicious on imaging.

Table 10. Follow-up schedule and procedures after TULSA (HIFU-PRO study). AE = adverse event; mpMRI = multiparametric magnetic resonance imaging; MRI-TBx = magnetic resonance imaging targeted biopsy; PSA = prostate-specific antigen; PSMA PET-CT = prostate-specific membrane antigen positron emission tomography-computed tomography; RALP = robot-assisted laparoscopic prostatectomy; QoL = quality of life; VAS = visual analog scale.

Arm	0-3 wk	3 wk	3-4 wk	3 mo	6 mo	9 mo	12 mo
Treat-and-resect	Catheter removal trial, uroflowmetry, PSA, AE review, VAS for pain, mpMRI at one wk	Uroflowmetry, AE review, VAS for pain functional/QoL questionnaires, mpMRI	RALP	Uroflowmetry, PSA, AE review, VAS for pain, functional/QoL questionnaires	Uroflowmetry, PSA, AE review, VAS for pain, functional/QoL questionnaires	Uroflowmetry, PSA, AE review, VAS for pain, functional/QoL questionnaires	Uroflowmetry, PSA, mpMRI, AE review, VAS for pain, functional/QoL questionnaires
Palliation	Catheter removal trial, uroflowmetry, PSA, AE review, VAS for pain	NA	NA	Uroflowmetry, PSA, cystoscopy, AE review, VAS for pain, functional/QoL questionnaires	Uroflowmetry, PSA, AE review, VAS for pain, functional/QoL questionnaires	Uroflowmetry, PSA, AE review, VAS for pain, functional/QoL questionnaires	Uroflowmetry, PSA, mpMRI, cystoscopy, AE review, VAS for pain, functional/QoL questionnaires
Salvage	Catheter removal trial, uroflowmetry, PSA, AE review, VAS for pain	NA	NA	Uroflowmetry, PSA, mpMRI, AE review, VAS for pain, functional/QoL questionnaires	Uroflowmetry, PSA, AE review, VAS for pain, functional/QoL questionnaires	Uroflowmetry, PSA, AE review, VAS for pain, functional/QoL questionnaires	Uroflowmetry, PSA, mpMRI, PSMA PET-CT, cystoscopy, MRI-TBx, AE review, VAS for pain, functional/QoL questionnaires

4.3.2 PROSTAGE-study

After consenting, study participants were referred for metastasis staging with all the following imaging modalities (**Figure 15**):

1. Standard imaging: ^{99}mTc-HMDP planar BS and CE-CT of the thorax, abdomen, and pelvis
2. Imaging under evaluation: ^{18}F-PSMA-1007 PET-CT, WBMRI including DWI, and ^{99}mTc-HMDP SPECT-CT

A detailed description of image acquisition for each imaging modality studied is given in the Supplemental Material related to the original publication numbered V in this thesis.

A total of six experienced modality-based experts (4 radiologists and 2 nuclear medicine physicians), two for each of the three imaging modalities, participated in the imaging readings. Each imaging modality was independently reviewed by the same pair of experts, blinded for the other modalities and the other readers, and informed only that the patients had a high risk of metastases. Lesions were interpreted in all modalities according to clinical expertise and following the current guidelines (Mottet et al. 2020, Fendler et al. 2017). Lesions were reported as malignant, equivocal or benign. Both pessimistic (equivocal lesions interpreted as malignant) and optimistic (equivocal interpreted as benign) analyses were performed to resolve equivocal lesion status. Data was collected on a RedCap electronic database (Harris et al. 2019). The software used for image interpretation is shown in **Figure 15**.

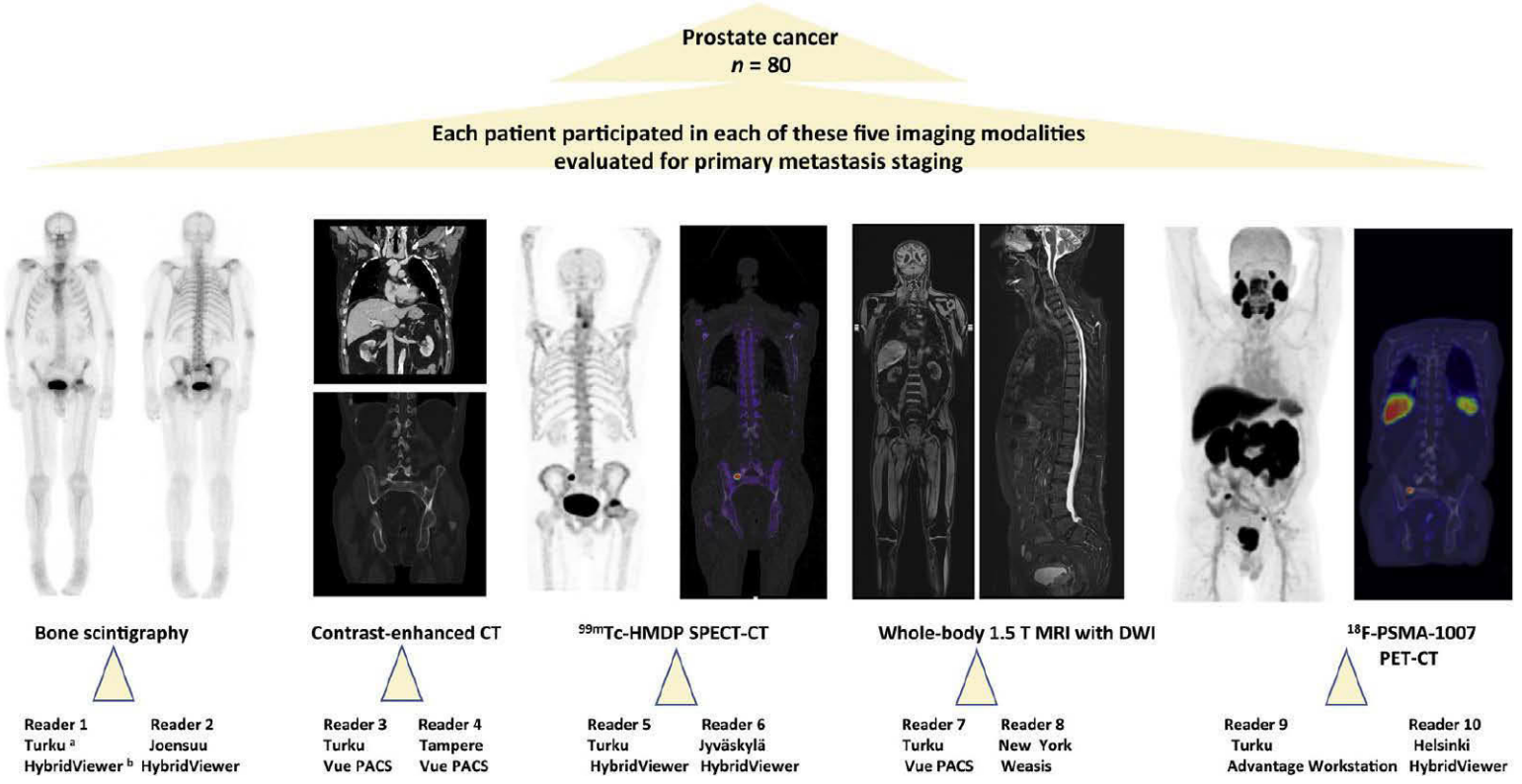

Figure 15. PROSTAGE study outline (from original publication V). CT = computed tomography; DWI = diffusion-weighted imaging; HMDP = hydroxymethylene diphosphonate; MRI = magnetic resonance imaging; PET = positron emission tomography; PSMA = prostate-specific membrane antigen; SPECT = single-photon emission computed tomography. [a] Location (city) of the reader. [b] Software used for image interpretation: HybridViewer (version 2.6 P; Hermes Medical Solutions, Stockholm, Sweden), Advantage Workstation (version 4.7; GE Healthcare, Buc, France), Weasis Medical Viewer (version 3.5.3; University of Geneva, Geneva, Switzerland), and Vue PACS (version 12.2.0.1007; Carestream Health Inc., Rochester, NY, USA).

For the validation of all reported lesions, the concept of a reference standard diagnosis was utilized, which included information on the examination results from all primary and follow-up imaging modalities, and clinical follow-up data (including PSA kinetics, and, when available, histopathological specimens). The reference standard diagnosis, either benign or malignant, was defined at the lesion level in a regularly organized consensus reading meetings by a multidisciplinary team, including two uro-oncologist, one uro-pathologist, two radiologists (CT and MRI experts), and two nuclear medicine physicians. PSMA PET-avid lesions lacking histopathological verification were rated as malignant only if there was a corresponding anatomical finding suspicious for malignancy at primary or follow-up MRI and/or CT. If there were no typical benign or malignant finding on MRI/CT within lesions associated with a tracer uptake, excluding normal physiological uptake areas, follow-up imaging was used to identify possible development of anatomical correspondence using MRI and/or CT from the region of interest. If follow-up imaging did not reveal anatomical correspondence, the lesion was considered non-malignant (false positive). The bone and soft tissue findings were compared at the patient, region, and lesion levels. The regions were divided into three categories according to the eighth edition of UICC 2009 TNM classification for PCa (Bierley et al. 2017).

4.4 Statistical analysis

In all studies the patient characteristics were summarized using descriptive statistics. In the TULSA studies, thermal targeting accuracy statistics including volumetric thermal target coverage and overlap, and linear targeting accuracy and precision, were executed in Matlab (R2018a, Mathworks Inc., Natick, MA). MRI-based volumetric calculations (prostate size, lesion volumes, non-perfused volume, histology-based complete necrosis volume) were measured using AW Server (GE Healthcare, Chicago, IL).

In the PROSTAGE study, the primary outcome measurement was the diagnostic accuracy assessed by the area under the receiver-operating characteristic curve (AUC) values of the detection of bone metastasis in the pessimistic analysis (equivocal lesions interpreted as malignant). The sample size calculation was based on our previously published pilot study SKELETA (Jambor et al. 2016), where AUC values of PET-CT and BS for bone metastasis detection were 0.91 and 0.72, respectively. We estimated that for the detection of a 0.19 difference in the AUC value using a two-tailed test with a power of 80% at a significance level of 0.05 in 2:1 ratio of sample sizes in negative/positive groups, 48 cases and 24 positive cases were required. Accounting for possible dropouts, the recruitment goal was 80 patients. The sensitivity, specificity, and accuracy values are reported with a 95% CI

and compared between modalities with Fisher's exact test. The inter-reader agreement at the patient level was defined using Cohen's kappa (95% CI). The AUC values were calculated using the trapezoid rule. The AUC values in the pessimistic analysis at the region level (bone) were calculated and compared using a method by Hanley and McNeal (Hanley & McNeal 1983). The analysis was performed using logistic regression. All p values of <0.05 were considered statistically significant. All statistical analyses were performed with the SAS system (version 9.4 for Windows; SAS Institute Inc., Cary, NC, USA).

4.5 Ethics

Both the two included prospective studies were conducted in compliance with the current revision of the Declaration of Helsinki guiding physicians and medical research involving human subjects (64th World Medical Association General Assembly, Fortaleza, Brazil, 2013). Prior to commencement of the studies, the study protocol, the patient information sheet, and the written informed consent were approved by the local ethics committee of the Hospital District of Southwest Finland.

5 Results

5.1 Study I

The primary objectives of Study I was to evaluate the safety and toxicity, accuracy and short-term evolution of cell-death after lesion-targeted TULSA.

Six patients were included and completed this study. Characteristics of the study population is shown in **Table 11** and location of the targeted lesions on MRI are presented in **Figure 16**. Eight lesions in the six study patients were ablated with TULSA, of which MRI-TBx revealed histopathology of ISUP GG ≥2 in five patients and ISUP GG 1 in one patient with high-volume disease based on MRI and histopathology. The first four patients had only one lesion, while the last two patients also had a secondary lesion (**Figure 16**).

The TULSA intervention was successful in every study patient, with the target ablation volumes of 7-19 ml in the prostates ranging from 42-82 ml. Median sonication time and in bore MRI time were 17 min (range: 11-52) and 117 min (range: 82-185), respectively. The TULSA was carried out under spinal anaesthesia in one patient and under general anaesthesia in the others. Suprapubic catheter was avoided and having no urinary drainage during the procedure did not compromise the procedure. All patients received transurethral Foley catheter immediately after the treatment and catheter removal was successful in each study patient at two to three days after TULSA. Two patients were discharged on the treatment day and four patients were admitted overnight due to logistical reasons. The technical feasibility and procedural outcomes are presented in **Table 12**.

None of the study patients experienced any treatment-related adverse event and there were no notable differences in functional/QoL questionnaires or uroflowmetry outcomes between baseline and three weeks after TULSA. Three patients having baseline erection sufficient for penetrations had successful penetrations after TULSA with normal antegrade ejaculations.

The RALP procedures at three weeks of TULSA treatment were uneventful. Minor localized inflammatory effects with periprostatic adhesions were noted including some fibrotic reaction of endopelvic and Denonvillier´s fascia, which did not compromise oncological radicality or nerve-sparing procedure in any of the study patient. All study patient presented negative surgical margins.

The thermal targeting accuracy measurements are shown in **Table 13**. Mean targeting accuracy was –0.5 ± 1.4 mm, with 95 ± 2% thermal coverage indicating minor undertreatment. The multimodality based volumetric correlations are shown in **Table 14**. Based on MRI measurement, the mean increase in total prostate volume was 29% one week after TULSA, decreasing at three weeks but remaining 4% greater than baseline. Non-perfused volume increased gradually over three weeks with a mean change of 36%. Locality and morphology of the three-week non-perfused volume correlated with the respective complete necrosis volume on histology in all patients (**Figure 17**). Three-week non-perfused volume was 19% (mean) larger than complete necrosis volume on histology after accounting for average total prostate volume shrinkage on histology of 26% (Jonmarker et al. 2006). Mean histological demarcation between complete necrosis and outer limit of thermal injury was 1.7 ± 0.4 mm (**Figure 18**).

Radiological and histopathological assessment of three-week treatment efficacy indicated no ablative or targeting failures. However, as expected based on the conservative treatment plan required in this treat-and-resect-study, 4/6 patients had residual cancer outside of the planned ablation volume, inside the pre-planned 3 mm safety margin near the neurovascular bundles at the prostate capsule.

Table 11. Baseline patient, disease and tumour characteristics on MRI (n=6). Between August 2017 and May 2018, six men were enrolled and all completed the study. All patients were Caucasian and had normal performance status (Eastern Cooperative Oncology Group = 0) (From original publication I). BMI = body mass index; cT = clinical tumour category; EAU = European Association of Urology; ISUP GG = International Society of Urological Pathology grade group; MRI-TBx = magnetic resonance imaging targeted biopsies; NA = not applicable (only primary lesion); PI-RADS = Prostate Imaging Reporting and Data System (from original publication I).

PATIENT AND DISEASE CHARACTERISTICS							PRIMARY LESION				SECONDARY LESION			
	AGE	BMI	PSA	cT	EAU risk group	ISUP GG	PI-RADS	Max diameter (mm)	Volume (ml)	MRI-TBx histology (ISUP GG)	PI-RADS	Max diameter (mm)	Volume (ml)	MRI-TBx histology (ISUP GG)
1	70	32	10	T2	Intermediate	3	3	16	0.6	3			NA	
2	70	27	4.6	T2	Intermediate	1	5	24	3	1			NA	
3	66	30	7.5	T3	High	2	5	19	1.5	2			NA	
4	70	33	36	T3	High	3	5	29	5.1	3			NA	
5	72	24	12	T2	High	4	4	8	0.4	4	4	9	0.2	4
6	54	25	7.8	T2	Intermediate	2	4	10	1	2	4	9	0.7	4

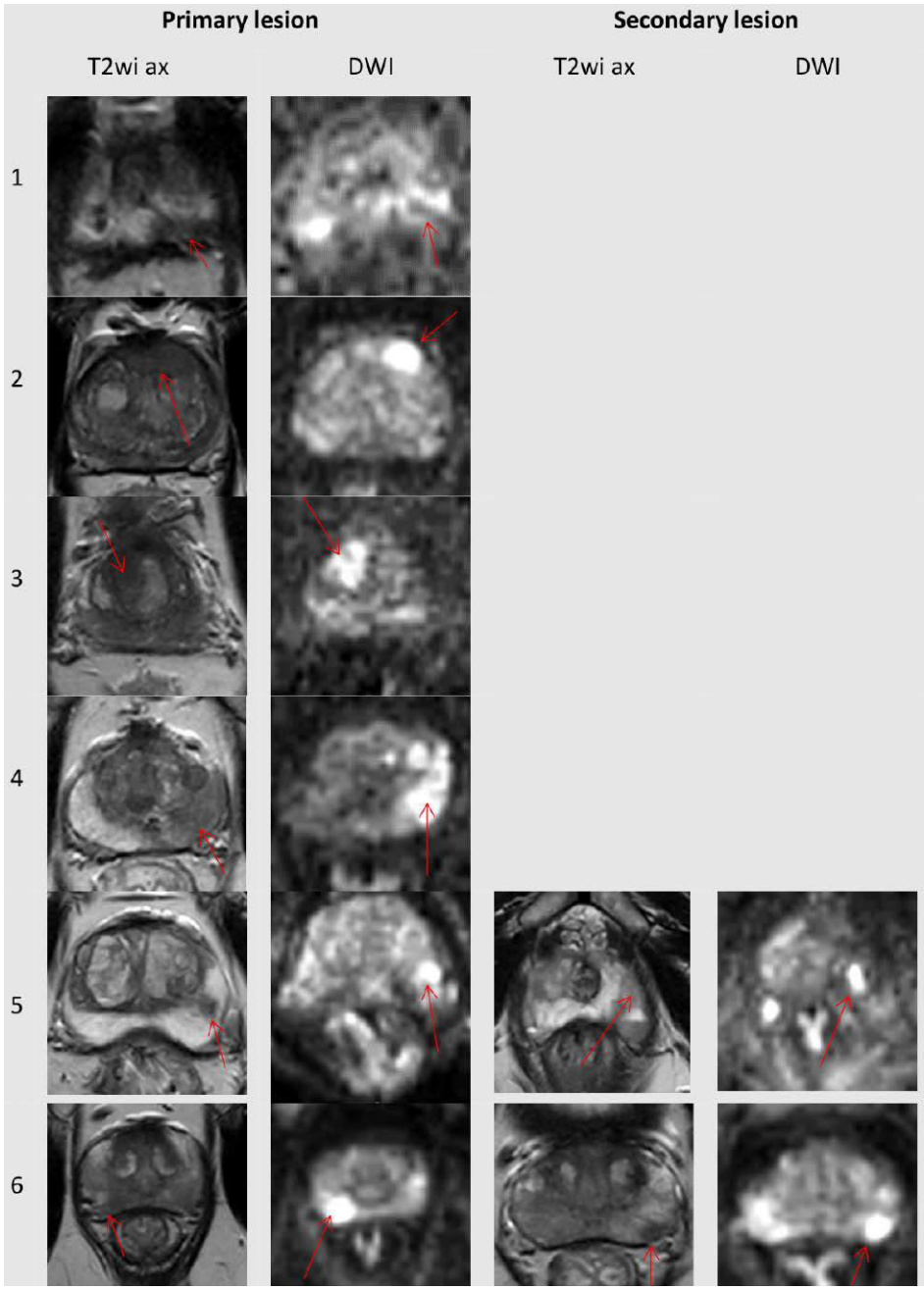

Figure 16. Locations of the targeted lesions on baseline MRI. Note the red arrow pointing to the lesion on each imaging sequence (from original publication I). DWI = diffusion-weighted imaging; T2wi ax = axial T2-weighted imaging

Table 12. Technical feasibility and procedural outcomes of lesion-targeted TULSA for PCa-lesion(s) (from original publication I).

	Max treatment radius (mm)	Sonication time (min)	In bore MRI-time (min)	Hospital stay (hours)	Catheterization time (days)
1	29.6	20	82	10.5	3
2	20.7	13	120	12	3
3	19.6	11	111	27	3
4	21.3	14	130	27	3
5	33.6	52	185	28	2
6	25.3	22	113	33	2

Table 13. Volumetric statistics of targeting accuracy (from original publication I). CEM = cumulative equivalent minutes at 43°C; SD = standard deviation.

	Individual data						All patients	
Temperature at control margin (57°C)	P1	P2	P3	P4	P5	P6	Mean	SD
Linear targeting accuracy (mm)	-0.7	0.4	-0.3	-0.2	-1.5	-0.5	-0.5	0.6
Linear targeting precision (mm)	2.1	1.1	0.7	0.7	2.3	1.2	1.4	0.7
Dice similarity coefficient	0.90	0.93	0.94	0.96	0.86	0.93	0.92	0.04
Volumetric coverage (%)	85.6	94.4	91.4	95.1	80.7	90.4	89.6	5.5

	Individual data						All patients	
Thermal dose at target boundary (240 CEM)	P1	P2	P3	P4	P5	P6	Mean	SD
Linear targeting accuracy (mm)	1.6	1.8	0.0	1.1	1.0	1.2	1.1	0.6
Linear targeting precision (mm)	2.8	1.9	1.1	1.8	2.7	2.3	2.1	0.6
Dice similarity coefficient	0.87	0.86	0.93	0.91	0.89	0.90	0.89	0.03
Volumetric coverage (%)	94.0	96.8	92.9	97.6	94.0	96.0	95.2	1.9

Table 14. Multimodality based volumetric correlation (from original publication I). CEM = cumulative equivalent minutes at 43°C; NA = not applicable; MRI = magnetic resonance imaging; NPV = non-perfused volume; TULSA = MRI-guided transurethral ultrasound ablation.

Parameter (ml)	Patients					
	1	2	3	4	5	6
Prostate volume on baseline MRI	65	65	42	51	82	55
1-week prostate volume POST-TULSA	75	83	62	68	98	NA
3-week prostate volume POST-TULSA	73	61	47	61	86	48
Target volume on treatment planning	16.8	10.5	7.0	13.0	10.1	18.6
Immediate POST-TULSA 55 °C isotherm volume	15.5	9.8	5.5	11.4	9.8	17.1
Immediate POST-TULSA 57 °C isotherm volume	13.1	8,0	4.5	9.3	7.3	15.0
Immediate POST-TULSA 240CEM isodose volume	22.5	14.8	7.8	16.0	14.5	26.2
Immediate POST-TULSA NPV	11.1	9.1	2.8	6.7	5.7	10
1-week POST-TULSA NPV	13.5	10.9	2	10.8	8.1	NA
3-week POST-TULSA NPV	15.9	9.6	4	10.7	9.3	13
Absolute and % change between immediate and 3-week NPV	4.8 (+43%)	0.5 (+6%)	1.2 (+43%)	4 (+60%)	3.6 (+63%)	1.8 (+19%)
Complete irreversible necrosis volume on histology	9.8	5.0	3.5	10.8	8.9	12.9

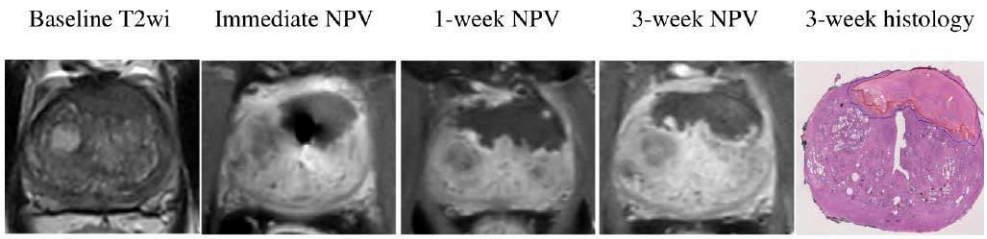

Figure 17. Baseline MRI identified an anterior 3 cc PI-RADS 5 lesion with a biopsy-concordant high-volume ISUP GG 1 PCa (MRI-TBx 4/4 positive cores, systematic biopsies negative). Post-treatment, 1- and 3-week non-perfused volume and 3-week whole-mount hematoxylin-eosin-stained slide demonstrate high volumetric and morphometric concordance. Note that complete necrosis reached the capsule and thermal damage was well-confined. Non-perfused volume covered the entire PI-RADS 5 lesion and no vital cancerous tissue was reported in the vicinity of the targeted lesion (from original publication I).

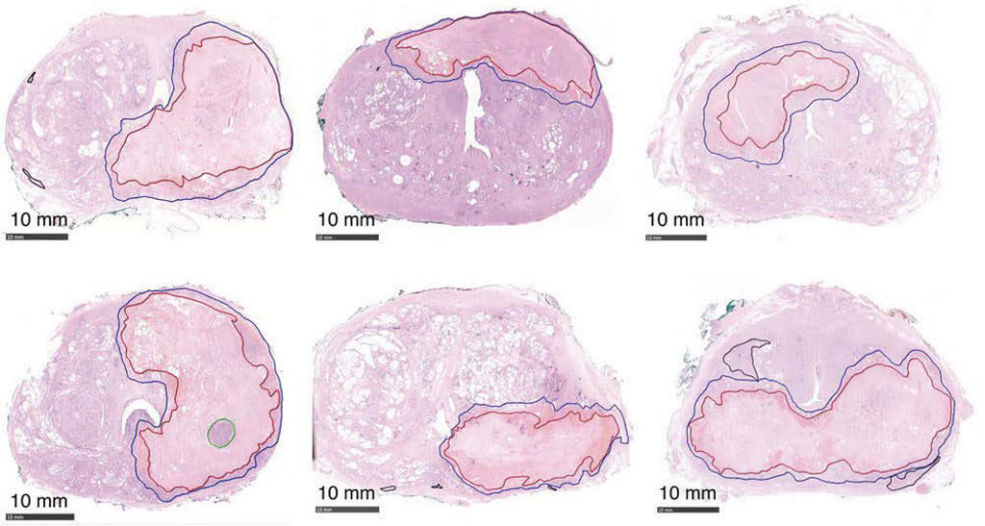

Figure 18. Annotated hematoxylin-eosin stained axial whole-mount slide mid from the RALP specimen from every study patient. The complete irreversible cell death inside the red boundary and margin zone between red and blue boundaries (outer limit of thermal injury). Mean distance between these boundaries was 1.7 ± 0.4 mm indicating sharp demarcation of the thermal injury (from original publication II).

5.2 Study II

The primary objectives of Study II were to evaluate histopathology of the removed prostate specimens from all six patients that completed the treat-and-resect study, and to characterize the immunoprofile and assess the viability of morphologically unaltered subregions of prostatic tissue within regions of coagulative necrosis on hematoxylin-eosin (H&E) staining after thermal ablation with TULSA. One of these

six patients presented with apparently viable tissue within the continuous area of coagulation necrosis on initial H&E staining. This patient presented with MRI-visible (5.1 cc PI-RADS 5 lesion) MRI-TBx-concordant high-volume (cancer core length 53 mm) ISUP GG 3 PCa in the left lobe. CT and BS were both negative for distant metastasis (**Figure 19**). ^{18}F-PSMA-1007 PET-CT imaging was also negative for extraprostatic disease and showed an intensive PSMA-uptake with a maximum standardized uptake (SUVmax) value of 81.1 in the left lobe of the prostate concordant with the MRI (**Figure 19 A**). The patient underwent left lobe hemiablation with TULSA and the treatment-day MRI-thermometry maps demonstrated a homogeneous and continuous cytocidal heating pattern extending into the prostate capsule completely containing the targeted predefined region including the targeted tumour (**Figure 19 B**). The three-week non-perfused volume covered the tumour without any enhancement observed inside the non-perfused volume indicating complete devascularization of the targeted region (**Figure 19 C**). The post-TULSA three-week RALP procedure was uneventful without perioperative adverse event. H&E stained analysis of the RALP specimen revealed a distinct round-shaped focus of morphologically viable adenocarcinoma in two consecutive slides 5mm apart from each other, retaining nuclear and cytological details and resembling ISUP GG 3 disease (**Figure 20**). Surprisingly, this focus was located in the central part of the ablated region, surrounded by complete irreversible cell death, coagulation necrosis, characterized by retention of cellular outline but loss of cytoplasmic and nuclear details, and the presence of haemorrhage and loosely woven collagen. This focus was situated in the zone where the highest temperature of 83.3°C was reached based on MRI-thermometry and was within a region of uniformly non-enhancing tissue on CE-MRI. Furthermore, this patient differed from the other five patients based on the finding that this patient had the most rapid heat response of all treatments (time from initiation of heating to peak: 12°C/min vs. median 7°C/min [IQR: 5.2-10]). Immunohistochemistry indicated that neither the apparently viable region nor the surrounding coagulation necrosis zone stained positively for cytokeratin 8, as assessed by Cam5.2 antibody. Instead, both the untreated benign region and apparent residual carcinoma just outside the ablated area within safety margin were cytokeratin 8 positive. This finding suggests that negative cytokeratin 8 staining (based on Cam5.2 antibody) distinguishes thermally-fixed and thermally-necrosed cells from vital and positively stained untreated tissue.

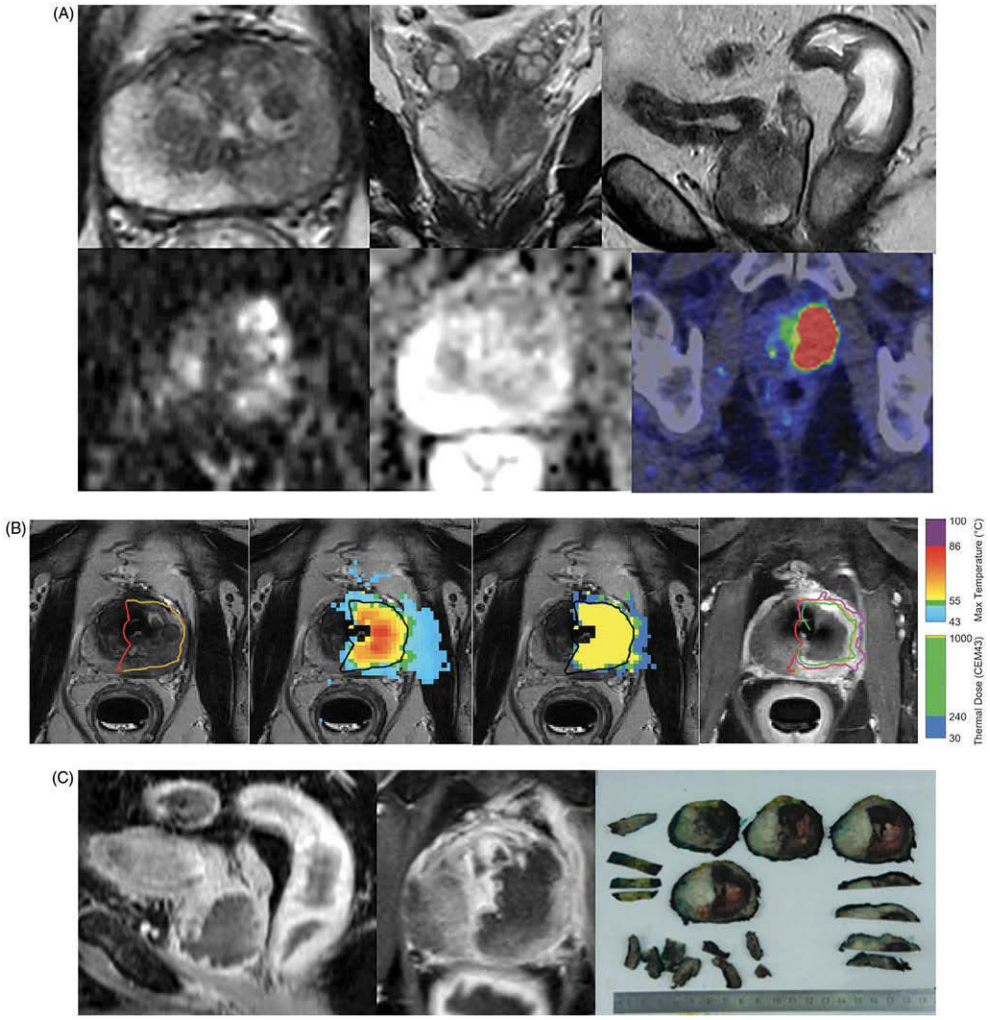

Figure 19. Multimodality based evaluation of the study patient presenting with thermal fixation. **A.** Axial, coronal and sagittal T2w images, DWI and apparent diffusion coefficient map images (left to right in order), and PSMA PET image showing PI-RADS 5 lesion with SUVmax of 81 on PSMA PET. **B.** Immediate post-treatment overlay images. On the left targeted region, on the middle maximum temperature and thermal dose maps, and on the right non-perfused volume. **C.** post-TULSA non-perfused volume on sagittal and axial images at 3 weeks prior to RALP procedure and the sliced RALP specimen on the right, in which thermal damage region is identified as the dark regions on the gross specimen (from original publication II).

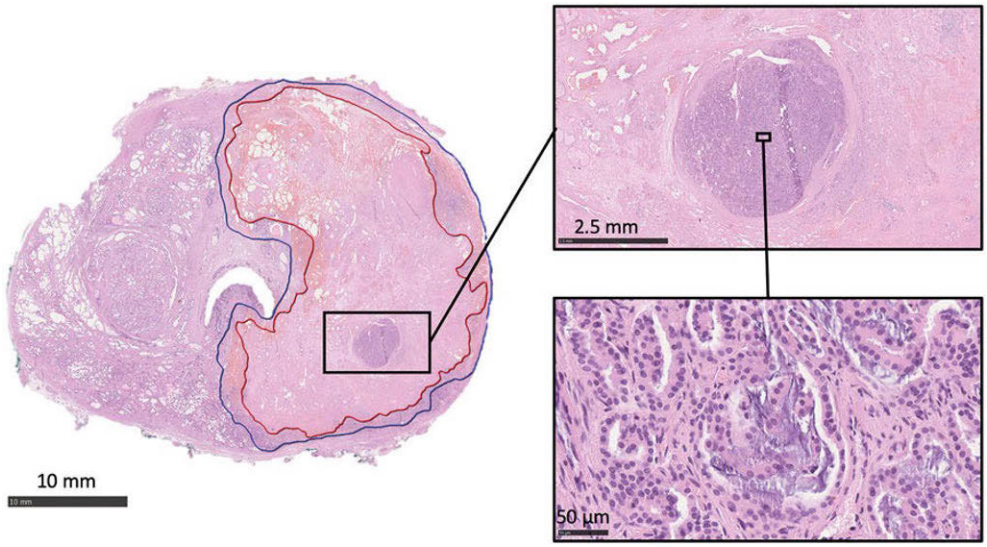

Figure 20. Histopathological analysis of prostatic thermal injury. An annotated axial H&E-stained whole-mount slide from the mid RALP specimen of the patient showing a complete irreversible cell death inside the red boundary delimiting coagulation necrosis zone and margin zone between red and blue boundaries. Magnification H&E images from the thermally-fixed area show well-preserved morphology resembling of ISUP GG 3 PCa (from original publication II).

5.3 Study III

The primary objectives of Study III were to evaluate the safety and feasibility of pTULSA in the treatment of gross haematuria and/or urinary retention in patients presenting with locally advanced PCa.

Ten patients were included and completed this study. Patient and disease characteristics of the study population are shown in **Table 15**. Prior to pTULSA, six patients had undergone external beam RT combined with 2-3-year ADT, while the other four patients were treated only with ADT. At enrolment eight patients had metastatic disease, five of which had castration resistant PCa. The median (range) age, Charlson Comorbidity Index score, Eastern Cooperative Oncology Group performance status, baseline PSA and prostate volume were 76.5 years (60–81), 10.5 (5–15), 2 (1–3), 18.5 ng/mL (0.23–140) and 35 cc (12–213), respectively. The median time between the initial PCa diagnosis and pTULSA was 30 months (range: 4-194). Half of the patients presented with clinical T4 tumours, while the other half had T3 tumours. Four patients with T4 tumours had direct invasion of the tumour in the bladder neck and/or posterior bladder wall. The median (range) length of follow-up was 427 days (80-738).

Table 15. Patient characteristics before pTULSA (n=10) (from original publication III). ECOG = Eastern Cooperative Oncology Group; PSA = prostate-specific antigen; CCI = Charlson comorbidity index; CRPC = castration-resistant prostate cancer; ADT = androgen deprivation therapy; pTURP = palliative transurethral resection of the prostate

Parameter	Value
Median age, year (range)	76.5 (60-81)
ECOG performance status, % (n)	
1	40% (4)
2	40% (4)
3	20% (2)
Median PSA, ng/ml (range)	18.5 (0.23-140)
Median prostate volume, ng/ml (range)	35 (12-213)
Radiological tumour stage, % (n)	
T3	50% (5)
T4	50% (5)
Median CCI (range)	10.5 (5-15)
CRPC, % (n)	
Yes	50% (5)
No	50% (5)
Primary cancer treatment, % (n)	
ADT	40% (4)
Radiation + ADT	60% (6)
Docetaxel	10% (1)
Continuous catheter, % (n)	
Yes	100% (10)
Documented metastatic disease, % (n)	
Yes	80% (8)
No	20% (2)
Urinary tract infection, % (n)	
Yes	80% (8)
No	20% (2)
pTURP before pTULSA, % (n)	
Yes	30% (3)
No	70% (7)
Anticoagulation, % (n)	
Yes	40% (4)
No	60% (6)

Prior to pTULSA all patients had continuous catheterization due to urinary retention. Nine patients also had history of recurrent and/or ongoing gross haematuria. All patients underwent pTULSA successfully with a mean ablation time of 37 min (range: 16-58) and ablation volume of 30.6 cc (range: 12-84). Two patients had a

suprapubic catheter during pTULSA procedure while the others did not have any urinary drainage during the procedure, receiving transurethral catheter afterwards. The mean hospitalization time was 28.6 h (range: 12-48) with one patient discharged on the treatment day, another on the second postoperative day and the others on the first postoperative day. Two Grade 2 and three Grade 1 adverse events were recorded, all related to urinary tract infection, of which two cases required hospitalization due to administration of intravenous antibiotics. Catheter removal at one week was successful in five patients. Two patients had their suprapubic catheter removed at three and nine months. Three patients underwent palliative TURP after pTULSA because of persistent bladder outlet obstruction. At the last follow-up visit 70% of the study patients were catheter-free, five patients after pTULSA alone and two patients after additional palliative TURP. Gross haematuria ceased in all patients at one week, continuing without occurrence of gross haematuria until the last follow-up visit. Comparing the 6 months preceding the pTULSA to 6 months after the average hospitalization time due to local complications decreased from 7.3 days (range: 0-20) before pTULSA to 1.4 days (0-7) after pTULSA. A successful pTULSA case is presented in **Figure 21**.

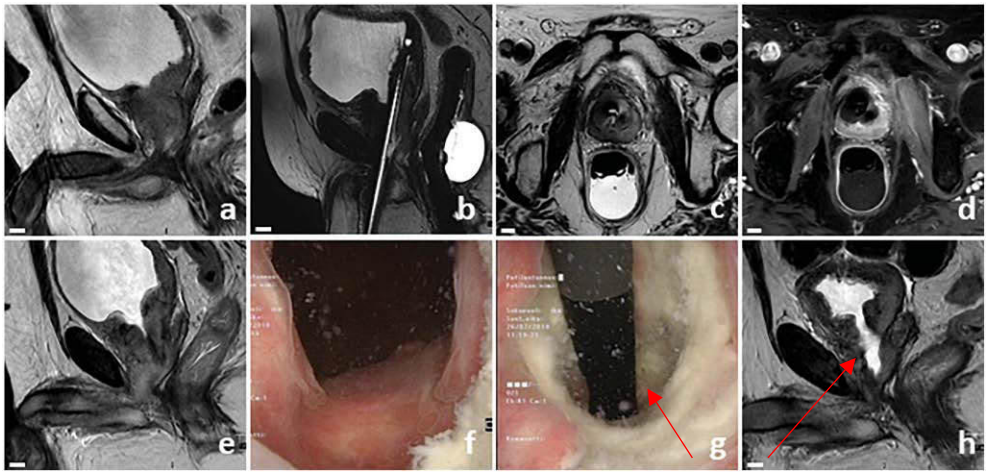

Figure 21. pTULSA case example. This patient suffered from locally advanced PCa causing urinary retention and recurrent gross haematuria. Baseline sagittal MRI image showed obstructive infiltration of PCa to the bladder neck and posterior bladder wall (a). Treatment-day MRI planning images showing the ultrasound applicator and endorectal cooling device (b and c). 19 cc of tumour around the bladder neck was targeted, with CE-MRI revealing immediate effects of ablation (d). Transurethral catheter removal was successful at 1 week, accompanied with a prostate volume increase from 35 to 40 cc on MRI (e). Cystoscopy revealed an open bladder neck at 3 months (f and g). A clear cavity (red arrows) could be seen around the proximal prostatic urethra on MRI, with a corresponding decrease in prostate volume to 12 cc at 12 months (h) (from original publication III).

5.4 Study IV

The primary objective of Study IV was to evaluate the safety and early oncological outcome of sTULSA in the treatment of localized radiorecurrent PCa.

Eleven patients were included and completed this study. Patient characteristics and disease history of the study population are shown in **Table 16** and **Table 17**. At the time of sTULSA, the median (IQR) patient age, prostate volume, PSA and time from initial PCa diagnosis was 69 years (68-74), 21 cc (18-24), 7.6 ng/mL (4.9-10) and 11 years (9.5-13), respectively. Ten patients had received external beam RT and one patient HDR brachytherapy as primary treatment. One patient also received second-line salvage HDR brachytherapy prior to sTULSA. Ten patients had histopathologically confirmed local recurrence before sTULSA, while one patient refused his screening biopsy. sTULSA was technically feasible in every study patient with a median (IQR) ablation time of 49 min (39-50) and ablation volume of 14 cc (13-17). Three patients underwent whole-gland ablation while eight patients underwent partial ablation. Nine patients received a transurethral catheter immediately after the treatment, while the other two patients received a suprapubic catheter prior to treatment. Each sTULSA was performed under general anaesthesia and all patients were discharged on the first postoperative day, with a median (IQR) duration of post-treatment catheterization of 7 days (1-14). One Grade 3 and three Grade 2 adverse events were reported, all related to urinary retention and urinary tract infection, all of which resolved with antibiotics. One patient who underwent whole-gland treatment had his retention treated by suprapubic catheter and six-month application of 2J stents (Grade 3) due to upper urinary tract dilatation. Ten patients were free of catheterization at one year, while one patient who had received prior salvage brachytherapy remained on intermittent catheterization. Cystoscopy in this patient at 9 months showed an open urethra and bladder neck, a large cavity within the prostate, and no stricture (**Figure 22**). No bowel-related adverse events of any grade were observed in any of the patient.

Table 16. Patient characteristics and disease history before sTULSA (from original publication IV). aADT = adjuvant androgen deprivation therapy; EBRT = external beam radiotherapy; HDR = high dose rate brachytherapy; IMRT = intensity-modulated radiation therapy; ISUP = International Society of Urological Pathology; PSA = prostate-specific antigen; sTULSA = salvage MRI-guided transurethral ultrasound ablation; 3D-CRT = three-dimensional conformal radiation therapy.

Patient Number	Clinical T-stage, at primary treatment	ISUP grade group, at primary treatment	PSA (ng/ml), at primary treatment	PCa diagnosis (year)	Radiation type	Radiation technique	Total Dose (Gy)	No of fiducial Seeds	aADT (months)	Highest PSA (ng/ml) post-radiation	Time from primary therapy to sTULSA (mo)	Age at sTULSA
1	T3	1	13	2006	EBRT	IMRT	78	3	6	15.2	147	69
2	T2	1	8.5	2005	EBRT	3D-CRT	72	0	12	5.5	157	69
3	T3	1	21	2007	EBRT	3D-CRT	72	0	continuous	8.6	138	69
4	T2	5	10	2009	EBRT	3D-CRT	72	0	36	3.3	114	69
5	T1	1	13	1999	EBRT	3D-CRT	68	0	6	16	237	80
6	T1	1	9.5	2008	EBRT	IMRT	72	3	no ADT	11	130	77
7	T1	2	14	2008	EBRT	IMRT	76	3	6	4.7	129	70
8	T2	1	9.4	2015	HDR	HDR	27	0	no ADT	8.3	48	66
9	T1	5	37	2004	EBRT[a]	IMRT	72	3	36	13	175	67
10	T1	1	13	2007	EBRT	3D-CRT	72	0	no ADT	9.5	144	81
11	T3	3	22	2010	EBRT	IMRT	72	3	36	2.15	109	62

[a]The patient received salvage HDR brachytherapy 3 x 9 Gy in 2011 due to histologically verified localized radiorecurrent PCa after EBRT.

Table 17. Radiorecurrent disease characteristics before sTULSA. Grey boxes indicate patients with bifocal disease (from original publication IV). ADT = androgen deprivation therapy; BIC = bicalutamide; CT = computed tomography; ISUP = International Society of Urological Pathology; MRI = magnetic resonance imaging; NA = not available; PET = positron emission tomography; PSMA = prostate-specific membrane antigen; PSA = prostate-specific antigen; Pt = patient; sTULSA = salvage MRI-guided transurethral ultrasound ablation; SUVmax = maximum standardized uptake value.

Pt.	ADT at enrolment, duration	MRI T-stage	PSA (ng/mL)	Prostate volume (cc)	No of positive biopsies / biopsies taken	Total length of biopsy material (mm)	Total cancer length (mm)	ISUP GG	Likert Score	Tumour diameter (mm)	SUVmax
1	BIC, 37 months	2c	1.9	18	4 / 6[a] 3 / 6	NA	NA	3 3	4 4	13 15	7.2 11.3
2	-	2a	5.5	37	3 / 8[b]	70	12	5	4	8	6.8
3	BIC, 37 months	2c	7.5	14	6 / 6[a] 4 / 6	96 75	45 27	3 3	4 4	19 19	48.1 48.1
4	-	2b	3.3	18	4 / 6[b]	84	8	5	5	11	44.6
5	-	2b	16	24	3 / 3[b]	32	22	3	5	20	23.3
6	-	2b	11	21	5 / 6[b]	59	28	3	5	17	5.4
7	-	2c	4.7	33	3 / 4[b] 4 / 4	70 50	21 25	4 2	4 4	16 9	17.7 8.1
8	Degarelix + BIC, 19 months	2b	0.1	24	1 / 3[b]	33	1.5	4	5	12	7.4
9	-	2c	13	21	7/9[b]	101	33	5	5	20	10.7
10	-	2c	9.5	20	Refused biopsy	-	-	-	5	18	49.6
11	BIC, 19 months	No lesion detected	0.1	16	1 / 12[a]	165	8	3	No lesion detected	No lesion detected	No lesion detected

[a] The patient underwent systematic biopsies. [b] The patient underwent MRI-TBx.

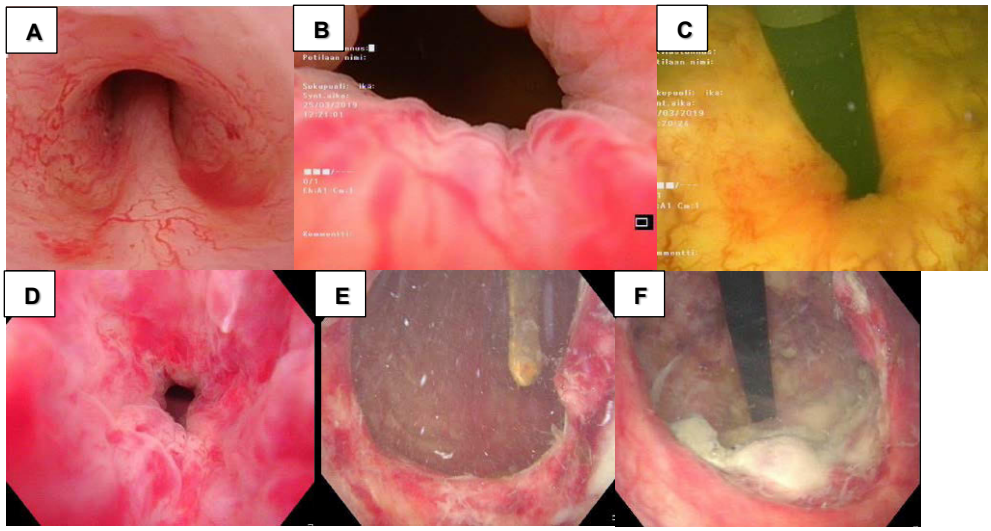

Figure 22. Pre- (A-C) and post-TULSA (D-F) cystoscopy images of a study patient that received whole-gland sTULSA: (A) the bulbotic and membranotic urethra, (B) bladder neck and (C) retroflexion of the bladder neck and the endoscope´s shaft as it traverses the bladder neck. (D-F) cystoscopy images are from the corresponding areas at 9 months after TULSA treatment, showing the patency of the urethra (D) as well as a clear cavity in the bladder neck (E) and inside the prostate (F). Note the tip of the suprapubic catheter (E) and the white necrotic tissue inside the prostate (F).

The uroflowmetry outcomes are demonstrated in **Figure 23**. The median declines in average flow rate, maximum flow rate and voided volume from baseline to 12 months were 27%, 24% and 54%, respectively. The median post-void residual improved threefold at 12 months.

The patient-reported functional outcomes are presented in **Table 18**. A minimal overall decrease in functional status was observed at 12 months. The Expanded Prostate Cancer Index Composite-26 irritative/obstructive domain was most affected, declining from a median score of 94 (IQR 88–94) at baseline to 75 (IQR 72–100) at 12 months. During one-year follow-up, three patients received mirabegron for urinary urgency; otherwise, no new medications affecting urinary or sexual function were required.

The 12-month oncological outcomes are summarized in **Table 19**. At 12 months, 10/11 patients were free of any cancer in the targeted ablation zone, confirmed with biopsy and imaging, and had low and stable PSA. There were one in-field and two out-of-field histopathologically confirmed recurrences at one year, all detected by ^{18}F-PSMA-1007 PET-CT. Only one of the three recurrences was detected by MRI. The median PSA decreased from 7.6 ng/ml (IQR 4.9–10) at baseline to a nadir value of 0.2 ng/ml (IQR 0.1–0.4) and was 0.23 ng/ml (IQR 0.2–0.9) at 12 months, corresponding to a decrease of 97%, despite discontinuation of ADT after TULSA

in those patients (n = 4) receiving ADT before TULSA. The median prostate volume reduction was 55% (IQR 44–63%) at 12 months. A successful sTULSA patient case is presented in **Figure 24**.

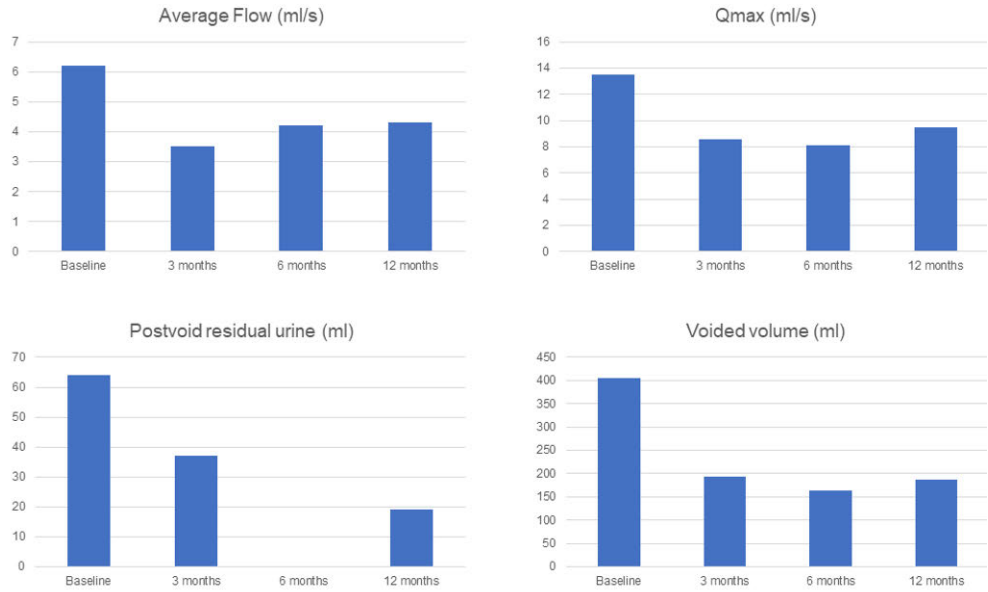

Figure 23. Uroflowmetry outcomes before and after sTULSA (from original publication IV). Qmax = maximum flow rate.

Table 18. Functional outcomes before and after sTULSA (from original publication IV). EPIC = Expanded Prostate Cancer Index Composite, IPSS = International Prostate Symptom Score, IIEF = International Index of Erectile Function.

Functional status questionnaires Median and interquartile range	**Baseline**	**3 months**	**6 months**	**12 months**
IPSS Urinary Symptom Score	8 (4-10)	12 (8-23)	10 (8-14)	7 (5-18)
IPSS Quality of Life	1 (0-3)	3 (2-4)	3 (1-4)	2 (1-3)
IIEF-5 Erectile Function	0 (0-3)	0 (0-1)	0 (0-2)	2 (0-3)
EPIC-26 Urinary Incontinence Domain	100 (100-100)	54 (36-100)	86 (47-100)	96 (46-100)
EPIC-26 Irritative/Obstructive Domain	94 (88-94)	81 (60-88)	75 (59-94)	75 (72-100)
EPIC-26 Bowel Domain	100 (88-100)	96 (88-100)	96 (81-100)	96 (90-100)
EPIC-26 Sexual Domain	18 (17-33)	17 (10-24)	15 (9-18)	15 (13-36)

Table 19. 12-month oncological outcomes after sTULSA (from original publication IV). ISUP = International Society of Urological Pathology; mpMRI = multi-parametric magnetic resonance imaging; PET = positron emission tomography; PSMA = prostate-specific membrane antigen; PSA = prostate-specific antigen; sTULSA = salvage MRI-guided transurethral ultrasound ablation; SV = seminal vesicles.

Patient	Biopsy					Imaging		PSA, ng/mL		
	In-field positive cores / total cores	Out-of-field[a] positive cores / total cores	Total Biopsy Material Length (mm)	Total Cancer Length (mm)	ISUP Grade Group	mpMRI	PSMA PET	Baseline	1-year post sTULSA	Biochemical failure
1	0 / 4	1 / 4	87	1.0	4	neg.	right, SV	1.9[b]	0.7[c]	no
2	0 / 4	-	60	-	-	neg.	neg.	5.5	1.4	no
3	0 / 4	-	69	-	-	neg.	neg.	7.5[b]	0.2[c]	no
4	0 / 4	-	48	-	-	neg.	neg.	3.3	0.3	no
5	1 / 2	0 / 2	20	1.5	2	neg.	left, lobe	16	1.4	no
6	0 / 4	-	43	-	-	neg.	neg.	11	0.2	no
7	0 / 6	-	53	-	-	neg.	neg.	4.7	0.2	no
8	0 / 5	-	75	-	-	neg.	neg.	0.1[b]	0.1[c]	no
9	0 / 4	1 / 2	75	4.0	4	pos.	right, SV	13	1.1[d]	yes
10	0 / 2	0 / 4	90	-	-	neg.	neg.	9.5	0.2	no
11	0 / 6	-	68	-	NA	neg.	neg.	0.1[b]	0.2[c]	no

[a] Out-of-field biopsies were only performed if imaging findings revealed anything suspicious. [b] Patients received ADT. [c] ADT was discontinued after sTULSA. [d] ADT was initiated after the diagnosis of biochemical failure and extraprostatic disease based on imaging at 6 months post-TULSA. ^{18}F-PSMA-1007 PET-CT of this patient showed recurrent tumour in the SV and two new lymph node metastases that had not been visible during preoperative imaging.

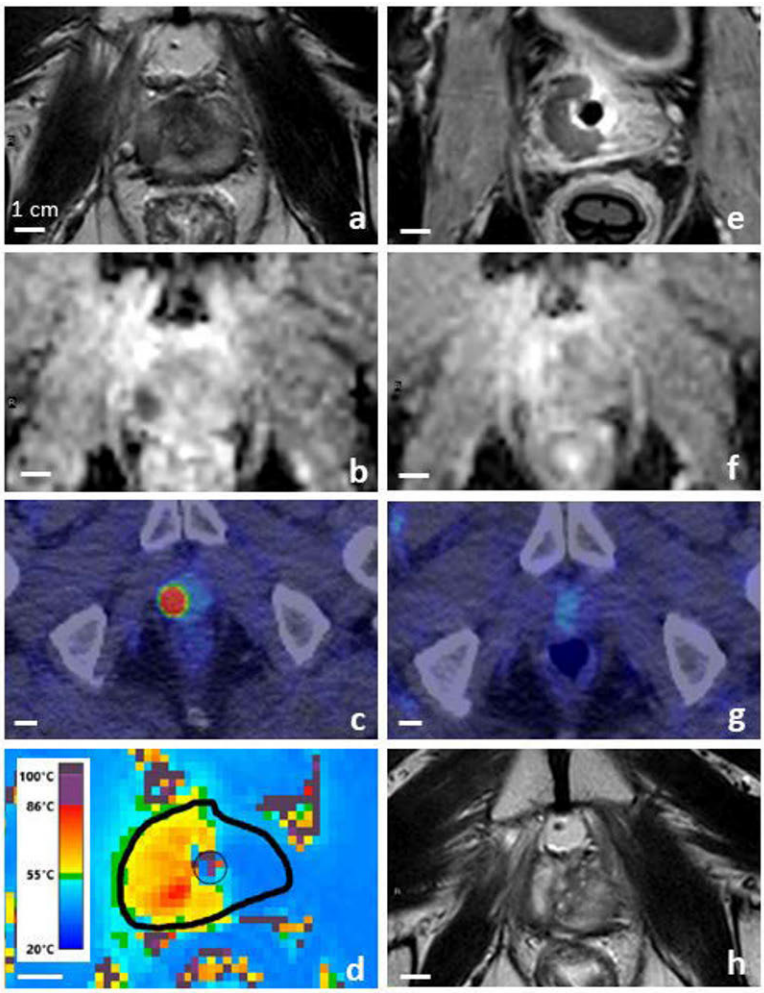

Figure 24. sTULSA patient case example. Screening T2w and DWI MRI imaging (a-b) revealed a distinct focus graded as Likert 5 lesion, which was also present on ^{18}F-PSMA-1007 PET-CT (maximum standardized uptake value of 44.6) (c). The patient received a targeted hemi-ablation (d), where the targeted prostate region reached a lethal minimum temperature of 55°C. The non-perfused volume can be visualized immediately after treatment which demonstrates the acute ablation effect (e). At 12 months the patient underwent additional follow-up imaging. mpMRI (f, h) and ^{18}F-PSMA-1007 PET-CT (g) were both negative. The prostate volume reduced by 56% at 12 months from 18 to 10cc. Imaging findings agreed with post-sTULSA biopsy which showed no vital cancer (from original publication IV).

5.5 Study V

The primary objective of the Study V was to compare standard staging modalities with more advanced imaging modalities in patients with primary high-risk PCa. The study flow chart is presented in **Figure 25**. Eighty patients were enrolled, and 79

patients completed the study. Except for one case of interrupted MRI due to unexpected claustrophobia, all patients were studied with all imaging modalities, resulting in 394 imaging examinations and 788 interpretations. The median interval per patient between the first and the last imaging study was 8 d (IQR: 6–9) and the median follow-up period per patient was 435 d (IQR: 378–557).

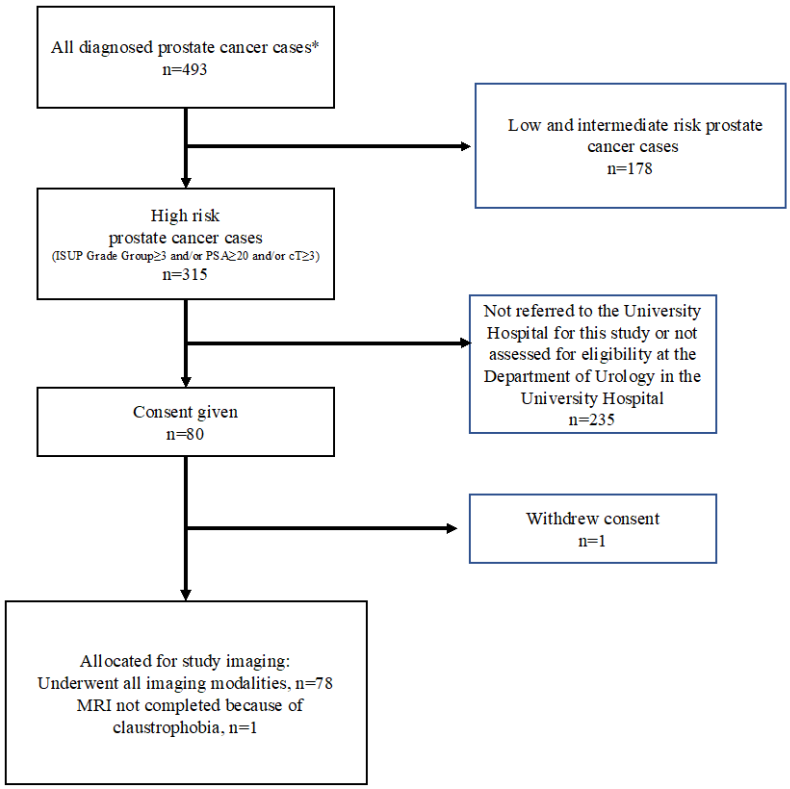

* All men in the Hospital District of Southwest Finland having a new diagnosis of prostate cancer during the period from March 2018 through May 2019. Study patients were identified for this study by the Department of Urology at the Turku University Hospital.

Figure 25. Study flow chart (from original publication V).

The patient and disease characteristics, and primary treatment methods are shown in **Table 20**. Of 79 patients, 20 had metastatic disease. There were no PSMA-negative bone metastases, but in one patient a PSMA-negative extraregional LN disease (M1a) was detected only with MRI.

Table 20. Patient demographics, disease characteristics and primary treatment methods (from original publication V). PSA, prostate-specific antigen; ISUP, International Society of Urological Pathology; RALP, robot-assisted laparoscopic prostatectomy; EBRT, external beam radiotherapy with (n=37) or without (n=1) ADT, androgen deprivation therapy; TULSA, transurethral ultrasound ablation of prostate, ADT; ADT with (n=4) or without (n=13) early chemotherapy with docetaxel. All patients were Caucasians and presented with good performance status at the time of enrolment (Eastern Cooperative Oncology Group Performance status 0-1). [1] Clinical T-stage was determined based on transrectal ultrasound and digital rectal examination before any imaging. [2] All patients with ISUP Grade Group 1 had PSA >20 ng/ml. [3] In two cases palliative transurethral resection of the prostate was performed due to bladder outlet obstruction prior to EBRT and one case underwent palliative TULSA combined with ADT.

Age, years; mean (sd)	70 (7)
PSA, ng/ml; median (IQR) (range)	12 (7-23) (3-2000)
Clinical T-stage; n (%)[1]	
cT1	7 (9)
cT2	38 (48)
cT3	27 (34)
cT4	8 (10)
Biopsy ISUP grade group; n (%)	
1[2]	3 (4)
2	1 (1)
3	29 (36)
4	13 (16)
5	34 (42)
Primary treatment methods; n (%)[3]	
RALP	5 (6)
RALP + lymphadenectomy	17 (21)
EBRT	38 (48)
TULSA	2 (3)
ADT	17 (21)
Watchful waiting	1 (1)

The experience of expert readers is presented in **Table 21**. Altogether 1137 malignant and 444 equivocal lesions were identified. The reported equivocal lesions were distributed among modalities as follows: BS 41 (reader 1: n = 18, and reader 2: n = 23), CT 208 (183 and 25), SPECT-CT 76 (34 and 42), MRI 85 (47 and 38), and PSMA PET-CT 34 (21 and 13). All 1581 lesions were consensus read, resulting in 212 lesions considered as malignant (the reference standard diagnosis): 129 bone, 53 extraregional LN, and 30 visceral.

Table 21. Expert readers background and experience (from original publication V). CT, computed tomography; NM, nuclear medicine physician; RAD, radiologist; SPECT-CT, single photon emission computed tomography-CT; WBMRI, whole-body magnetic resonance imaging; PSMA PET-CT, prostate-specific membrane antigen positron emission tomography-CT.

Reader	Institution	Specialty	Software	Modality	Modality based reading experience (years)	Number of reads of assigned modality
1	Turku, Finland	NM	Hermes	Bone scintigraphy	6	2200
2	Joensuu, Finland	NM	Hermes	Bone scintigraphy	37	10000
3	Turku, Finland	RAD	Vue PACS	CT	25	4000
4	Tampere, Finland	RAD	Vue PACS	CT	20	4000
5	Turku, Finland	NM	Hermes	SPECT-CT	20	1000
6	Jyväskylä, Finland	NM	Hermes	SPECT-CT	15	1000
7	Turku, Finland	RAD	Vue PACS	wbMRI	12	300
8	New York, USA	RAD	Weasis	wbMRI	3	200
9	Helsinki, Finland	NM	AW	PSMA PET-CT	23	500
10	Helsinki, Finland	NM	Hermes	PSMA PET-CT	17	1400

The results of the analyses at patient level are shown in **Table 22**. PSMA PET-CT detected metastatic disease in 11/20 of patients in whom standard imaging (combination of BS and CT) was negative and in 6/20 of patients in whom all other imaging modalities were negative. The inter-reader agreement values (kappa) in the pessimistic analysis at the patient level were 0.56 (95% CI: 0.34–0.77), 0.02 (95% CI: 0.11–0.14), 0.46 (95% CI: 0.26–0.66), 0.34 (95% CI: 0.11–0.56), and 0.82 (95% CI: 0.69–0.95) for BS, CT, SPECT-CT, wbMRI, and PSMA PET-CT, respectively.

At the region level (bone), PSMA PET-CT was significantly more sensitive than other imaging modalities. The AUC values for bone metastases detection with PSMA PET-CT were 0.90 (95% CI: 0.85–0.95) and 0.91 (95% CI: 0.87–0.96) for readers 1 and 2, respectively, while the AUC values for BS, CT, SPECT-CT, and WBMRI were 0.71 (95% CI: 0.58–0.84) and 0.8 (95% CI: 0.67–0.92), 0.53 (95% CI: 0.39–0.67) and 0.66 (95% CI: 0.54–0.77), 0.77 (95% CI: 0.65–0.89) and 0.75

(95% CI: 0.62–0.88), and 0.85 (95% CI: 0.74–0.96) and 0.67 (95% CI: 0.54–0.80), respectively, for the other four pairs of readers. The number of all malignant and equivocal lesions reported by each reader and their concordance with the reference standard diagnosis are shown in **Table 23**. The total numbers of false positive lesions were 22 for PET reader 1 and 30 for PET reader 2. The mean SUVmax values of all true positive and false positive lesions were 10.5 (range: 2.3–55.4) and 5.4 (range: 2.8–10.5), respectively. There were six and 12 false positive metastatic patients according to PET readers 1 and 2, respectively.

Table 22. Sensitivity, specificity and accuracy of both readers of each imaging modality in pessimistic and optimistic analysis at the patient level (from original publication V). CT, computed tomography; SPECT-CT, single photon emission computed tomography-CT; WBMRI, whole-body magnetic resonance imaging; DWI, diffusion-weighted imaging; PSMA PET-CT, prostate-specific membrane antigen positron emission tomography-CT. Planar bone scintigraphy was excluded from the patient level analysis due to inability to assess soft tissues. Metastatic disease was revealed by standard imaging (combination of BS and CT), SPECT-CT, WBMRI and PSMA PET-CT in 9/20, 11/20, 13/20 and 19/20 of the patients, respectively.

Imaging modality and reader	Pessimistic analysis			Optimistic analysis		
	Sensitivity (95%CI)	Specificity (95%CI)	Accuracy (95%CI)	Sensitivity (95%CI)	Specificity (95%CI)	Accuracy (95%CI)
CT 1	0.57 (0.36-0.78)[1,2]	0.33 (0.21-0.45)[1,2]	0.39 (0.27-0.52)[1,2]	0.43 (0.22-0.64)[1,2]	0.79 (0.69-0.90)	0.70 (0.58-0.81)[2]
CT 2	0.43 (0.22-0.64)[1,2]	0.95 (0.89-1.01)[1,2]	0.81 (0.71-0.91)	0.33 (0.13-0.53)[1,2]	0.98 (0.95-1.02)[2]	0.81 (0.71-0.91)
SPECT-CT 1	0.67 (0.47-0.87)[2]	0.74 (0.63-0.85)	0.72 (0.61-0.84)	0.52 (0.31-0.73)[1,2]	0.97 (0.92-1.01)[2]	0.85 (0.76-0.94)
SPECT-CT 2	0.57 (0.36-0.78)[1,2]	0.86 (0.77-0.95)	0.78 (0.68-0.84)[2]	0.33 (0.13-0.53)[1,2]	0.98 (0.95-1.01)[2]	0.81 (0.71-0.94)
WBMRI + DWI 1	0.67 (0.47-0.87)[2]	0.80 (0.70-0.91)	0.77 (0.66-0.88)	0.67 (0.47-0.87)	0.96 (0.91-1.01)[2]	0.88 (0.80-0.97)
WBMRI + DWI 2	0.52 (0.31-0.74)[1,2]	0.82 (0.72-0.92)	0.74 (0.63-0.86)	0.43 (0.22-0.64)[1,2]	0.96 (0.91-1.01)[2]	0.82 (0.72-0.92)
PSMA PET-CT 1	0.90 (0.78-1.00)	0.76 (0.65-0.87)	0.80 (0.69-0.90)	0.86 (0.71-1.00)	0.90 (0.82-0.97)	0.89 (0.80-0.97)
PSMA PET-CT 2	0.95 (0.86-1.00)	0.79 (0.69-0.90)	0.84 (0.74-0.93)	0.95 (0.86-1.00)	0.81 (0.71-0.91)	0.85 (0.76-0.94)

[1] Statistically significant difference (P<0.05) compared to PSMA PET-CT 1. [2] Statistically significant difference (P<0.05) compared to PSMA PET-CT 2.

Table 23. The total number of reported lesions by both readers of each imaging modality and their concordance with the reference standard diagnosis at lesion level (from original publication V). BS, bone scintigraphy; CT, computed tomography; SPECT-CT, single photon emission computed tomography-CT; WBMRI, whole-body magnetic resonance imaging; DWI, diffusion-weighted imaging; PSMA PET-CT, prostate-specific membrane antigen positron emission tomography-CT. There were 212 malignant lesions (reference standard diagnoses) in the patient cohort, of which 129 were bone and 83 soft tissue lesions.

Imaging modality and reader number	Number of positive lesions reported	Number of true positive lesions	Detection rate of true positive lesions	Number of false positive lesions	Number of false negative lesions	Number of equivocal lesions reported	Ratio of equivocal to all detected lesions
BS 1	45	41	19%	4	88	18	29%
BS 2	57	51	24%	6	78	23	29%
CT 1	158	106	50%	52	106	183	54%
CT 2	82	74	35%	8	138	25	23%
SPECT-CT 1	106	99	47%	7	113	34	24%
SPECT-CT 2	76	67	32%	9	145	42	36%
WBMRI+DWI 1	95	88	42%	7	124	47	33%
WBMRI+DWI 2	131	78	37%	53	134	38	22%
PSMA PET-CT 1	205	183	86%	22	29	21	9%
PSMA PET-CT 2	182	152	72%	30	60	13	7%

6 Discussion

6.1 Main findings and discussion of the substudies

6.1.1 Summary

As the diagnosis of PCa shifts toward earlier stages of the disease through PSA screening and advances in imaging methodology, we can treat PCa at a more local stage with the goal of eradicating csPCa with less functional impairment. More precise therapy can be given by combining modern MRI technology with ablative treatment systems, allowing lesion to be visualized in real-time to improve targeting accuracy, while MRI-thermometry can monitor the treatment response in real time and CE-MRI confirms the treatment response during the procedure. TULSA is a promising method utilizing these advanced MRI techniques.

We investigated the utility of TULSA in the treatment of PCa in the following settings in a prospective phase 1 trial: FT of localized PCa, palliative therapy, and treatment of locally recurrent PCa after RT. To summarize the results, TULSA seems to ablate prostate tissue efficiently, predictably, accurately and safely, whether it is treatment-naive or radiotherapy-treated prostate tissue. The thermal damage is precisely delimited by the planned treatment area with sharp demarcation of thermal injury. The method can be deployed anywhere in the prostate, either whole-gland or focal. Furthermore, TULSA appears to achieve local symptom relief in palliative patients and encouraging preliminary oncological control in salvage patients.

In the second section of the doctoral thesis, we investigated the diagnostic performance of advanced imaging, particularly PSMA PET and MRI, in metastasis staging of patients with high-risk PCa, as well as in the treatment planning and treatment response assessment of TULSA. In summary, PSMA PET outperformed other imaging modalities in primary metastasis staging of high-risk PCa. Compared to MRI, PSMA PET appears to more accurately identify the post-TULSA extent of local recurrence in radiorecurrent PCa.

6.1.2 Discussion of the TULSA substudies

In a prospective treat-and-3-week-resect study (Study I) we reported our initial experience with lesion-targeted TULSA in the treatment of MRI-visible biopsy-concordant csPCa in six patients and demonstrated safe, accurate and effective in-field ablation of these lesions.

In contrast to a phase 1 study including 30 patients with localized PCa undergoing whole-gland TULSA with conservative margins (Chin et al. 2016), our approach using lesion-targeted ablation caused no urinary tract infections or urinary retention in our study patients. This is most likely related to the smaller ablation volumes achieved with the lesion-targeted approach. Other contributing factors include a substantially shorter catheterization time, 2-3 days compared to two weeks, and the avoidance of pre-TULSA cystoscopy and suprapubic catheter. Overall, no perioperative complications were observed in our study and there were no significant differences in any of the functional and QoL questionnaires or uroflowmetry results between baseline and 3 weeks after TULSA, emphasizing the low toxicity of this treatment approach.

Previous treat-and-immediate-resect studies investigating a similar technology examined thermal injury after TULSA only in the acute state (Chopra et al. 2012, Ramsay et al. 2017). In contrast, our study evaluated delayed thermal injury by following the short-term radiological and histopathological evolution of ablation, which was assessed after a 3-week follow-up period between the TULSA and RALP procedures. The non-perfused volume gradually increased in size by an average of 36% at 3 weeks, indicating that immediate post-procedure non-perfused volume substantially underestimates the size of the ablated volume. Based on histopathological analysis of the RP specimens, the mean delayed thermal injury between complete necrosis and the outer limit of thermal injury across all study patients was 1.7 ± 0.4 mm, which is in close agreement with previous treat-and-immediate-resect studies (Chopra et al. 2012), and also shows a sharp demarcation of the delayed thermal injury. There was clear morphometric and volumetric concordance between radiology and histology in all targeted tumours. However, the 3-week non-perfused volume was 19% larger than the delayed necrosis volume, which is consistent with previously reported results of ablative therapy in a similar study design (Lindner et al. 2010, Bomers et al. 2017). Our study was the first to demonstrate that ablation and subsequent coagulation necrosis to the capsule and beyond can be obtained with TULSA. This finding is clinically relevant because a significant proportion of PCas are in the vicinity of the capsule or infiltrate into the capsule.

In our study population 50% presented with intermediate-risk and 50% with high-risk disease. This ratio differs from previous studies exploring similar technology but in mainly low-risk disease (Chin et al. 2016, Ramsay et al. 2017).

Our study confirms the tissue-type independence of TULSA ablation, and was the first to demonstrate that aggressive, predominantly Gleason pattern 4 tumours will respond to TULSA with complete histopathologically verified cell death.

Limitations of this study included a small sample size with a heterogeneous patient population containing intermediate to high-risk tumours. Longer-term toxicity could not be explored, although a favourable 3-week safety and toxicity profile may predict longer-term functional outcomes. Because of the treat-and-resect study design, longer-term oncological outcomes could not be assessed. Since a conservative treatment strategy was ethically required near the neurovascular bundle, this contributed to residual PCa found at histopathology in four patients, all of which was outside the targeted region and within the 3mm safety margins. This limitation was an expected result and concordant with treatment planning, demonstrating accurate targeting and a sharp demarcation of thermal injury. Importantly, there was no histopathologically documented in-field residual cancer in any of the study patients. Although one of six study patients presented with apparently viable cancer cells within the ablated region at initial H&E-stained histopathology, further analysis of MRI-thermometry, 3-week non-perfused volume and immunohistochemistry demonstrated that these cells had undergone thermal fixation and were non-viable.

Study II reviewed the concept of thermal fixation using this patient case, which was the first report of thermal fixation in the prostate after TULSA. As demonstrated in the results section, the cause of thermal fixation in this particular case was probably the most rapid and one of the highest heat responses in the tissue. It is known that sufficiently high and rapid temperature rise in the tissue can cause denaturation of the structural and enzymatic protein constituents of tissue, so that they are ablee to resist the typical repair/breakdown pathways of the body (Coad et al. 2003, He et al. 2004). Therefore, thermally-fixed cells maintain their cytocidal staining characteristics and preserved nuclear chromatin, which gives histological staining appearance (in this case H&E staining) similar to viable cells. In particular, loss of cytokeratin 8 staining (as assessed by Cam5.2 antibody) was indicative of severe cellular damage in both thermally-fixed and thermally-necrosed regions. Our detailed description of staining outcomes in whole-mount tissues acquired three weeks after treatment, supported by MRI-thermometry and CE-MRI, provides an important addition to the limited literature on thermal fixation. These observations provide guidance for pathologists reviewing the increasing number of post-ablation histopathological specimens in the future. The literature review of thermal fixation is included in **Table 24**.

Table 24. Previous literature of thermal fixation (from original publication II). CE-MRI=contrast-enhanced magnetic resonance imaging; CITT = conductive interstitial thermal therapy; CK = cytokeratin; FLA = focal laser ablation; H&E = hematoxylin-eosin; HIFU = high intensity focused ultrasound; HP = histopathology; ICH = immunohistochemistry; NADH = nicotinamide adenine dinucleotide; LITT=laser interstitial thermal therapy; MW= microwave; PCNA = proliferating nuclear antigen; PSA = prostate-specific antigen; RFA = radiofrequency ablation; SS = supravital staining; TTC = triphenyl tetrazolium chloride; vWF = von Willebrand factor.

Author	Therapy device	Material	Methods				Validation of thermal fixation
			SS	HP	IHC	Others	
Van Leenders et al. 2000	HIFU	9 human prostates *in vivo*		H&E; uranyl acetate; lead citrate	CK8; anti-PSA; panCK; Ki67	Electron microscopy	Thermal fixation indicated by H&E in 6 prostates; non-viability confirmed by CK8 negativity and electron microscopy
Bhowmick et al. 2004	Heating with copper block	10 human prostate tissue samples *in vitro*		H&E		Fluorescence microscope (EthD-2 and Hoechst 33342 dyes)	Thermal fixation indicated by H&E; non-viability confirmed by fluorescence microscopy
Boyes et al. 2007	Transurethral ultrasound	7 canine prostates *in vivo*	TTC	H&E		CE-MRI	Non-viability confirmed by TTC unstaining; thermally fixated in H&E-staining
Lindner et al. 2010	FLA	4 human prostates *in vivo*		H&E	CK8 (CAM 5.2)	CE-MRI	Thermal fixation indicated by H&E; non-viability confirmed by CK8 negativity and CE-MRI
Stafford et al. 2010	LITT	7 canine prostates *in vivo*		H&E	vWF	CE-MRI	Thermal fixation in every prostate in H&E; non-viability confirmed by vWF
Germer et al. 1998	LITT	55 rabbit livers *in vivo*		H&E; silver nitrate; azan		CE-MRI	Non-viability indicated by morphology with H&E; non-viability confirmed by CE-MRI
Coad et al. 2003	RFA	4 human livers *in vivo*		H&E		CE-MRI: CE-CT	Thermal fixation in every liver in H&E; non-viability confirmed by CE-MRI or CE-CT

Author	Therapy device	Material	Methods				Validation of thermal fixation
			SS	HP	IHC	Others	
Leslie et al. 2008	HIFU	6 human livers *in vivo*	TTC	H&E	Factor VIII	CE-MRI	Thermal fixation in 1 indicated by lack of post-mortem autolysis in morphology; non-viability confirmed by Factor VIII and CE-MRI
Courivaud et al. 2014	HIFU	4 + 5 swine livers *in vivo*[a]		H&E		CE-MRI	Thermal fixation in 7 livers in H&E; non-viability confirmed by CE-MRI and by presence of foreign-body giant cells
Hennings et al. 2009	CITT	8 nipples of one swine in vivo; 8 rabbit VX2 carcinomas *in vivo*	TTC	H&E	Anti-PCNA	Autofluorescence microscopy	Thermal fixation indicated by H&E; non-viability confirmed by TTC and autofluorescence microscopy
He et al. 2004	MW thermal therapy	5 + 7 + 8 porcine kidneys *in vitro* or *in vivo*[b]		H&E			Thermal fixation in every kidney; non-viability indicated by morphology with H&E
Wu et al. 2006	HIFU	23 human breasts *in vivo*	NADH	Uranyl acetate; lead citrate; H&E	biotin-streptavidin-peroxidase; CA15-3; VEGF	Electron microscopy	Thermal fixation in 11 breast tumours indicated by H&E; non-viability confirmed by NADH and electron microscopy

[a] Four ablated and euthanized after immediate MRI; five in survival study, euthanized after 1-week MRI.

[b] Four animals, five kidneys in vitro; six animals, seven kidneys in vivo 2-hour perfusion; four animals, eight kidneys in vivo 7-day perfusion.

In Study III, TULSA was evaluated for the first time in the treatment of local symptoms and complications due to locally advanced PCa in a palliative setting. We demonstrated the safety and feasibility of TULSA for the ablation of large tumours, some of which infiltrated the bladder and posterior bladder wall. Furthermore, catheter removal was successful for five patients at one week post-TULSA and 50% of the patients were catheter-free at 1 year with no subsequent palliative TURP.

In locally advanced PCa, gross haematuria can be related to bladder outlet obstruction or direct invasion of PCa to the urinary tract. These complications are difficult to manage and can require repeat invasive procedures and/or hospital admission. Previous RT can cause radiation urethritis or cystitis which may result in bleeding, and concurrent anticoagulation compounds this risk. In the current study, recurrent/ongoing gross haematuria ceased for all nine patients who had this symptom before pTULSA, with the added benefit that pTULSA can also relieve bladder outlet obstruction in an outpatient setting with a relatively short hospitalization time.

TULSA has some inherent advantages compared to existing surgical interventions for treating local symptoms and complications caused by locally advanced PCa. The resection of malignant prostatic tissue during TURP may potentially cause tumour spillage and systemic tumour dissemination (Moreno et al. 1997, Hanks et al. 1983). In addition, the clinical success rate of palliative TURP is moderate and carries notable surgical and anaesthetic risks which increase with age and may exclude those who cannot discontinue anticoagulation (Heidenreich et al. 2015, Marszalek et al. 2007, Crain et al. 2004, Pelletier et al. 2018, Gnanapragasam et al. 2006). Alternative surgical options including palliative prostatectomy and cystoprostatectomy with urinary diversion may be considered, but due to their technical complexity, they are available only for patients with good performance status and at centres with extensive experience (Pfister et al. 2011, Haidl et al. 2018). There is only limited evidence for the efficacy of palliative RT (Din et al. 2009, Cameron et al. 2015) and prostate arterial embolization (Pereira et al. 2016, Chen et al. 2017) in the treatment of gross haematuria caused by locally advanced PCa. Non-surgical options including ADT and other systemic therapy can achieve notable response in metastasis, but have a minimal effect on the prostate itself (Haidl et al. 2018). In contrast, TULSA enables bloodless incision-free ablation of prostatic tissue, providing a minimally invasive option for the treatment of gross haematuria and bladder outlet obstruction, and with an ablation pattern that is tailored to each patient's tumour and comorbidities.

Limitations in this study included a small sample size and a non-randomized study setting with no control arm. Research on palliative intervention includes challenges in measuring validated efficacy outcomes in a patient population undergoing a rapid decline in health (Khafagy et al. 2007). We therefore focused on catheter-free and gross-haematuria-free time, and a reduced need for hospitalization.

We published the first evaluation of TULSA for the treatment of localized radiorecurrent PCa in Study IV, found it safe and technically feasible for all patients, and demonstrated promising early-stage oncological control and low toxicity.

At one-year follow-up there were adverse events (three grade 2 and one grade 3) caused by infection and urinary retention, comparing favourably with other salvage intervention modalities. There were no serious complications such as urethral strictures or bowel related adverse event after sTULSA. Although rare, these complications have been reported after salvage interventions using other ablative modalities (Chade et al. 2012, Crouzet et al. 2017, Siddiqui et al. 2016, Peters et al. 2013). Based on patient reported functional questionnaires, sTULSA had a minor impact on QoL, the most significant a modest 20% deterioration of irritative/obstruction symptom scores, which corresponded to declines in average flow rates and maximum flow rates at 12 months. As there are no other studies using TULSA in previously treated patients, these adverse effects upon functional outcomes appear to be related to its effect upon a previously irradiated prostate and prostatic urethra. These functional impairments were not seen in earlier studies of whole-gland TULSA for the primary treatment of organ-confined PCa, in which the benign prostatic hyperplasia component was also treated (Chin et al. 2016, Elterman et al. 2020).

At one year 10/11 patients were free of cancer in the targeted ablation volume while 2/11 patients had an out-of-field recurrence. Of the three patients with biopsy-proven local recurrence, the only one having an in-field recurrence and receiving partial sTULSA, presented with a slowly rising PSA. At biopsy 1.5 mm of vital cancerous tissue (ISUP GG 2) was found in the tip of one biopsy core. This recurrence was visible only on ^{18}F-PSMA-1007 PET-CT, and appeared at the periphery of the ablated region, suggesting targeting failure rather than ablation failure. This patient has been placed on active monitoring due to a low and stable PSA of 1.4 ng/ml. The second patient who had also undergone partial sTULSA, underwent a second partial sTULSA targeted to the biopsy-proven out-of-field recurrence in the base of the seminal vesicle, which was also detected by ^{18}F-PSMA-1007 PET-CT. This second sTULSA was well tolerated, and the patient had a low and stable PSA of 0.89 ng/ml at 12 mo after the second sTULSA. The third patient, who had undergone whole-gland sTULSA, experienced BCR at 6 months post-TULSA. ^{18}F-PSMA-1007 PET-CT showed recurrent tumour in the seminal vesicle and two new LN metastases that had not been visible during preoperative imaging. This patient was given ADT.

Treatment monitoring after nonsurgical salvage therapy is challenging, particularly after partial treatment. In this study we used PSA, ^{18}F-PSMA-1007 PET-CT, mpMRI, and 12-month biopsies for monitoring of oncological outcomes. ^{18}F-PSMA-1007 PET-CT detected all three biopsy-proven recurrences, in contrast to mpMRI, which detected only one. There was no BCR nor histologically verified

recurrence within the prostate in any of the patients with negative ^{18}F-PSMA-1007 PET-CT.

TULSA has several potential advantages over existing nonsurgical salvage interventions with regard to patient selection, ablation patterns, and ablation time. Partial cryotherapy is mainly restricted to recurrent anterior tumours because it allows less spatial control. Organ-protective warming tools render cryotherapy potentially less effective for apical and periurethral tumours (Van Son et al. 2018, Ganzer et al. 2018). On the other hand, HIFU offers high spatial control, but since it requires a longer completion time for ablation and is more restrictive in terms of treatment volume, it is used more often for posterior tumours (Ingrosso et al. 2020). Since HIFU is delivered transrectally, treatment of anterior tumours with this modality may be challenging. In contrast, TULSA has the distinct advantage of being delivered transurethrally, offers high spatial control by combining the precision of the ultrasound heat source with thermometry monitoring, and can also treat large tissue volumes in a relatively short time. These advantages enable TULSA to be used anywhere in the prostate, for either whole or partial gland ablation.

Limitations of this study include the small sample size, the non-randomized study design without a control arm, and short-term oncological follow-up. The limitations of TULSA technology are primarily financial, including relatively complex technical requirements, prolonged in-bore magnet time and MR-compatible anaesthesia equipment.

6.1.3 Discussion of the PROSTAGE substudy

In Study V, the PROSTAGE study, we compared the diagnostic performance of conventional and advanced imaging modalities in primary metastasis staging of men with high-risk PCa. We found that ^{18}F-PSMA-1007 PET-CT was superior to the other imaging modalities studied for the detection of distant metastasis.

A recent Australian multicentre RCT (proPSMA) including 300 patients reported superiority of ^{68}Ga-PSMA-11 PET-CT over conventional imaging (combination of BS and CT) in the primary staging of high-risk PCa (Hofman et al. 2020). The study included a cross-over setting in which patients were imaged in the second phase by comparative imaging if no more than two metastases were detected in the first phase imaging. The study demonstrated that Ga-PSMA-11 PET-CT had a 27% better accuracy in identifying LN or distant metastases compared to conventional imaging. Despite these promising results, the superiority of PSMA PET-CT over other new imaging methods, especially wbMRI, requires further study. Evidence indicates that wbMRI is an effective method for the overall staging of PCa and has been shown to provide better detection of distant metastasis than traditional imaging (Lecouvet et al. 2012). Furthermore, the optimal tracer for PSMA PET imaging has yet to be

determined. The new ^{18}F-labeled PET markers, DCFPyL and PSMA-1007, are promising PSMA targeting ligands (Giesel et al. 2018, Cardinale et al. 2017) that offer a potentially better alternative to PCa imaging (Kesch et al. 2017).

In the PROSTAGE study, the diagnostic performance of conventional imaging studies (CT and BS) was compared to more advanced imaging studies (99mTc-HMDP SPECT-CT, wbMRI with DWI, ^{18}F-PSMA-1007 PET-CT) in primary staging of men with high-risk PCa. In this study all patients were imaged by all five imaging methods, and each imaging method was reported by two independent experts blinded to results from the other modalities. The median time per patient between the first and last imaging was only 8 days and the median follow-up was 435 days. So-called hard criteria were used to validate the imaging findings, with only PSMA-avid imaging findings having either histopathological evidence or an anatomical correspondence at either primary or follow-up imaging were accepted as evidence of PCa metastasis. In cases where the nature of the PSMA-avid lesion remained uncertain after the first-line imaging, follow-up imaging was performed using CT and/or 3T mpMRI from the region of interest to search for the development of an anatomically corresponding lesion. In this study 25% (20/79) of the patients were diagnosed with distant metastatic disease, of which ^{18}F-PSMA-1007 PET-CT detected the most, 95% (19/20). However, another 15% (12/79) of the patients were diagnosed with false positive metastatic disease. In other words, these patients had a PSMA-avid lesion without histopathological proof of PCa or anatomical correspondence in the primary or one-year follow-up imaging. The mean SUVmax value was 5.4 (range: 2.8–10.5) in false positive PSMA-avid lesions and 10.5 (range: 2.3–55.4) in true positive PSMA-avid lesions. In addition to these false positive lesions, subtle PSMA-uptake was frequently found in bones, especially in the ribs.

Our patient data were similar to those in the proPSMA study, in which 16% (48/300) of their patients were diagnosed with metastatic disease. However, only 6% of cases (18/300) were diagnosed with metastases using hard criteria for validation. Imaging findings that were interpreted as metastases in the proPSMA study with soft criteria were interpreted as false positives in the our PROSTAGE study due to our stricter validation criteria. These more stringent validation criteria may have contributed to the relatively high number of false positive PSMA PET findings reported in our study.

In addition to the non-randomized study design, a limitation of the PROSTAGE study was the small number of histopathologically-confirmed distant metastases. The inherent challenge in investigating the diagnostic performance of modern imaging methods with improved sensitivity for metastasis detection, such as PSMA PET-CT, is that they are likely to identify smaller lesions, some of which lack an anatomically corresponding lesion necessary for successful image-guided biopsy. Furthermore, it is ethically questionable to biopsy lesions which are detectable only

with PSMA, because a negative biopsy result does still not completely rule out the possibility of metastasis, while the significance of a positive finding in treatment planning is also unclear. There is not yet evidence that radical treatment of a single metastasis would improve treatment outcomes.

One of the strengths of the PROSTAGE study was the long clinical and imaging follow-up, which provided a more reliable assessment of the nature of PSMA-avid lesions. The use of hard validation criteria, as in our study, may be closer to the truth than the soft validation criteria used in the proPSMA study, but an appreciation of this challenge is necessary when interpreting PSMA PET-CT scans for the planning of patient care.

In studies of newer and more sensitive imaging methods, one of the main objectives is to determine the impact of the new imaging method on the choice of treatment received by the patient. In the proPSMA study, PSMA PET-CT changed the treatment plan in the first phase in 28% of patients and in the second phase after traditional imaging in 27% of patients. In the PROSTAGE study, the corresponding number for PSMA PET was 18%. However, a change in treatment plans is not always the same as a better treatment outcome. If the validation criteria are soft, more PSMA-avid lesions are accepted as metastases and treatment plans are more likely to be changed. In the worst-case scenario, the patient may be denied radical curative-intent therapy due to “false positive” metastatic disease. Because of this potential risk associated with PSMA PET imaging, at the design phase of the PROSTAGE study it was prospectively decided not to prohibit radical treatment in patients with suspected metastatic disease based on PSMA PET-CT alone.

Based on the proPSMA and PROSTAGE studies, we know that PSMA PET can detect metastatic, often oligometastatic, disease at an earlier stage than traditional imaging, but there is still much uncertainty as to how these more precise findings should affect therapeutic decisions (Lecouvet et al. 2018). The STAMPEDE study demonstrated a survival benefit from prostate irradiation combined with ADT in patients with primarily oligometastatic disease detected by conventional imaging methods (Burdett et al. 2019). Studies are underway to investigate the benefits of radical treatment of metastases with stereotactic ablative radiotherapy in men with oligometastatic recurrence (Phillips et al. 2020). The radical treatment of local tumours and solitary metastases in primary PCa is under investigation (Connor et al. 2020, Kim et al. 2017).

6.2 Implications and future perspectives

PCa is the most common cancer in men, heterogeneous in its disease spectrum, with some diseases leading to death despite radical treatment and some not requiring any treatment. Established methods of radical therapy, including RP and RT, treat the

entire gland regardless of where the underlying pathology is located and therefore affect urogenital function, since structures maintaining these functions in the immediate vicinity of the prostate will be affected. With the shift of PCa diagnosis to earlier stages of the disease, and with the development of new imaging techniques, it has become possible to give targeted therapy to men with PCa. In addition, the overall extent of the disease can also be more reliably determined with modern imaging, with the added benefit of improved tumor characterization. Image-guided ablative cancer therapy and the FT approach have gained acceptance as new technologies have emerged in PCa management. There are also significant limitations related to the FT approach for the treatment of PCa. Although partial surgery and FT are accepted options in selected patients in almost all solid cancers, the legitimacy of FT in PCa remains controversial as this malignancy is frequently multifocal. Although mpMRI is highly sensitive for detecting csPCa at the patient level, its diagnostic performance at the lesion level is limited. MRI also tends to underestimate the size of the tumour. Other challenges in FT include the ability of imaging methods to distinguish cancer from healthy tissue with sufficient accuracy and to develop a highly accurate energy delivery system. The protocols for postoperative surveillance after FT have yet to be established.

In this doctoral thesis we have shown that TULSA is safe and feasible for various PCa treatment indications, providing personalized, targeted care. The promising phase 1 results of TULSA in the treatment of localized PCa, encouraged us to progress to phase 2 studies (PRO-TULSA-PCa, NCT03814252), in which 35 of 60 patients have already been treated with TULSA. The results of this study should be available in the spring of 2022. The encouraging results of the salvage patient group allowed us to move to a phase 2 study and expand the cohort to 40 patients (HIFU-PRO, NCT03350529), 25 of whom have already received the sTULSA treatment.

PSMA PET-CT has established its position in the diagnosis of BCR after radical therapy. Although PSMA PET-CT improves the detection of metastasis in primary PCa, there is currently no oncological endpoint evidence that patients would benefit from an earlier diagnosis of (oligo) metastatic disease with PSMA PET-CT. In addition, all risk classifications and treatment recommendations in current use are based on studies that have used only traditional imaging methods for metastasis staging. For these reasons, the EAU guidelines continue to strongly recommend the use of BS and CT in primary staging of men with high-risk PCa. Accordingly, PSMA PET-CT has not yet replaced traditional imaging modalities in primary staging in our hospital district, but is strongly recommended for restaging recurrent disease after first-line therapy.

7 Summary/Conclusions

In these feasibility studies TULSA was shown to successfully ablate treatment-naive and radiotherapy-treated prostate tissue efficiently, accurately and safely.

Studies I-II demonstrated that TULSA enables lesion-targeted treatment of localized PCa, keeping a 3 mm safety margin from the neurovascular bundle, and had considerably fewer short-term adverse events than whole-gland TULSA using a similar safety margin. Accurate and efficient targeted ablation of PCa lesions was demonstrated by histopathological evaluation of RP specimens. Histopathology in one patient revealed thermally fixed nonviable cells after TULSA. This artefact may result in the misinterpretation of treatment failure if this phenomenon is not recognized and confirmative immunohistochemistry is not performed. Our results indicate that Cam5.2 staining for cytokeratin 8 is a reliable method for distinguishing thermally fixed from viable cells.

Study III demonstrated the feasibility of pTULSA for the palliative ablation of locally advanced PCa giving a long-term control of haematuria, a reduced hospitalization time and relief of lower urinary tract obstruction in some cases.

Study IV demonstrated the feasibility of sTULSA for the ablation of radiorecurrent PCa with encouraging early-stage oncological control and low toxicity. Preliminary results suggest the superiority of PSMA PET-CT over mpMRI for monitoring treatment outcome.

In Study V PSMA PET-CT outperformed other imaging modalities for detecting distant PCa metastases, but at the expense of false positive bone lesions.

In conclusion, these studies have demonstrated the effectiveness of ^{18}F-PSMA-1007 PET-CT in PCa diagnosis and the effectiveness of TULSA in PCa therapy.

Acknowledgements

Research for this thesis was carried out in the Departments of Urology and Radiology and in the Turku HIFU Research Centre, all at the University of Turku and Turku University Hospital, from 2016-2020, with assistance from the Department of Medical Physics, the Department of Biostatistics, the Department of Pathology, the Department of Clinical Physiology and Nuclear Medicine, and the Turku PET Centre.

The most influential persons behind the thesis are my supervisor's Adjunct Professor Peter Boström, Professor Roberto Blanco and Adjunct Professor Pekka Taimen. I can vividly remember my first meeting about the TULSA project at Roberto´s office, where Peter introduced me to Roberto and said "here is a guy who makes things happen when he gets involved". We launched an ambitious TULSA project that has required much work but has been even more rewarding. Peter, Roberto and Pekka, I am grateful for your trust and my good fortune in having you as supervisors and mentors during the early stages of my research career. Peter, I warmly recall the many long discussions we have had about the scientific aspects of prostate cancer after long days of clinical work and your ability to come up with new ideas and find new approaches in situations where I thought we had come to a dead end.

I wish to thank Professor Boris Hadaschik and Adjunct Professor Jukka Perälä for their thorough review of the thesis and constructive criticism which considerably improved the quality of this thesis.

Professor Peter Dean, our scientific discussions have gone on for countless evenings and for hours on end, even the time I was running around Hirvensalo during our telephone discussion. You have always been available to teach me ever more about scientific thinking and writing.

I am especially grateful to the late Professor Risto Santti, who ignited my interest in anatomy and scientific research from the beginning of my medical studies, and continued to advise and help me up until his very recent death.

I owe my deepest gratitude to the entire Turku HIFU research group: Pietari Mäkelä, Heikki Pärssinen, Pertti Nurminen, Antero Horte, Aida Steiner, Visa Suomi, Jani Saunavaara, Teija Sainio, Kalle Koskensalo, Antti Viitala, Emil Ylijoki, Lauri

Eklund, Ilari Virtanen, Cameron Wright and Ari Katila, and the PROSTAGE research group: Otto Ettala, Simona Malaspina, Ivan Jambor, Minna Sandell, Sami Kajander, Irina Rinta-Kiikka, Jukka Schildt, Ekaterina Saukko, Pentti Rautio, Kirsi Timonen, Tuomas Matikainen, Tommi Noponen, Jani Saunavaara, Eliisa Löyttyniemi, Pekka Taimen, Jukka Kemppainen, Peter Dean, Roberto Blanco, Hannu Aronen, Marko Seppänen and Peter Boström.

My thanks also go to the research nurses in the Department of Urology: Heidi Aaltonen, Kaisa Reunanen, Laura Lindén and Sara Karnell, and the radiology technologists in the Department of Radiology (TG3-MRI): Mira Hallenberg, Fanny Nyroos, Kari Jarkko, Kaisa Saarinen, Viivi Magerholm, Satu Holmström, Miia Airola, Jouni Nyroos, Anni Koskinen, Ville Roppola, Iina Luoma-Aho and Säde Korpinen, and the anesthesia nurses in the Department of Anesthesiology: Anneke Van Vliet, Erika Tamminen, Ella Helander and Jaana Kujanpää. I would also like to thank the members of the follow-up committee for doctoral training: Johanna Virtanen and Saila Kauhanen.

I wish to express my gratitude to my fellow colleagues at the Turku University Hospital: Matti Laato, Kimmo Kuusisto, Pekka Kinnala, Esa Kähkönen, Antero Horte, Sari Liesjärvi, Antti Salminen, Otto Ettala, Kari Syvänen, Pertti Nurminen, Saku Mäkelä, Harri Backman, Juha Knaapila, Ilkka Nikulainen, Ville Sell, Lauri Reunanen (now working at the Satakunta Central Hospital) and Jukka Häkkinen (now working at Mehiläinen Oulu), and Jouni Huttunen, Niilo Hendolin and Tapani Liukkonen at the Mikkeli Central Hospital. You have played important roles in my development as an academic surgeon.

I am fortunate to have my old friends who remind me that there really is more to life than medicine. I thank you all for your social support and lifelong friendship. Sports, especially tennis, have been an important part of my life and an important balancing factor alongside the challenges of work and research.

I wish to express my dearest thanks to my parents, Anu and Henrik, and my siblings, Eerik, Selina and Saara, who have given me such wonderful support throughout my life. I especially thank my father, Henrik, for inspiring me in my academic career with his example. I fondly remember my recently departed grandfather, Johannes Anttinen, as my role model, a dedicated surgeon and scientist.

I thank my dear mother and mother-in-law, Anu and Maija, for your generous help, particularly caring for our children, making it possible for me to carry out the work for this thesis.

My greatest gratitude goes to my dear spouse, Suvi, the mother of my two dear children Leevi and Matilda. In addition to your own challenging work, you have always taken care of the home, the children, and me.

This work could not have been accomplished without funding. I would like to thank the Finnish Urological Association, the Finnish Urological Research

Foundation, the Finnish Medical Foundation, the Turku University Hospital Research Foundation, the Turku University Foundation, the Emil Aaltonen Foundation, the Ida Montin Foundation, the Paulo Foundation, the Päivikki and Sakari Sohlberg Foundation, the Finnish Cultural Foundation and the Cancer Foundation Finland for their support.

May 2021
Mikael Anttinen

References

Ahmed, H. U., Arya, M., Freeman, A., & Emberton, M. (2012). Do low-grade and low-volume prostate cancers bear the hallmarks of malignancy? *Lancet Oncol,* 13(11), e509-e517.

Ahmed, H. U., Bosaily, A. E., Brown, L. C., Gabe, R., Kaplan, R., Parmar, M. K., et al. (2017). Diagnostic accuracy of multi-parametric MRI and TRUS biopsy in prostate cancer (PROMIS): A paired validating confirmatory study. *Lancet*, 389(10071), 815-822.

Albertsen, P. C., Hanley, J. A., & Fine, J. (2005). 20-year outcomes following conservative management of clinically localized prostate cancer. *JAMA*, 293(17), 2095-2101.

Algaba, F., & Montironi, R. (2010). Impact of prostate cancer multifocality on its biology and treatment. *J Endourol*, 24(5), 799-804.

American Cancer Society, A. 2008. Cancer facts and figures 2008. American Cancer Society.

Arora, R., Koch, M. O., Eble, J. N., Ulbright, T. M., Li, L., & Cheng, L. (2004). Heterogeneity of gleason grade in multifocal adenocarcinoma of the prostate. *Cancer*, 100(11), 2362-2366.

Asimakopoulos, A. D., Miano, R., Virgili, G., Vespasiani, G., & Agrò, E. F. (2012). HIFU as salvage first-line treatment for palpable, TRUS-evidenced, biopsy-proven locally recurrent prostate cancer after radical prostatectomy: A pilot study. *Urol Oncol*, 30(5), 577-583.

Bahler, C. D., Green, M., Hutchins, G. D., Cheng, L., Magers, M. J., Fletcher, J., et al. (2019). Prostate specific membrane antigen targeted positron emission tomography of primary prostate cancer: Assessing accuracy with whole mount pathology. *J Urol*, 203(1), 92-99.

Bass, E. J., Pantovic, A., Connor, M., Gabe, R., Padhani, A. R., Rockall, A., et al. (2020). A systematic review and meta-analysis of the diagnostic accuracy of biparametric prostate MRI for prostate cancer in men at risk. *Prostate Cancer Prostatic Dis*, 1-16.

Bhowmick, S., Coad, J. E., Swanlund, D. J., & Bischof, J. C. (2004). In vitro thermal therapy of AT-1 dunning prostate tumours. *Int J Hyperthermia*, 20(1), 73-92.

Bierley, J. D., Gospodarowicz, M. K., & Wittekind, C. (2017). TNM classification of malignant tumors. UICC International Union Against Cancer. 8th edn.

Biermann, K., Montironi, R., Lopez-Beltran, A., Zhang, S., & Cheng, L. (2010). Histopathological findings after treatment of prostate cancer using high-intensity focused ultrasound (HIFU). *Prostate*, 70(11), 1196-1200.

Bill-Axelson, A., Holmberg, L., Garmo, H., Taari, K., Busch, C., Nordling, S., et al. (2018). Radical prostatectomy or watchful waiting in prostate cancer—29-year follow-up. *New Engl J Med, 379*(24), 2319-2329.

Bokhorst, L. P., Valdagni, R., Rannikko, A., Kakehi, Y., Pickles, T., Bangma, C. H., et al. (2016). A decade of active surveillance in the PRIAS study: An update and evaluation of the criteria used to recommend a switch to active treatment. *Eur Urol*, 70(6), 954-960.

Bomers, J. G. R., Cornel, E. B., Futterer, J. J., Jenniskens, S. F. M., Schaafsma, H. E., Barentsz, J. O., et al. (2017). MRI-guided focal laser ablation for prostate cancer followed by radical prostatectomy: Correlation of treatment effects with imaging. *World J Urol*, 35(5), 703-711.

Bonekamp, D., Wolf, M. B., Roethke, M. C., Pahernik, S., Hadaschik, B. A., Hatiboglu, G., et al. (2019). Twelve-month prostate volume reduction after MRI-guided transurethral ultrasound ablation of the prostate. *Eur Radiol*, 29, 299-308.

Boyes, A., Tang, K., Yaffe, M., Sugar, L., Chopra, R., & Bronskill, M. (2007). Prostate tissue analysis immediately following magnetic resonance imaging guided transurethral ultrasound thermal therapy. *J Urol*, 178(3), 1080-1085.

Bratan, F., Niaf, E., Melodelima, C., Chesnais, A. L., Souchon, R., Mège-Lechevallier, F., et al. (2013). Influence of imaging and histological factors on prostate cancer detection and localisation on multiparametric MRI: A prospective study. *Eur Radiol*, 23(7), 2019-2029.

Bray, F., Ferlay, J., Soerjomataram, I., Siegel, R. L., Torre, L. A., & Jemal, A. (2018). Global cancer statistics 2018: GLOBOCAN estimates of incidence and mortality worldwide for 36 cancers in 185 countries. *CA Cancer J Clin*, 68(6), 394-424.

Burdett, S., Boeve, L. M., Ingleby, F. C., Fisher, D. J., Rydzewska, L. H., Vale, C. L., et al. (2019). Prostate radiotherapy for metastatic hormone-sensitive prostate cancer: A STOPCAP systematic review and meta-analysis. *Eur Urol*, 76(1), 115-24

Burtnyk, M., Chopra, R., & Bronskill, M. (2010). Simulation study on the heating of the surrounding anatomy during transurethral ultrasound prostate therapy: A 3D theoretical analysis of patient safety. *Med Phys*, 37(6Part1), 2862-2875.

Burtnyk, M., Chopra, R., & Bronskill, M. J. (2009). Quantitative analysis of 3-D conformal MRI-guided transurethral ultrasound therapy of the prostate: Theoretical simulations. *Int J Hyperther*, 25(2), 116-131.

Burtnyk, M., Hill, T., Cadieux-Pitre, H., & Welch, I. (2015). Magnetic resonance image guided transurethral ultrasound prostate ablation: A preclinical safety and feasibility study with 28-day followup.(2015). *J Urol*, 193(5), 1669-1675.

Burtnyk, M., N'Djin, W. A., Kobelevskiy, I., Bronskill, M., & Chopra, R. (2010). 3D conformal MRI-controlled transurethral ultrasound prostate therapy: Validation of numerical simulations and demonstration in tissue-mimicking gel phantoms. *Phys Med Biol*, 55(22), 6817.

Byar, D. P., Mostofi, F. K., & Veterans Administration Cooperative Urological Research Group. (1972). Carcinoma of the prostate: Prognostic evaluation of certain pathologic features in 208 radical prostatectomies. *Cancer*, 30(1), 5-13.

Böni, R. A., Sulser, T., Jochum, W., Romanowski, B., Debatin, J. F., & Krestin, G. P. (1997). Laser ablation-induced changes in the prostate: Findings at endorectal MR imaging with histologic correlation. *Radiology*, 202(1), 232-236.

Calais, J., Ceci, F., Eiber, M., Hope, T. A., Hofman, M. S., Rischpler, C., et al. (2019). 18F-fluciclovine PET-CT and 68Ga-PSMA-11 PET-CT in patients with early biochemical recurrence after prostatectomy: A prospective, single-centre, single-arm, comparative imaging trial. *Lancet Oncol*, 20(9), 1286-1294.

Cameron, M. G., Kersten, C., Vistad, I., van Helvoirt, R., Weyde, K., Undseth, C., et al. (2015). Palliative pelvic radiotherapy for symptomatic incurable prostate cancer–A prospective multicenter study. *Radiother Oncol*, 115(3), 314-320.

Cardinale, J., Schäfer, M., Benešová, M., Bauder-Wüst, U., Leotta, K., Eder, M., et al. (2017). Preclinical evaluation of 18F-PSMA-1007, a new prostate-specific membrane antigen ligand for prostate cancer imaging. *J Nucl Med*, 58(3), 425-431.

Carlsson, S., Assel, M., Ulmert, D., Gerdtsson, A., Hugosson, J., Vickers, A., et al. (2017). Screening for prostate cancer starting at age 50–54 years. A population-based cohort study. *Eur Urol*, 71(1), 46-52.

Catalona, W. J., Partin, A. W., Slawin, K. M., Brawer, M. K., Flanigan, R. C., Patel, A., et al. (1998). Use of the percentage of free prostate-specific antigen to enhance differentiation of prostate cancer from benign prostatic disease: A prospective multicenter clinical trial. *JAMA*, 279(19), 1542-1547.

Chade, D. C., Eastham, J., Graefen, M., Hu, J. C., Karnes, R. J., Klotz, L., et al. (2012). Cancer control and functional outcomes of salvage radical prostatectomy for radiation-recurrent prostate cancer: A systematic review of the literature. *Eur Urol*, 61(5), 961-971.

Chen, J., Shin, J. H., Tsao, T., Ko, H., Yoon, H., Han, K., et al. (2017). Prostatic arterial embolization for control of hematuria in patients with advanced prostate cancer. *J Vasc Interv Radiol*, 28(2), 295-301.

Chin, J. L., Billia, M., Relle, J., Roethke, M. C., Popeneciu, I. V., Kuru, T. H., et al. (2016). Magnetic resonance imaging–guided transurethral ultrasound ablation of prostate tissue in patients with localized prostate cancer: A prospective phase 1 clinical trial. *Eur Urol*, 70(3), 447-455.

Choi, Y. H., Yu, J. W., Jeong, B. C., Seo, S. I., Jeon, S. S., Lee, H. M., et al. (2019). Histological characteristics of the largest and secondary tumors in radical prostatectomy specimens and implications for focal therapy. *Diagnostic Pathol*, 14(1), 1-6.

Chopra, R., Burtnyk, M., Haider, M. A., & Bronskill, M. J. (2005). Method for MRI-guided conformal thermal therapy of prostate with planar transurethral ultrasound heating applicators. *Phys Med Biol*, 50(21), 4957.

Chopra, R., Colquhoun, A., Burtnyk, M., N'djin, W. A., Kobelevskiy, I., Boyes, A., et al. (2012). MR imaging–controlled transurethral ultrasound therapy for conformal treatment of prostate tissue: Initial feasibility in humans. *Radiology*, 265(1), 303-313.

Chopra, R., Tang, K., Burtnyk, M., Boyes, A., Sugar, L., Appu, S., et al. (2009). Analysis of the spatial and temporal accuracy of heating in the prostate gland using transurethral ultrasound therapy and active MR temperature feedback. *Phys Med Biol*, 54(9), 2615.

Chopra, R., Wachsmuth, J., Burtnyk, M., Haider, M. A., & Bronskill, M. J. (2006). Analysis of factors important for transurethral ultrasound prostate heating using MR temperature feedback. *Phys Med Biol*, 51(4), 827.

Chu, K. F., & Dupuy, D. E. (2014). Thermal ablation of tumours: Biological mechanisms and advances in therapy. *Nat Rev Cancer*, 14(3), 199-208.

Coad, J. E., Kosari, K., Humar, A., & Sielaff, T. D. (2003). Radiofrequency ablation causes 'thermal fixation'of hepatocellular carcinoma: A post-liver transplant histopathologic study. *Clin Transplant*, 17(4), 377-384.

Cole, A. I., Morgan, T. M., Spratt, D. E., Palapattu, G. S., He, C., Tomlins, S. A., et al. (2016). Prognostic value of percent gleason grade 4 at prostate biopsy in predicting prostatectomy pathology and recurrence. *J Urol*, 196(2), 405-411.

Connor, M. J., Shah, T. T., Horan, G., Bevan, C. L., Winkler, M., & Ahmed, H. U. (2020). Cytoreductive treatment strategies for de novo metastatic prostate cancer. *Nat Rev Clin Oncol*, 17(3), 168-182.

Cooperberg, M. R., Moul, J. W., & Carroll, P. R. (2005). The changing face of prostate cancer. *J Clin Oncol, 23*(32), 8146-8151.

Corfield, J., Perera, M., Bolton, D., & Lawrentschuk, N. (2018). 68 ga-prostate specific membrane antigen (PSMA) positron emission tomography (PET) for primary staging of high-risk prostate cancer: A systematic review. *World J Urol*, 36(4), 519-527.

Courivaud, F., Kazaryan, A. M., Lund, A., Orszagh, V. C., Svindland, A., Marangos, I. P., et al. (2014). Thermal fixation of swine liver tissue after magnetic resonance-guided high-intensity focused ultrasound ablation. *Ultrasound Med Biol*, 40(7), 1564-1577.

Crain, D. S., Amling, C. L., & Kane, C. J. (2004). Palliative transurethral prostate resection for bladder outlet obstruction in patients with locally advanced prostate cancer. *J Urol*, 171(2), 668-671.

Crouzet, S., Blana, A., Murat, F. J., Pasticier, G., Brown, S. C., Conti, G. N., et al. (2017). Salvage high-intensity focused ultrasound (HIFU) for locally recurrent prostate cancer after failed radiation therapy: Multi-institutional analysis of 418 patients. *BJU Int*, 119(6), 896-904.

Crouzet, S., Chapelon, J. Y., Rouviere, O., Mege-Lechevallier, F., Colombel, M., Tonoli-Catez, H., et al. (2014). Whole-gland ablation of localized prostate cancer with high-intensity focused ultrasound: Oncologic outcomes and morbidity in 1002 patients. *Eur Urol*, 65(5), 907-914.

D'Amico, A. V., Whittington, R., Malkowicz, S. B., Schultz, D., Blank, K., Broderick, G. A., et al. (1998). Biochemical outcome after radical prostatectomy, external beam radiation therapy, or interstitial radiation therapy for clinically localized prostate cancer. *Jama*, 280(11), 969-974.

Daneshmand, S., Quek, M. L., Stein, J. P., Lieskovsky, G., Cai, J., Pinski, J., et al. (2004). Prognosis of patients with lymph node positive prostate cancer following radical prostatectomy: Long-term results. *J Urol*, 172(6 Part 1), 2252-2255.

De Carlo, F., Celestino, F., Verri, C., Masedu, F., Liberati, E., & Di Stasi, S. M. (2014). Retropubic, laparoscopic, and robot-assisted radical prostatectomy: Surgical, oncological, and functional outcomes: A systematic review. *Urol Int, 93*(4), 373-383.

Donaldson, I. A., Alonzi, R., Barratt, D., Barret, E., Berge, V., Bott, S., et al. (2015). Focal therapy: Patients, interventions, and outcomes—a report from a consensus meeting. *Eur Urol*, 67(4), 771-777.

Donovan, J. L., Hamdy, F. C., Lane, J., Mason, M., Metcalfe, C., Walsh, E., et al. (2016). Patient-reported outcomes after monitoring, surgery, or radiotherapy for prostate cancer. *N Engl J Med*, 375, 1425-1437.

Drost, F. H., Osses, D. F., Nieboer, D., Steyerberg, E. W., Bangma, C. H., Roobol, M. J., et al. (2019). Prostate MRI, with or without MRI-targeted biopsy, and systematic biopsy for detecting prostate cancer. *Cochrane Database of Syst Rev,* (4)

Duijzentkunst, D. S., Peters, M., van Zyp, JRN van der Voort, Moerland, M. A., & van Vulpen, M. (2016). Focal salvage therapy for local prostate cancer recurrences after primary radiotherapy: A comprehensive review. *World J Urol*, 34(11), 1521-1531.

Eder, M., Schäfer, M., Bauder-Wüst, U., Hull, W., Wängler, C., Mier, W., et al. (2012). 68Ga-complex lipophilicity and the targeting property of a urea-based PSMA inhibitor for PET imaging. *Bioconj Chem*, 23(4), 688-697.

Elterman, D., Li, W., Hatiboglu, G., Relle, J., Zorn, K. C., Bhojani, N., et al. (2020). Relief of lower urinary tract symptoms after MRI-guided transurethral ultrasound ablation (TULSA) for localized prostate cancer: Subgroup analyses in patients with concurrent cancer and benign prostatic hyperplasia. *J Endourol*. https://doi.org/10.1089/end.2020.0511

Epstein, J. I., Allsbrook Jr, W. C., Amin, M. B., Egevad, L. L., & ISUP Grading Committee. (2005). The 2005 international society of urological pathology (ISUP) consensus conference on gleason grading of prostatic carcinoma. *Am J Surg Pathol*, 29(9), 1228-1242.

Epstein, J. I., Egevad, L., Amin, M. B., Delahunt, B., Srigley, J. R., & Humphrey, P. A. (2016). The 2014 international society of urological pathology (ISUP) consensus conference on gleason grading of prostatic carcinoma. *Am J Surg Pathol*, 40(2), 244-252.

Epstein, J. I., Walsh, P. C., Carmichael, M., & Brendler, C. B. (1994). Pathologic and clinical findings to predict tumor extent of nonpalpable (stage t1 c) prostate cancer. *JAMA*, 271(5), 368-374.

Epstein, M. M., Edgren, G., Rider, J. R., Mucci, L. A., & Adami, H. (2012). Temporal trends in cause of death among swedish and US men with prostate cancer. *J Natl Cancer Inst*, 104(17), 1335-1342.

Epstein, J. I., Zelefsky, M. J., Sjoberg, D. D., Nelson, J. B., Egevad, L., Magi-Galluzzi, C., et al. (2016). A contemporary prostate cancer grading system: A validated alternative to the gleason score. *Eur Urol*, 69(3), 428-435.

Erickson, A., Sandeman, K., Lahdensuo, K., Nordling, S., Kallajoki, M., Seikkula, H., et al. (2018). New prostate cancer grade grouping system predicts survival after radical prostatectomy. *Hum Pathol*, 75, 159-166.

Even-Sapir, E. (2005). Imaging of malignant bone involvement by morphologic, scintigraphic, and hybrid modalities. *J Nucl Med*, 46(8), 1356-1367.

Even-Sapir, E., Metser, U., Flusser, G., Zuriel, L., Kollender, Y., Lerman, H., et al. (2004). Assessment of malignant skeletal disease: Initial experience with 18F-fluoride PET/CT and comparison between 18F-fluoride PET and 18F-fluoride PET/CT. *J Nucl Med*, 45(2), 272-278.

Even-Sapir, E., Metser, U., Mishani, E., Lievshitz, G., Lerman, H., & Leibovitch, I. (2006). The detection of bone metastases in patients with high-risk prostate cancer: 99mTc-MDP planar bone scintigraphy, single-and multi-field-of-view SPECT, 18F-fluoride PET, and 18F-fluoride PET/CT. *J Nucl Med*, 47(2), 287-297.

Fendler, W. P., Eiber, M., Beheshti, M., Bomanji, J., Ceci, F., Cho, S., et al. (2017). 68 ga-PSMA PET/CT: Joint EANM and SNMMI procedure guideline for prostate cancer imaging: Version 1.0. *Eur J Nucl Med Mol Imaging*, 44(6), 1014-1024.

Fenton, J. J., Weyrich, M. S., Durbin, S., Liu, Y., Bang, H., & Melnikow, J. (2018). Prostate-specific Antigen–Based screening for prostate cancer: Evidence report and systematic review for the US preventive services task force. *JAMA*, 319(18), 1914-1931.

Finnish Cancer Registry. (2019). Tilastot. https://syoparekisteri.fi/tilastot/tautitilastot/

Fitzmaurice, C., Dicker, D., Pain, A., Hamavid, H., Moradi-Lakeh, M., MacIntyre, M. F., et al. (2015). The global burden of cancer 2013. *JAMA Oncol*, 1(4), 505-527.

Fütterer, J. J., Briganti, A., De Visschere, P., Emberton, M., Giannarini, G., Kirkham, A., et al. (2015). Can clinically significant prostate cancer be detected with multiparametric magnetic resonance imaging? A systematic review of the literature. *Eur Urol*, 68(6), 1045-1053.

Gandaglia, G., Abdollah, F., Schiffmann, J., Trudeau, V., Shariat, S. F., Kim, S. P., et al. (2014). Distribution of metastatic sites in patients with prostate cancer: A population-based analysis. *Prostate*, 74(2), 210-216.

Gandaglia, G., Fossati, N., Zaffuto, E., Bandini, M., Dell'Oglio, P., Bravi, C. A., et al. (2017). Development and internal validation of a novel model to identify the candidates for extended pelvic lymph node dissection in prostate cancer. *Eur Urol*, 72(4), 632-640.

Gandaglia, G., Ploussard, G., Valerio, M., Mattei, A., Fiori, C., Fossati, N., et al. (2019). A novel nomogram to identify candidates for extended pelvic lymph node dissection among patients with clinically localized prostate cancer diagnosed with magnetic resonance imaging-targeted and systematic biopsies. *Eur Urol*, 75(3), 506-514.

Ganzer, R., Arthanareeswaran, V. K. A., Ahmed, H. U., Cestari, A., Rischmann, P., Salomon, G., et al. (2018). Which technology to select for primary focal treatment of prostate cancer?—European section of urotechnology (ESUT) position statement. *Prostate Cancer Prostatic Dis*, 21(2), 175-186.

Germer, C., Isbert, C. M., Albrecht, D., Ritz, J. P., Schilling, A., Roggan, A., et al. (1998). Laser-induced thermotherapy for the treatment of liver metastasis. *Surg Endoscopy*, 12(11), 1317-1325.

Gill, I. S., Azzouzi, A., Emberton, M., Coleman, J. A., Coeytaux, E., Scherz, A., et al. (2018). Randomized trial of partial gland ablation with vascular targeted phototherapy versus active surveillance for low risk prostate cancer: Extended followup and analyses of effectiveness. *J Urol, 200*(4), 786-793.

Giesel, F. L., Will, L., Lawal, I., Lengana, T., Kratochwil, C., Vorster, M., et al. (2018). Intraindividual comparison of 18F-PSMA-1007 and 18F-DCFPyL PET/CT in the prospective evaluation of patients with newly diagnosed prostate carcinoma: A pilot study. *J Nucl Med*, 59(7), 1076-1080.

Gleason, D. F. (1966). Classification of prostatic carcinomas. *Cancer Chemother Rep*, 50, 125-8.

Gnanapragasam, V. J., Kumar, V., Langton, D., Pickard, R. S., & Leung, H. Y. (2006). Outcome of transurethral prostatectomy for the palliative management of lower urinary tract symptoms in men with prostate cancer. *Int J Urol*, 13(6), 711-715.

Godtman, R., Holmberg, A., Khatami, E., Stranne, A., Hugosson, J. J. (2012). Outcome following active surveillance of men with screen-detected prostate cancer. results from the göteborg randomised population-based prostate cancer screening trial. *Eur Urol*, 63(1), 101-107.

Haas, G. P., Delongchamps, N., Brawley, O. W., Wang, C. Y., & de la Roza, G. (2008). The worldwide epidemiology of prostate cancer: Perspectives from autopsy studies. *Can J Urol*, 15(1), 3866.

Haidl, F., & Heidenreich, A. (2018). The significance of palliative surgery in castration-resistant prostate cancer. *Aktuelle Urol*, 49(5), 405-411.

Hamdy, F. C., Donovan, J. L., Lane, J. A., Mason, M., Metcalfe, C., Holding, P., et al. (2016). 10-year outcomes after monitoring, surgery, or radiotherapy for localized prostate cancer. *New Engl J Med*, 375(15), 1415-1424.

Hanks, G. E., Leibel, S., & Kramer, S. (1983). The dissemination of cancer by transurethral resection of locally advanced prostate cancer. *J Urol*, 129(2), 309-311.

Hanley, J. A., & McNeil, B. J. (1983). A method of comparing the areas under receiver operating characteristic curves derived from the same cases. *Radiology*, 148(3), 839-843.

Harris, P. A., Taylor, R., Minor, B. L., Elliott, V., Fernandez, M., O'Neal, L., et al. (2019). The REDCap consortium: Building an international community of software platform partners. *J Biomed Inform*, 95, 103208.

Hatiboglu, G., Popeneciu, V., Bonekamp, D., Burtnyk, M., Staruch, R., Pahernik, S., et al. (2020). Magnetic resonance imaging-guided transurethral ultrasound ablation of prostate tissue in patients with localized prostate cancer: Single-center evaluation of 6-month treatment safety and functional outcomes of intensified treatment parameters. *World J Urol*, 38(2), 343-350.

He, X., McGee, S., Coad, J. E., Schmidlin, F., Iaizzo, P. A., Swanlund, D. J., et al. (2004). Investigation of the thermal and tissue injury behaviour in microwave thermal therapy using a porcine kidney model. *Int J Hyperthermia*, 20(6), 567-593.

Heidenreich, A., Porres, D., & Pfister, D. (2015). The role of palliative surgery in castration-resistant prostate cancer. *Oncol Res Treat*, 38(12), 670-677.

Helyar, V., Mohan, H. K., Barwick, T., Livieratos, L., Gnanasegaran, G., Clarke, S. E., et al. (2010). The added value of multislice SPECT/CT in patients with equivocal bony metastasis from carcinoma of the prostate. *Eur J Nucl Med Mol Imaging*, 37(4), 706-713.

Hennings, L., Kaufmann, Y., Griffin, R., Siegel, E., Novak, P., Corry, P., et al. (2009). Dead or alive? autofluorescence distinguishes heat-fixed from viable cells. *Int J Hyperther*, 25(5), 355-363.

Herlemann, A., Wenter, V., Kretschmer, A., Thierfelder, K. M., Bartenstein, P., Faber, C., et al. (2016). 68Ga-PSMA positron emission tomography/computed tomography provides accurate staging of lymph node regions prior to lymph node dissection in patients with prostate cancer. *Eur Urol*, 70(4), 553-557.

Hofman, M. S., Lawrentschuk, N., Francis, R. J., Tang, C., Vela, I., Thomas, P., et al. (2020). Prostate-specific membrane antigen PET-CT in patients with high-risk prostate cancer before curative-intent surgery or radiotherapy (proPSMA): A prospective, randomised, multi-centre study. *Lancet*, 395(10231), 1208-1216

Hølund, B. (1980). Latent prostatic cancer in a consecutive autopsy series. *Scand J Urol Nephrol*, 14(1), 29-35.

Hövels, A., Heesakkers, R., Adang, E. M., Jager, G. J., Strum, S., Hoogeveen, Y. L., et al. (2008). The diagnostic accuracy of CT and MRI in the staging of pelvic lymph nodes in patients with prostate cancer: A meta-analysis. *Clinical Radiol*, 63(4), 387-395.

Ilic, D., Evans, S. M., Allan, C. A., Jung, J. H., Murphy, D., & Frydenberg, M. (2017). Laparoscopic and robotic-assisted versus open radical prostatectomy for the treatment of localised prostate cancer. *Cochrane Database Syst Rev,* (9).

Ilic, D., Neuberger, M. M., Djulbegovic, M., & Dahm, P. (2013). Screening for prostate cancer. *Cochrane Database Syst Rev*, (1).

Ingrosso, G., Becherini, C., Lancia, A., Caini, S., Ost, P., Francolini, G., et al. (2020). Nonsurgical salvage local therapies for radiorecurrent prostate cancer: A systematic review and meta-analysis. *Eur Urol Oncol*, 3(2), 183-197.

Jambor, I., Boström, P. J., Taimen, P., Syvänen, K., Kähkönen, E., Kallajoki, M., et al. (2017). Novel biparametric MRI and targeted biopsy improves risk stratification in men with a clinical suspicion of prostate cancer (IMPROD trial). *J Magn Reson Imaging*, 46(4), 1089-1095.

Jambor, I., Kuisma, A., Ramadan, S., Huovinen, R., Sandell, M., Kajander, S., et al. (2016). Prospective evaluation of planar bone scintigraphy, SPECT, SPECT/CT, 18F-NaF PET/CT and whole body 1.5 T MRI, including DWI, for the detection of bone metastases in high risk breast and prostate cancer patients: SKELETA clinical trial. *Acta Oncol*, 55(1), 59-67.

Jambor, I., Kähkönen, E., Taimen, P., Merisaari, H., Saunavaara, J., Alanen, K., et al. (2015). Prebiopsy multiparametric 3T prostate MRI in patients with elevated PSA, normal digital rectal examination, and no previous biopsy. *J Magn Reson Imaging*, 41(5), 1394-1404.

Jambor, I., Verho, J., Ettala, O., Knaapila, J., Taimen, P., Syvänen, K. T., et al. (2019). Validation of IMPROD biparametric MRI in men with clinically suspected prostate cancer: A prospective multi-institutional trial. *PLOS Med*, 16(6), e1002813.

Janssen, J., Woythal, N., Meißner, S., Prasad, V., Brenner, W., Diederichs, G., et al. (2017). [68 ga] PSMA-HBED-CC uptake in osteolytic, osteoblastic, and bone marrow metastases of prostate cancer patients. *Mol Imaging Biol*, 19(6), 933-943.

Jereczek-Fossa, B. A., Rojas, D. P., Zerini, D., Fodor, C., Viola, A., Fanetti, G., et al. (2019). Reirradiation for isolated local recurrence of prostate cancer: Mono-institutional series of 64 patients treated with salvage stereotactic body radiotherapy (SBRT). *Br J Radiol*, 92(1094), 20180494.

Johnson, D. C., Raman, S. S., Mirak, S. A., Kwan, L., Bajgiran, A. M., Hsu, W., et al. (2019). Detection of individual prostate cancer foci via multiparametric magnetic resonance imaging. *Eur Urol*, 75(5), 712-720.

Jones, C. U., Hunt, D., McGowan, D. G., Amin, M. B., Chetner, M. P., Bruner, D. W., et al. (2011). Radiotherapy and short-term androgen deprivation for localized prostate cancer. *New Engl J Med,* 365(2), 107-118.

Jonmarker, S., Valdman, A., Lindberg, A., Hellström, M., & Egevad, L. (2006). Tissue shrinkage after fixation with formalin injection of prostatectomy specimens. Virchows Archiv, 449(3), 297-301.

Kalapara, A. A., Nzenza, T., Pan, H. Y., Ballok, Z., Ramdave, S., O'Sullivan, R., et al. (2020). Detection and localisation of primary prostate cancer using 68gallium prostate-specific membrane antigen positron emission tomography/computed tomography compared with multiparametric magnetic resonance imaging and radical prostatectomy specimen pathology. *BJU Int*, 126(1), 83-90.

Kalbasi, A., Li, J., Berman, A. T., Swisher-McClure, S., Smaldone, M., Uzzo, R. G., et al. (2015). Dose-escalated irradiation and overall survival in men with nonmetastatic prostate cancer. *JAMA Oncol*, 1(7), 897-906.

Karavitakis, M., Winkler, M., Abel, P., Livni, N., Beckley, I., & Ahmed, H. U. (2011). Histological characteristics of the index lesion in whole-mount radical prostatectomy specimens: Implications for focal therapy. *Prostate Cancer Prostatic Dis*, 14(1), 46-52.

Kasivisvanathan, V., Rannikko, A. S., Borghi, M., Panebianco, V., Mynderse, L. A., Vaarala, M. H., et al. (2018). MRI-targeted or standard biopsy for prostate-cancer diagnosis. *New Engl J Med*, 378(19), 1767-1777.

Kesch, C., Kratochwil, C., Mier, W., Kopka, K., & Giesel, F. L. (2017). 68Ga or 18F for prostate cancer imaging? *J Nucl Med*, 58(5), 687-688.

Kesch, C., Vinsensia, M., Radtke, J. P., Schlemmer, H. P., Heller, M., Ellert, E., et al. (2017). Intraindividual comparison of 18F-PSMA-1007 PET/CT, multiparametric MRI, and radical prostatectomy specimens in patients with primary prostate cancer: A retrospective, proof-of-concept study. *J Nucl Med*, 58(11), 1805-1810.

Khafagy, R., Shackley, D., Samuel, J., O'Flynn, K., Betts, C., & Clarke, N. (2007). Complications arising in the final year of life in men dying from advanced prostate cancer. *J Palliat Med*, 10(3), 705-711.

Kim, J., Park, J. S., & Ham, W. S. (2017). The role of metastasis-directed therapy and local therapy of the primary tumor in the management of oligometastatic prostate cancer. *Investig Clin Urol*, 58(5), 307-316.

Klotz, L., Pavlovich, C. P., Chin, J., Hatiboglu, G., Koch, M., Penson, D., et al. (2020). MRI-guided transurethral ultrasound ablation of prostate cancer. J Urol. https://doi.org/10.1097/JU.0000000000001362

Klotz, L., Vesprini, D., Sethukavalan, P., Jethava, V., Zhang, L., Jain, S., et al. (2015). Long-term follow-up of a large active surveillance cohort of patients with prostate cancer. *J Clin Oncol*, 33(3), 272-277.

Knaapila, J., Jambor, I., Ettala, O., Taimen, P., Verho, J., Perez, I. M., et al. (2020). Negative predictive value of biparametric prostate magnetic resonance imaging in excluding significant prostate

cancer: A pooled data analysis based on clinical data from four prospective, registered studies. *Eur Urol Focus*. https://doi.org/10.1016/j.euf.2020.04.007

Knaapila, J., Jambor, I., Perez, I. M., Ettala, O., Taimen, P., Verho, J., et al. (2020). Prebiopsy IMPROD biparametric magnetic resonance imaging combined with prostate-specific antigen density in the diagnosis of prostate cancer: An external validation study. *Eur Urol Oncol*, 3(5), 648-656.

Komori, T., Narabayashi, I., Matsumura, K., Matsuki, M., Akagi, H., Ogura, Y., et al. (2007). 2-[fluorine-18]-fluoro-2-deoxy-D-glucose positron emission tomography/computed tomography versus whole-body diffusion-weighted MRI for detection of malignant lesions: Initial experience. *Ann Nucl Med*, 21(4), 209-215.

Kuriyama, M., Wang, M. C., Lee, C., Papsidero, L. D., Killian, C. S., Inaji, H., et al. (1981). Use of human prostate-specific antigen in monitoring prostate cancer. *Cancer Res, 41*(10), 3874-3876.

Kweldam, C. F., Kümmerlin, I. P., Nieboer, D., Verhoef, E. I., Steyerberg, E. W., Van der Kwast, Theodorus H, et al. (2016). Disease-specific survival of patients with invasive cribriform and intraductal prostate cancer at diagnostic biopsy. *Mod Pathol, 29*(6), 630-636.

Le, J. D., Tan, N., Shkolyar, E., Lu, D. Y., Kwan, L., Marks, L. S., et al. (2015). Multifocality and prostate cancer detection by multiparametric magnetic resonance imaging: Correlation with whole-mount histopathology. *Eur Urol*, 67(3), 569-576.

Lecouvet, F. E., El Mouedden, J., Collette, L., Coche, E., Danse, E., Jamar, F., et al. (2012). Can whole-body magnetic resonance imaging with diffusion-weighted imaging replace tc 99m bone scanning and computed tomography for single-step detection of metastases in patients with high-risk prostate cancer? *Eur Urol*, 62(1), 68-75.

Lecouvet, F. E., Geukens, D., Stainier, A., Jamar, F., Jamart, J., d'Othée, B. J., et al. (2007). Magnetic resonance imaging of the axial skeleton for detecting bone metastases in patients with high-risk prostate cancer: Diagnostic and cost-effectiveness and comparison with current detection strategies. *J Clin Oncol*, 25(22), 3281-3287.

Lecouvet, F. E., Oprea-Lager, D. E., Liu, Y., Ost, P., Bidaut, L., Collette, L., et al. (2018). Use of modern imaging methods to facilitate trials of metastasis-directed therapy for oligometastatic disease in prostate cancer: A consensus recommendation from the EORTC imaging group. *Lancet Oncol*, 19(10), e534-e545.

Lecouvet, F. E., Vande Berg, B. C., Malghem, J., Omoumi, P., & Simoni, P. (2009). Diffusion-weighted MR imaging: Adjunct or alternative to T1-weighted MR imaging for prostate carcinoma bone metastases? *Radiology*, 252(2), 624.

Leslie, T. A., Kennedy, J. E., Illing, R. O., Ter Haar, G. R., Wu, F., Phillips, R. R., et al. (2008). High-intensity focused ultrasound ablation of liver tumours: Can radiological assessment predict the histological response? *BJR*, 81(967), 564-571.

Levesque, M., Hu, H., Diamandis, E. P., & D'Costa, M. (1995). Prostate-Specific antigen expression by various tumors. *J Clin Lab Anal*, 9(2), 123-128.

Lindner, U., Lawrentschuk, N., Weersink, R. A., Davidson, S. R., Raz, O., Hlasny, E., et al. (2010). Focal laser ablation for prostate cancer followed by radical prostatectomy: Validation of focal therapy and imaging accuracy. *Eur Urol*, 57(6), 1111-1114.

Løvf, M., Zhao, S., Axcrona, U., Johannessen, B., Bakken, A. C., Carm, K. T., et al. (2019). Multifocal primary prostate cancer exhibits high degree of genomic heterogeneity. *Eur Urol*, 75(3), 498-505.

Luboldt, W., Küfer, R., Blumstein, N., Toussaint, T. L., Kluge, A., Seemann, M. D., et al. (2008). Prostate carcinoma: Diffusion-weighted imaging as potential alternative to conventional MR and 11 C-choline PET/CT for detection of bone metastases. *Radiology*, 249(3), 1017-1025.

Maenhout, M., Peters, M., van Vulpen, M., Moerland, M. A., Meijer, R. P., van den Bosch, Maurice AAJ, et al. (2017). Focal MRI-guided salvage high-dose-rate brachytherapy in patients with radiorecurrent prostate cancer. *Technol Cancer Res T*, 16(6), 1194-1201.

Marszalek, M., Ponholzer, A., Rauchenwald, M., & Madersbacher, S. (2007). Palliative transurethral resection of the prostate: Functional outcome and impact on survival. *BJU Int*, 99(1), 56-59.

Matta, R., Chapple, C. R., Fisch, M., Heidenreich, A., Herschorn, S., Kodama, R. T., et al. (2019). Pelvic complications after prostate cancer radiation therapy and their management: An international collaborative narrative review. *Eur Urol, 75*(3), 464-476.

Maurer, T., Eiber, M., Schwaiger, M., & Gschwend, J. E. (2016). Current use of PSMA–PET in prostate cancer management. *Nat Rev Urol*, 13(4), 226.

McNeal, J. E. (1981). The zonal anatomy of the prostate. *Prostate, 2*(1), 35-49.

McNeal, J. E. (1992). Cancer volume and site of origin of adenocarcinoma in the prostate: Relationship to local and distant spread. Human Pathology, 23(3), 258-266.

McNeal, J. E., Redwine, E. A., Freiha, F. S., & Stamey, T. A. (1988). Zonal distribution of prostatic adenocarcinoma: Correlation with histologic pattern and direction of spread. *Am J Surg Pathol*, 12(12), 897-906.

Mease, R. C., Foss, C. A., & Pomper, M. G. (2013). PET imaging in prostate cancer: Focus on prostate-specific membrane antigen.*Cur Top Med Chem, 13*(8), 951-962.

Merisaari, H., Jambor, I., Ettala, O., Boström, P. J., Montoya Perez, I., Verho, J., et al. (2019). IMPROD biparametric MRI in men with a clinical suspicion of prostate cancer (IMPROD trial): Sensitivity for prostate cancer detection in correlation with whole-mount prostatectomy sections and implications for focal therapy. *J Magn Reson Imaging, 50*(5), 1641-1650.

Moreno, J. G., O'Hara, S. M., Long, J. P., Veltri, R. W., Ning, X., Alexander, A. A., et al. (1997). Transrectal ultrasound-guided biopsy causes hematogenous dissemination of prostate cells as determined by RT-PCR. *Urology*, 49(4), 515-520.

Mottet, N., van den Bergh, Roderick CN, Briers, E., Van den Broeck, T., Cumberbatch, M. G., De Santis, M., et al. (2020). EAU-EANM-ESTRO-ESUR-SIOG guidelines on prostate Cancer—2020 update. part 1: Screening, diagnosis, and local treatment with curative intent. *Eur Urol.*

Mouraviev, V., Mayes, J. M., Sun, L., Madden, J. F., Moul, J. W., & Polascik, T. J. (2007). Prostate cancer laterality as a rationale of focal ablative therapy for the treatment of clinically localized prostate cancer. *Cancer*, 110(4), 906-910.

Mouraviev, V., Villers, A., Bostwick, D. G., Wheeler, T. M., Montironi, R., & Polascik, T. J. (2011). Understanding the pathological features of focality, grade and tumour volume of early-stage prostate cancer as a foundation for parenchyma-sparing prostate cancer therapies: Active surveillance and focal targeted therapy. *BJU Int*, 108(7), 1074-1085.

Nair, S. M., Hatiboglu, G., Relle, J., Hetou, K., Hafron, J., Harle, C., et al. (2020). MRI-Guided transurethral ultrasound ablation in patients with localized prostate cancer: Three year outcomes of a prospective phase I study. *BJU Int*. https://doi.org/10.1111/bju.15268

Nair, S. M., Stern, N., Dewar, M., Siddiqui, K., Smith, E., Gomez, J. A., et al. (2020). Salvage open radical prostatectomy for recurrent prostate cancer following MRI-guided transurethral ultrasound ablation (TULSA) of the prostate: Feasibility and efficacy. *Scan J Urol*, 1-5.

Napoli, A., Anzidei, M., De Nunzio, C., Cartocci, G., Panebianco, V., De Dominicis, C., et al. (2013). Real-time magnetic resonance–guided high-intensity focused ultrasound focal therapy for localised prostate cancer: Preliminary experience. *Eur Urol*, 63(2), 395-398.

Neal, D. E., Metcalfe, C., Donovan, J. L., Lane, J. A., Davis, M., Young, G. J., et al. (2020). Ten-year mortality, disease progression, and treatment-related side effects in men with localised prostate cancer from the ProtecT randomised controlled trial according to treatment received. *Eur Urol*, 77(3), 320-330.

Nevoux, P., Ouzzane, A., Ahmed, H. U., Emberton, M., Montironi, R., Presti Jr, J. C., et al. (2012). Quantitative tissue analyses of prostate cancer foci in an unselected cystoprostatectomy series. *BJU Int*, 110(4), 517-523.

Oishi, M., Gill, I. S., Ashrafi, A. N., Lin-Brande, M., Nassiri, N., Shin, T., et al. (2019). Primary whole-gland cryoablation for prostate cancer: Biochemical failure and clinical recurrence at 5.6 years of follow-up. *Eur Urol*, 75(2), 208-214.

Padhani, A. R., Weinreb, J., Rosenkrantz, A. B., Villeirs, G., Turkbey, B., & Barentsz, J. (2019). Prostate imaging-reporting and data system steering committee: PI-RADS v2 status update and future directions. *Eur Urol*, 75(3), 385-396.

Pasoglou, V., Michoux, N., Peeters, F., Larbi, A., Tombal, B., Selleslagh, T., et al. (2014). Whole-body 3D T1-weighted MR imaging in patients with prostate cancer: Feasibility and evaluation in screening for metastatic disease. *Radiology*, 275(1), 155-166.

Pelletier, J., Cyr, S., Julien, A., Fradet, Y., Lacombe, L., & Toren, P. (2018). Contemporary outcomes of palliative transurethral resection of the prostate in patients with locally advanced prostate cancer. *Urol Oncol*, , 36. (8) pp. 363. e7-363. e11.

Pereira, K., Halpern, J. A., McClure, T. D., Lewis, N. A., Kably, I., Bhatia, S., et al. (2016). Role of prostate artery embolization in the management of refractory haematuria of prostatic origin. *BJU Int*, 118(3), 359-365.

Perera, M., Papa, N., Roberts, M., Williams, M., Udovicich, C., Vela, I., et al. (2020). Gallium-68 prostate-specific membrane antigen positron emission tomography in advanced prostate cancer—updated diagnostic utility, sensitivity, specificity, and distribution of prostate-specific membrane antigen-avid lesions: A systematic review and meta-analysis. *Eur Urol, 77*(4), 403-417.

Peters, M., Moman, M. R., van der Poel, Henk G, Vergunst, H., de Jong, I. J., Vijverberg, P. L., et al. (2013). Patterns of outcome and toxicity after salvage prostatectomy, salvage cryosurgery and salvage brachytherapy for prostate cancer recurrences after radiation therapy: A multi-center experience and literature review. *World J Urol*, 31(2), 403-409.

Pfister, D., Porres, D., Epplen, R., & Heidenreich, A. (2011). Palliative radical (cysto) prostatectomy in locally advanced castration-resistant prostate cancer. *Der Urologe.Ausg.A*, 50(9), 1101-1105.

Phillips, R., Shi, W. Y., Deek, M., Radwan, N., Lim, S. J., Antonarakis, E. S., et al. (2020). Outcomes of observation vs stereotactic ablative radiation for oligometastatic prostate cancer: The ORIOLE phase 2 randomized clinical trial. *JAMA Oncol*, 6, 650-9.

Pooli, A., Johnson, D. C., Shirk, J., Markovic, D., Sadun, T. Y., Sisk Jr, A. E., et al. (2021). Predicting pathological tumor size in prostate cancer based on multiparametric prostate magnetic resonance imaging and preoperative findings. *J Urol*, 205(2), 444-451.

Postema, A. W., de Reijke, T. M., Ukimura, O., van den Bos, W., Azzouzi, A. R., Barret, E., et al. (2016). Standardization of definitions in focal therapy of prostate cancer: Report from a delphi consensus project. *World J Urol*, 34(10), 1373-1382.

Priester, A., Natarajan, S., Khoshnoodi, P., Margolis, D. J., Raman, S. S., Reiter, R. E., et al. (2017). Magnetic resonance imaging underestimation of prostate cancer geometry: Use of patient specific molds to correlate images with whole mount pathology. *J Urol*, 197(2), 320-326.

Privé, B. M., Israël, B., Schilham, M. G., Muselaers, C. H., Zámecnik, P., Mulders, P. F., et al. (2020). Evaluating F-18-PSMA-1007-PET in primary prostate cancer and comparing it to multi-parametric MRI and histopathology. Prostate Cancer Prostatic Dis. https://doi.org/10.1038/s41391-020-00292-2.

Purysko, A. S., Rosenkrantz, A. B., Turkbey, I. B., & Macura, K. J. (2020). RadioGraphics update: PI-RADS version 2.1—A pictorial update. *RadioGraphics*, 40(7), E33-E37.

Ramsay, E., Mougenot, C., Staruch, R., Boyes, A., Kazem, M., Bronskill, M., et al. (2017). Evaluation of focal ablation of magnetic resonance imaging defined prostate cancer using magnetic resonance imaging controlled transurethral ultrasound therapy with prostatectomy as the reference standard. *J Urol*, 197(1), 255-261.

Reddy, D., Shah, T. T., van Son, M., Guillaumier, S., Hosking-Jervis, F., Dudderidge, T., et al. (2020). Oncological Outcomes of 356 Patients Undergoing Salvage Focal Ablative HIFU Or Cryotherapy Following Radiation Failure. *J Clin Oncol*, 38(15suppl), 5582-5582.

Reeve, B. B., Stover, A. M., Jensen, R. E., Chen, R. C., Taylor, K. L., Clauser, S. B., et al. (2012). Impact of diagnosis and treatment of clinically localized prostate cancer on health-related quality of life for older americans: A population-based study. *Cancer*, 118(22), 5679-5687.

Resnick, M. J., Koyama, T., Fan, K., Albertsen, P. C., Goodman, M., Hamilton, A. S., et al. (2013). Long-term functional outcomes after treatment for localized prostate cancer. *N Engl J Med*, 368(5), 436.

Rhee, H., Thomas, P., Shepherd, B., Gustafson, S., Vela, I., Russell, P. J., et al. (2016). Prostate specific membrane antigen positron emission tomography may improve the diagnostic accuracy of multiparametric magnetic resonance imaging in localized prostate cancer. *J Urol*, 196(4), 1261-1267.

Rischmann, P., Gelet, A., Riche, B., Villers, A., Pasticier, G., Bondil, P., et al. (2017). Focal high intensity focused ultrasound of unilateral localized prostate cancer: A prospective multicentric hemiablation study of 111 patients. *Eur Urol*, 71(2), 267-273.

Rischpler, C., Beck, T. I., Okamoto, S., Schlitter, A. M., Knorr, K., Schwaiger, M., et al. (2018). 68Ga-PSMA-HBED-CC uptake in cervical, celiac, and sacral ganglia as an important pitfall in prostate cancer PET imaging. *J Nucl Med*, 59(9), 1406-1411.

Rosset, R., Bratan, F., Crouzet, S., Tonoli-Catez, H., Mège-Lechevallier, F., Gelet, A., et al. (2017). Can pre-and postoperative magnetic resonance imaging predict recurrence-free survival after whole-gland high-intensity focused ablation for prostate cancer? *Eur Radiol*, 27(4), 1768-1775.

Rouvière, O., Lyonnet, D., Raudrant, A., Colin-Pangaud, C., Chapelon, J. Y., Bouvier, R., et al. (2001). MRI appearance of prostate following transrectal HIFU ablation of localized cancer. *Eur Uro*l, 40(3), 265-274.

Rouvière, O., Puech, P., Renard-Penna, R., Claudon, M., Roy, C., Mège-Lechevallier, F., et al. (2019). Use of prostate systematic and targeted biopsy on the basis of multiparametric MRI in biopsy-naive patients (MRI-FIRST): A prospective, multicentre, paired diagnostic study. *Lancet Oncol*, 20(1), 100-109.

Sæter, T., Vlatkovic, L., Waaler, G., Servoll, E., Nesland, J. M., Axcrona, K., et al. (2017). Intraductal carcinoma of the prostate on diagnostic needle biopsy predicts prostate cancer mortality: A population-based study. *Prostate*, 77(8), 859-865.

Sanda, M. G., Dunn, R. L., Michalski, J., Sandler, H. M., Northouse, L., Hembroff, L., et al. (2008). Quality of life and satisfaction with outcome among prostate-cancer survivors. *N Engl J Med*, 358(12), 1250-1261.

Sapareto, S. A., & Dewey, W. C. (1984). Thermal dose determination in cancer therapy. *Int J Radiat Oncol • Biol • Phys*, 10(6), 787-800.

Sauter, G., Steurer, S., Clauditz, T. S., Krech, T., Wittmer, C., Lutz, F., et al. (2016). Clinical utility of quantitative gleason grading in prostate biopsies and prostatectomy specimens. *Eur Urol*, 69(4), 592-598.

Scheltema, M. J., van den Bos, W., Siriwardana, A. R., Kalsbeek, A. M., Thompson, J. E., Ting, F., et al. (2017). Feasibility and safety of focal irreversible electroporation as salvage treatment for localized radiorecurrent prostate cancer. *BJU Int*, 120, 51-58.

Schröder, F. H., Hugosson, J., Roobol, M. J., Tammela, T. L., Zappa, M., Nelen, V., et al. (2014). The european randomized study of screening for prostate cancer–prostate cancer mortality at 13 years of follow-up. *Lancet*, 384(9959), 2027-2035.

Shah, T. T., Peters, M., Eldred-Evans, D., Miah, S., Yap, T., Faure-Walker, N. A., et al. (2019). Early-medium-term outcomes of primary focal cryotherapy to treat nonmetastatic clinically significant prostate cancer from a prospective multicentre registry. *Eur Urol*, 76(1), 98-105.

Sheikhbahaei, S., Werner, R. A., Solnes, L. B., Pienta, K. J., Pomper, M. G., Gorin, M. A., et al. (2019). Prostate-specific membrane antigen (PSMA)-targeted PET imaging of prostate cancer: An update on important pitfalls. *Semin Nulc Med,* 49(4), 255-270.

Siddiqui, K., Chopra, R., Vedula, S., Sugar, L., Haider, M., Boyes, A., et al. (2010). MRI-guided transurethral ultrasound therapy of the prostate gland using real-time thermal mapping: Initial studies. *Urology*, 76(6), 1506-1511.

Siddiqui, K. M., Billia, M., Al-Zahrani, A., Williams, A., Goodman, C., Arifin, A., et al. (2016). Long-term oncologic outcomes of salvage cryoablation for radio-recurrent prostate cancer. *J Urol*, 196(4), 1105-1111.

Siddiqui, M. M., Rais-Bahrami, S., Turkbey, B., George, A. K., Rothwax, J., Shakir, N., et al. (2015). Comparison of MR/ultrasound Fusion–Guided biopsy with ultrasound-guided biopsy for the diagnosis of prostate cancer. *JAMA*, 313(4), 390-397.

Silver, D. A., Pellicer, I., Fair, W. R., Heston, W. D., & Cordon-Cardo, C. (1997). Prostate-specific membrane antigen expression in normal and malignant human tissues. *Clin Cancer Res*, 3(1), 81-85.

Stabile, A., Orczyk, C., Hosking-Jervis, F., Giganti, F., Arya, M., Hindley, R. G., et al. (2019). Medium-term oncological outcomes in a large cohort of men treated with either focal or hemi-ablation using high-intensity focused ultrasonography for primary localized prostate cancer. *BJU Int*, 124(3), 431-440.

Stafford, R. J., Shetty, A., Elliott, A. M., Klumpp, S. A., McNichols, R. J., Gowda, A., et al. (2010). Magnetic resonance guided, focal laser induced interstitial thermal therapy in a canine prostate model. *J Urol*, 184(4), 1514-1520.

Stamey, T. A., Yang, N., Hay, A. R., McNeal, J. E., Freiha, F. S., & Redwine, E. (1987). Prostate-specific antigen as a serum marker for adenocarcinoma of the prostate. *New Engl J Med*, 317(15), 909-916.

Su, S. L., Huang, I., Fair, W. R., Powell, C. T., & Heston, W. D. (1995). Alternatively spliced variants of prostate-specific membrane antigen RNA: Ratio of expression as a potential measurement of progression. *Cancer Res*, 55(7), 1441-1443.

Suh, C. H., Shinagare, A. B., Westenfield, A. M., Ramaiya, N. H., Van den Abbeele, A D, & Kim, K. W. (2018). Yield of bone scintigraphy for the detection of metastatic disease in treatment-naive prostate cancer: A systematic review and meta-analysis. *Clin Radiol*, 73(2), 158-167.

Sweat, S. D., Pacelli, A., Murphy, G. P., & Bostwick, D. G. (1998). Prostate-specific membrane antigen expression is greatest in prostate adenocarcinoma and lymph node metastases. *Urology*, 52(4), 637-640.

Tateishi, U., Morita, S., Taguri, M., Shizukuishi, K., Minamimoto, R., Kawaguchi, M., et al. (2010). A meta-analysis of 18 F-fluoride positron emission tomography for assessment of metastatic bone tumor. *Ann Nucl Med*, 24(7), 523-531.

Tay, K. J., Scheltema, M. J., Ahmed, H. U., Barret, E., Coleman, J. A., Dominguez Escrig, J., et al. (2017). Patient selection for prostate focal therapy in the era of active surveillance: An international delphi consensus project. *Prostate Cancer Prostatic Dis*, 20(3), 294-299.

Tay, K. J., Amin, M. B., Ghai, S., Jimenez, R. E., Kench, J. G., Klotz, L., et al. (2019). Surveillance after prostate focal therapy. *World J Urol*, 37(3), 397-407.

Taylor, K. L., Luta, G., Hoffman, R. M., Davis, K. M., Lobo, T., Zhou, Y., et al. (2018). Quality of life among men with low-risk prostate cancer during the first year following diagnosis: The PREPARE prospective cohort study. *Transl Behav Med*, 8(2), 156-165.

Thoeny, H. C., Froehlich, J. M., Triantafyllou, M., Huesler, J., Bains, L. J., Vermathen, P., et al. (2014). Metastases in normal-sized pelvic lymph nodes: Detection with diffusion-weighted MR imaging. *Radiology*, 273(1), 125-135.

Thompson, I. M., Pauler, D. K., Goodman, P. J., Tangen, C. M., Lucia, M. S., Parnes, H. L., et al. (2004). Prevalence of prostate cancer among men with a prostate-specific antigen level≤ 4.0 ng per milliliter. *New Engl J Med*, 350(22), 2239-2246.

Tisseverasinghe, S. A., & Crook, J. M. (2018). The role of salvage brachytherapy for local relapse after external beam radiotherapy for prostate cancer. *Transl Androl Urol*, 7(3), 414.

Tonttila, P. P., Lantto, J., Pääkkö, E., Piippo, U., Kauppila, S., Lammentausta, E., et al. (2016). Prebiopsy multiparametric magnetic resonance imaging for prostate cancer diagnosis in biopsy-naive men with suspected prostate cancer based on elevated prostate-specific antigen values: Results from a randomized prospective blinded controlled trial. *Eur Urol*, 69(3), 419-425.

Tosoian, J. J., Mamawala, M., Epstein, J. I., Landis, P., Wolf, S., Trock, B. J., et al. (2015). Intermediate and longer-term outcomes from a prospective active-surveillance program for favorable-risk prostate cancer. *J Clin Oncol*, 33(30), 3379-3385.

Tran, H., Kwok, J., Pickles, T., Tyldesley, S., & Black, P. C. (2014). Underutilization of local salvage therapy after radiation therapy for prostate cancer. *Urol Oncol*, 32(5), 701-706.

Tsuzuki, T. (2015). Intraductal carcinoma of the prostate: a comprehensive and updated review. *Int J Urol*, 22(2), 140-145.

Ukimura, O., Coleman, J. A., De La Taille, A., Emberton, M., Epstein, J. I., Freedland, S. J., et al. (2013). Contemporary role of systematic prostate biopsies: indications, techniques, and implications for patient care. *Eur Urol*, 63(2), 214-230.

Uprimny, C., Kroiss, A. S., Decristoforo, C., Fritz, J., von Guggenberg, E., Kendler, D., et al. (2017). 68 ga-PSMA-11 PET/CT in primary staging of prostate cancer: PSA and gleason score predict the intensity of tracer accumulation in the primary tumour. *Eur J Nucl Med and Mol Imaging*, 44(6), 941-949.

Valerio, M., Cerantola, Y., Eggener, S. E., Lepor, H., Polascik, T. J., Villers, A., et al. (2017). New and established technology in focal ablation of the prostate: A systematic review. *Eur Urol*, 71(1), 17-34.

van der Leest, M., Cornel, E., Israel, B., Hendriks, R., Padhani, A. R., Hoogenboom, M., et al. (2019). Head-to-head comparison of transrectal ultrasound-guided prostate biopsy versus multiparametric prostate resonance imaging with subsequent magnetic resonance-guided biopsy in biopsy-naïve men with elevated prostate-specific antigen: A large prospective multicenter clinical study. *Eur Urol*, 75(4), 570-578.

van der Poel, Henk G, van den Bergh, Roderick CN, Briers, E., Cornford, P., Govorov, A., Henry, A. M., et al. (2018). Focal therapy in primary localised prostate cancer: The european association of urology position in 2018. *Eur Urol*, 74(1), 84-91.

van Kalmthout, L. W., van Melick, H. H., Lavalaye, J., Meijer, R. P., Kooistra, A., de Klerk, J. M., et al. (2020). Prospective validation of gallium-68 prostate specific membrane antigen-positron emission tomography/computerized tomography for primary staging of prostate cancer. J Urol, 203(3), 537-545.

van Leenders, G. J., Beerlage, H. P., Ruijter, E. T., de la Rosette, J. J, & van de Kaa, C. A. (2000). Histopathological changes associated with high intensity focused ultrasound (HIFU) treatment for localised adenocarcinoma of the prostate. *J Clin Pathol*, 53(5), 391-394.

van Leenders, G. J., van der Kwast, Theodorus H, Grignon, D. J., Evans, A. J., Kristiansen, G., Kweldam, C. F., et al. (2020). The 2019 international society of urological pathology (ISUP) consensus conference on grading of prostatic carcinoma. Am J Surg Pathol, 44, e87–e99.

van Leeuwen, P. J., Emmett, L., Ho, B., Delprado, W., Ting, F., Nguyen, Q., et al. (2017). Prospective evaluation of 68Gallium-prostate-specific membrane antigen positron emission tomography/computed tomography for preoperative lymph node staging in prostate cancer. *BJU Int*, 119(2), 209-215.

Van Son, M., Peters, M., Moerland, M., Kerkmeijer, L., Lagendijk, J., & Van der Voort van Zyp, Jochem. (2018). Focal salvage treatment of radiorecurrent prostate cancer: A narrative review of current strategies and future perspectives. *Cancers*, 10(12), 480.

Venkitaraman, R., Cook, G., Dearnaley, D. P., Parker, C. C., Khoo, V., Eeles, R., et al. (2009). Whole-body magnetic resonance imaging in the detection of skeletal metastases in patients with prostate cancer. *J Med Imaging Radiat Oncol*, 53(3), 241-247.

von Eyben, F. E., & Kairemo, K. (2014). Meta-analysis of 11C-choline and 18F-choline PET/CT for management of patients with prostate cancer. *Nucl Med Commun*, 35(3), 221-230.

Wallitt, K. L., Khan, S. R., Dubash, S., Tam, H. H., Khan, S., & Barwick, T. D. (2017). Clinical PET imaging in prostate cancer. *Radiographics*, 37(5), 1512-1536.

Wegelin, O., van Melick, H. H., Hooft, L., Bosch, J. R., Reitsma, H. B., Barentsz, J. O., et al. (2017). Comparing three different techniques for magnetic resonance imaging-targeted prostate biopsies:

A systematic review of in-bore versus magnetic resonance imaging-transrectal ultrasound fusion versus cognitive registration. is there a preferred technique? *Eur Urol*, 71(4), 517-531.

Wei, L., Wang, J., Lampert, E., Schlanger, S., DePriest, A. D., Hu, Q., et al. (2017). Intratumoral and intertumoral genomic heterogeneity of multifocal localized prostate cancer impacts molecular classifications and genomic prognosticators. *Eur Urol*, 71(2), 183-192.

Wein, A. J., Kavoussi, L. R., Partin, A. W., & Peters, C. (2016). Campbell-Walsh urology.

Wilt, T. J., Jones, K. M., Barry, M. J., Andriole, G. L., Culkin, D., Wheeler, T., et al. (2017). Follow-up of prostatectomy versus observation for early prostate cancer. *N Engl J Med*, 377(2), 132-142.

Wise, A. M., Stamey, T. A., McNeal, J. E., & Clayton, J. L. (2002). Morphologic and clinical significance of multifocal prostate cancers in radical prostatectomy specimens. *Urology*, 60(2), 264-269.

Woo, S., Suh, C. H., Eastham, J. A., Zelefsky, M. J., Morris, M. J., Abida, W., et al. (2019). Comparison of magnetic resonance imaging-stratified clinical pathways and systematic transrectal ultrasound-guided biopsy pathway for the detection of clinically significant prostate cancer: A systematic review and meta-analysis of randomized controlled trials. *Eur Urol Oncol, 2*(6), 605-616.

Woodrum, D. A., Gorny, K. R., & Mynderse, L. A. (2018). Mr-guided prostate interventions. *Top Magn Res Imaging*, 27(3), 141-151.

Wu, F., Wang, Z., Cao, Y., Xu, Z., Zhou, Q., Zhu, H., et al. (2006). Heat fixation of cancer cells ablated with high-intensity–focused ultrasound in patients with breast cancer. *Am J Surg*, 192(2), 179-184.

Yacoub, J.H., & Oto, A. (2018). MR imaging of prostate zonal anatomy. *Radiol Clin*, 56(2), 197-209

Yilmaz, B., Turkay, R., Colakoglu, Y., Baytekin, H. F., Ergul, N., Sahin, S., et al. (2019). Comparison of preoperative locoregional Ga-68 PSMA-11 PET-CT and mp-MRI results with postoperative histopathology of prostate cancer. *Prostate*, 79(9), 1007-1017.

Zlotta, A. R., Egawa, S., Pushkar, D., Govorov, A., Kimura, T., Kido, M., et al. (2013). Prevalence of prostate cancer on autopsy: Cross-sectional study on unscreened caucasian and asian men. *J Natl Cancer Inst*, 105(14), 1050-1058.

Zumsteg, Z. S., Spratt, D. E., Romesser, P. B., Pei, X., Zhang, Z., Polkinghorn, W., et al. (2015). The natural history and predictors of outcome following biochemical relapse in the dose escalation era for prostate cancer patients undergoing definitive external beam radiotherapy. *Eur Urol*, 67(6), 1009-1016.

TURUN
YLIOPISTO
UNIVERSITY
OF TURKU

Painosalama Oy, Turku, Finland 2021

ISBN 978-951-29-8463-3 (PRINT)
ISBN 978-951-29-8464-0 (PDF)
ISSN 0355-9483 (Print)
ISSN 2343-3213 (Online)